Hungarian University of Agriculture and Life Sciences

Doctoral (PhD) Dissertation

Enhanced Efficiency Zn Coated Urea to Reduce the N_2O Emissions and Increasing the Crop Growth

A Dissertation Submitted for the Degree of Doctor of Philosophy at the Doctoral School of Environmental Sciences, Hungarian University of Agriculture and Life Sciences

by
Wajid Umar

Gödöllő, Hungary

2022

Title: Enhanced Efficiency Zn Coated Urea to Reduce the N_2O Emissions and Increasing the Crop growth

Name of Doctoral School: Environmental Science

Discipline: Environmental Science

Head of Doctoral School: **Csákiné Dr. Michéli Erika**

Professor, DSC.
Institute of Environmental Science
Department of Soil Science

Supervisor(s): **Dr. Imre Czinkota, PhD**

Associate Professor, PhD
Institute of Environmental Science
Department of Agrochemistry

Dr. Miklós Gulyás

Associate Professor, PhD
Institute of Environmental Science
Department of Agrochemistry

…..…..…….. …….

Approval of Head of Doctoral School ……

Approval of Supervisor(s)

DECLARATION

This dissertation is my original work and has not been presented for a degree at any other university. No part of this dissertation may be reproduced without prior permission of the author and/or the Hungarian University of Agriculture and Life Sciences.

_____ Date_____

Wajid Umar

DECLARATION BY SUPERVISORS

This dissertation has been submitted with our approval as supervisors.

_____ Date_____

Imre Czinkota

Associate Professor, PhD
Institute of Environmental Science
Department of Agrochemistry

_____ Date_____

Miklós Gulyás

Associate Professor, PhD
Institute of Environmental Science
Department of Agrochemistry

DEDICATION

This work is dedicated to:

My beloved parents, Umar Khan and Mehmooda Beghum. I had promised to make them the happiest parents through the achievement of monumental academic success, and I hope that I have partly fulfilled the promise.

My dad, Umar Khan, not only worked so hard to provide for the family but also inculcated our principles of hard work and encouraged me to believe in myself.

My siblings (M. Yasin, G. Rasool, Khalid, Shahid, Sajid, Abid, and Abida) and my best friend Farheen for your support, encouragement, inspiration, affection, love, and steadfast partnership for success in my life. You all have been my support system.

Table of Contents

List of Figures

List of Tables

List of Equations

1. INTRODUCTION

Nitrogen (N) is the most abundant and vital nutrient in plants. It is a central part of several compounds, such as proteins and nucleotides (Xie et al., 2022). Therefore, it plays a significant role in the growth and development of plants. Apart from the crops that can fix the N from the atmosphere, e.g., legumes, all other non-leguminous plants need N (20-50 g) to produce about 1 kg of biomass (Xu et al., 2012; Xie et al., 2021). External N application in the agroecosystem is necessary to sustain crop yield and production (Umar et al., 2020).

To meet the growing population's global food demand, a significantly higher amount of N is applied as chemical fertilizers in the agroecosystem (Wang et al., 2021c). During the green revolution period (1960-2009), synthetic N fertilizers were used extensively for producing maize, rice, and wheat (Yang et al., 2017). According to Galloway et al. (2008), the global utilization of N fertilizers is about 1.5 x 10^8 t annually. It is regrettable that currently, the nitrogen use efficiency (NUE) is very low (30-50%) in the agroecosystem (Umar et al., 2020; Wang et al., 2021c). In the modern agricultural system, about 50-70% of the applied N in the form of synthetic fertilizers is lost in the environment (Ladha et al., 2005; Umar et al., 2022), leading to substantial economic losses of about 81 million US dollar annually (Subbarao et al., 2012). Apart from the losses in the field, the production of chemical N fertilizers by the Haber-Bosch process consumes about 3-5% of global natural gas annually (Harindintwali et al., 2021). Natural gas consumption releases about 450 million tons of carbon dioxide (CO_2) every year, equivalent to 1% of emissions by humans (Service, 2019; Harindintwali et al., 2021).

In addition, the N lost to the environment from the applied fertilizers significantly impacts the climate and ultimately leads to environmental degradation and toxicity (Fowler et al., 2013; Umar et al., 2022). The higher amount of lost N in the environment causes a change in biodiversity and ecosystem productivity. On the other hand, it also leads to nitrate pollution and eutrophication of freshwater bodies, degradation of air quality, ozone depletion, and greenhouse gas emissions (Harindintwali et al., 2021; Cui et al., 2020a). According to an estimate, the world population will touch the mark of 9 billion by 2050, and to feed the whole population; food production should have to be increased up to 70-100% (Godfray et al., 2010). In that scenario, the reliance on food production will increase on the synthetic N fertilizers produced by the Haber-Bosch process (Coskun et al., 2017). The global N fertilizer application will double at the rate of 3.8 x 10^7 t, ultimately leading to higher N losses and

environmental pollution problems (Subbarao et al., 2012; Umar et al., 2020). After applying the N fertilizer, it can be converted into NH_4^+ and NO_3^- forms through the mineralization process by microorganisms and soil enzymes (Ali et al., 2017). Plants and microbes absorb N in these inorganic forms, and it becomes part of the biological organisms (Ros et al., 2011; Harindintwali et al., 2021). The soil colloids have a strong affinity toward NH_4^+-N, but after complete saturation of clay colloids, the remaining NH_4^+-N can leach from the soil (Liu et al., 2016). NH_4^+-N can be converted to NH_3 by decomposing microbes and released into the atmosphere. Figure 1 showed the N gains and losses in agroecosystems.

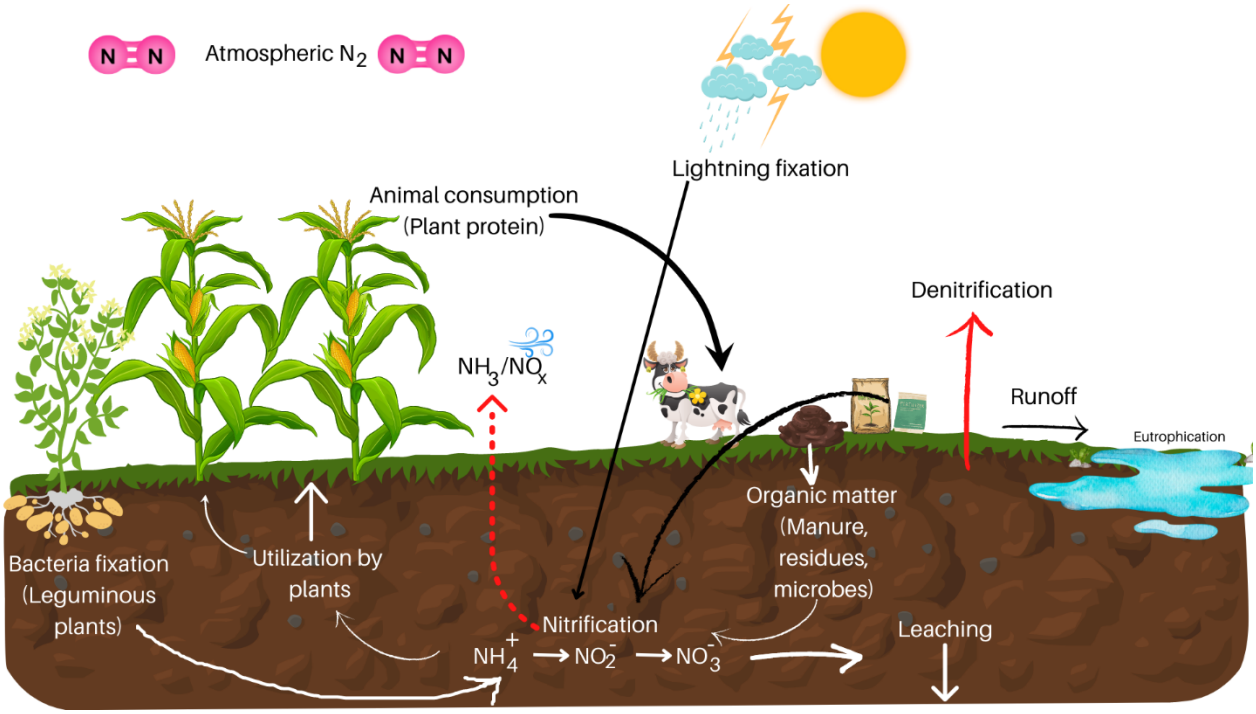

Figure 1: Nitrogen cycling in the agroecosystems

On the other hand, it can also be converted to NO_3^--N through the process of nitrification and might leads to the production of N_2O during the process. The NO_3^--N can go through the denitrification process, leading to the production of N_2O, N_2, and NO (Saggar et al., 2013). Besides, NO_3-N can leach with the infiltrating water and cause groundwater contamination (Zhao et al., 2022).

Agriculture is one of the major contributors to N_2O emissions, a potent greenhouse gas playing a significant role in global warming and ultimately in climate change (Reay et al., 2012; Umar et al., 2022). It is reported that N_2O has 296 times higher global warming potential than CO_2 over 100 years (Xie et al., 2019). Nitrification and denitrification are the major processes in producing N_2O from agricultural soils. The production of N_2O increases when a higher amount of N fertilizer is applied

compared to the crop requirement (Thangarajan et al., 2018; Machado et al., 2020). According to the Intergovernmental Panel on Climate Change (IPCC), nitrogen fertilizers are considered a source of N_2O emissions suggesting an emission factor (EF) of 1.6% as compared to 0.6% for crop residues under similar circumstances (IPCC, 2019). Over the last three decades, the concentration of N_2O is increased at the rate of 0.73 ppb yr^{-1} in the atmosphere (Stocker et al., 2013). More than 50% of the global N_2O is emitted from the agricultural fields receiving N fertilizers (Tian et al., 2020). Agricultural practices such as the amount of N applied, method of application, and soil moisture contents significantly influence the N_2O emission (Liu et al., 2017). The response of N_2O emission is not always linear as it highly depends on the amount of fertilizer applied. Field studies reported that N_2O emission response was non-linear when a higher amount of N fertilizer was used compared to the crop needs (Song et al., 2018; Signor et al., 2013).

Adopting relevant management practices is necessary to overcome the above-mentioned fertilizer losses and environmental hazards. The 4R strategy needed to be adapted to reduce the loss of nutrients, increase plant utilization, and ultimately increase crop yield and production. From the 4R system, the "Right source/fertilizer" is one of the main components. It has been found that slow-release fertilizers (SRFs) and controlled-release fertilizers (CRFs) have already gained much attention from farmers and researchers (Rahman et al., 2021). The SRFs are known for the slow release of nutrients but the nutrient release factors such as period, pattern, and rate are uncontrollable and mostly depend on the soil conditions, weather, storage, and transportation (Rajan et al., 2021). These fertilizers are prepared mainly by physically coating the fertilizer granules with organic/inorganic hydrophobic material. The hydrophobic materials act as a wall to prevent the rapid release of nutrients by reducing the water penetration and bursting of the fertilizer granules ultimately increasing the nutrient use efficiency and reducing the environmental impact (Andelkovic et al., 2018). The release of nutrients from SRFs also depends on biological and chemical actions (Ransom et al., 2020). Such as the sulfur-coated urea (SCU) coating prevents urea's solubility until the sulfur is oxidized, and the release mainly depends on the microbial activity and soil condition. Recently it was reported that the biobased polymer coating significantly increases the duration of N release from urea (Zhang et al., 2021b).

Similarly, another study reported a significant reduction in the release of N from an encapsulated urea fertilizer (Elhassani et al., 2019). Apart from the chemically synthesized hydrophobic coating materials, the use of clay minerals such as zeolite and bentonite for coating and incorporating fertilizer was also reported. Higher cation exchange capacity and slow-release properties of bentonite increased the N-release duration in a study by Hermida and Agustian (2019). This slow release of N reduces the

fertilizer losses to the environment. It is stated that slow-release N fertilizer reduced the N_2O emission by 49-66% and increased the NUE by 51-70% in the spring maize system (Lyu et al., 2021).

As we know, there are 18 essential nutrients for plants, and from them, some are required in higher quantities, known as a macronutrient (Umar et al., 2021). One of the macronutrients we discussed above is N, but some elements are required in minimal quantities and are known as micronutrients. Even though they are needed in smaller amounts, their deficiency can affect plant growth and development like a macronutrient deficiency. Of those micronutrients, Zinc (Zn) is one of the vital and essential nutrients in the soil-plant system as it contributes to several bio-physical roles (Nriagu, 2019; Castillo-Gonzalez et al., 2018). Zn is categorized into the elements required in trace amounts and is highly important to carry out normal metabolic functions (Sturikova et al., 2018). However, a higher concentration of Zn can be lethal to the living organism as it becomes toxic above optimal limits (Nriagu, 2019; Natasha et al., 2022, Niragu, 2007). Therefore, it is crucial to supply Zn at optimal concentration for sustainably carrying out the metabolic task without causing its toxicity and deficiency (Sturikova et al., 2018).

As an essential plant nutrient, Zn participates in several Physico-chemical and biological processes (Noman et al., 2019). Zn is necessary for activating more than 300 enzymes because it is one of the main structural components of all six classes of enzymes (McCall et al., 2000; Natasha et al., 2022). Because it is an integral part of the enzymes like superoxide dismutase (SOD), Zn plays a significant role in cellular defense mechanisms by tackling free radicals (Castillo-Gonzalez et al., 2018). The other vital functions of Zn in plants include the synthesis of proteins, regulation of gene expressions, involvement in carbohydrate and phosphate metabolism, and along with that, it is the structural part of bio-membranes (Noman et al., 2019; Sturikova et al., 2018). Hence, the deficiency of Zn can hamper all these biological and physical processes in plants.

Nevertheless, the toxicity of Zn can be as lethal as its deficiency because plants cannot perform their metabolic and other important functions properly under higher Zn concentration (Bankaji et al., 2019; Sidhu et al., 2020; Tibbett et al., 2021). The deficiency of Zn can trigger the deficiency of other nutrients of the same radii as it reduces their uptake by plants and their translocation inside the plant body (Bankaji et al., 2019). Under such circumstances, Zn disturbs transpiration, photosynthesis, and other related functions in plants (Chakraborty and Mishra, 2020; Mateos-Naranjo et al., 2018). Based on the dual behavior of Zn (essential and toxic) it is imperative to check its functions in the soil-plant system and it's environmental/applied levels.

Zn is the 23rd most abundant element in the earth's crust. The most-reported common range of Zn in soils globally is about 10-300 mg/kg with an overall soil Zn level of 50-55 mg/kg (Sharma et al., 2013; Umar et al., 2021). On the other hand, Gupta et al. (2016) stated that the range of Zn varied in mineral (50 mg/kg) and organic soils (66 mg/kg). In important Zn ores, their concentration is about 5-15% (Kabata-Pendias, 2011). The important Zn minerals are hemimorphite and smithsonite which are commonly known as Zn silicates and Zn carbonates respectively (Louha et al., 2021). Different activities contribute to soil Zn levels such as smelting and mining of the Zn (Tu et al., 2020; Shi et al., 2021).

The soils such as sandy soils, histosols, and the soils that originated from weathered parent material are low in Zn contents. On the other hand, there are some soils such as vertisol, calcareous soils, and saline soils that contain low plant-available Zn (Mossa et al., 2020). Zn deficiency is common globally (Akhter et al., 2020). It is stated that about 30% of soils with agricultural activity and about 50% of soils with paddy cultivation are deficient in Zn (Alloway, 2009). Fixation and low solubility are the main causes of Zn deficiency. Mainly the Phyto available Zn is the Zn present in the soil solution pool (Mossa et al., 2020). The range of soil-soluble, soil-exchangeable, and water-soluble Zn is 0.004-0.27 mg/L, 0.1-2 mg/kg, and 0.0000004-0.004 mg/kg respectively (Kabata-Pendias, 2011; Gupta et al., 2016). The plant availability of Zn and its leaching potential varies based on the soil type. The Zn availability highly depends on the clay part of the soil. The Zn solubility and availability decrease in soils with higher organic matter and clay contents, lower levels of Mn and P, and higher Al and Fe oxides (Małecki et al., 2016). The higher availability of Zn in acidic, sandy, and lighter texture soils is because of low organic matter (Moreno-Lora and Delgado, 2020). The low availability of Zn in calcareous soils because of higher clay contents, higher $CaCO_3$, and higher pH leads to the chemisorption of Zn (Wang et al., 2017b). There is a negative correlation between the pH and Zn solubility, Higher pH leads to the sorption of Zn, and at a pH greater than 8 Zn binds with clays and organic matter (Salinitro et al., 2020). In addition to the factors explained above other factors like electrical conductivity (EC), soil moisture and cation exchange capacity (CEC) also affect the Phyto availability of Zn (Moreno-Lora and Delgado, 2020; Salinitro et al., 2020).

One of the key steps to reducing the Zn deficiency in plants is the application of Zn-containing fertilizers (Liu et al., 2020; Zhang et al., 2020). There are several types of fertilizers used to overcome Zn deficiency. From them, zinc sulfate ($ZnSO_4$) and zinc oxide (ZnO) is the most commonly used Zn fertilizer. According to Yusefi-Tanha et al. (2020), the solubility of zinc chloride (ZnCl2) is much higher (432g/100mL water) as compared to ZnSO4 (57g/100 mL of water). Recently, the use of Zn-

containing fertilizers such as NPK-Zn, Zn-coated phosphatic fertilizers, Urea-Zn, and Zn-coated urea has been gaining importance (Irfan et al., 2018; Umar et al., 2022). In the recent past, studies have also been performed to test the importance of zinc oxide nanoparticles (ZnO NPs) in crop production and Zn biofortification in crops (Dimkpa et al., 2020b; Singh et al., 2019; Umar et al., 2021).

Nanoparticles (NPs) are materials that have particles size ranging from 1 to 100 nm (Reda et al., 2021; El-Saadony et al., 2021). The NPs possess properties different than the bulk materials. Previous studies reported that NPs have better Physico-chemical and biological properties as compared to bulk materials (Adhikari et al., 2020). The application of NPs as a fertilizer improved plant growth and development (Dimkpa and Bindraban, 2016). The most common features of nano-fertilizers have been discussed by Guru et al. (2015) that are as follows:

1) These are sustainable and cost-effective sources of nutrients
2) They deliver the appropriate amount of nutrients to plants when applied in soil or as foliar
3) The efficiency of nano-fertilizers is much higher than bulk materials
4) They help in reducing the environmental pollution caused by nutrients

There are different types of Zn NPs such as ZnSe, ZnS, and quantum dots but the most commonly used are ZnO NPs. The role of ZnO NPs as Zn nano-fertilizers vastly investigated during the past couple of years (Sturikova et al., 2018). According to the study conducted by Umar et al. (2021), ZnO NPs significantly improved the growth, development, and yield of maize (*Zea mays L.*) crop. It was also stated that the use of ZnO NPs as fertilizer significantly increased the grain Zn concentration in maize. The application of ZnO NPs in rice improved the NPK uptake and Zn contents in the grains as compared to Zn salt (Yang et al., 2021).

In addition to the chemical nano-fertilizers, the use of naturally occurring clay materials such as zeolite and bentonite as fertilizer/nutrient carriers is gaining importance. These clay materials are famous for their higher absorption capacity and CEC and slow-release properties (Umar et al., 2022). The major portion of bentonite consists of the clay mineral montmorillonite. Bentonite can be used for the improvement of sandy soils, where it can increase the macro-micronutrients, CEC of the soil, and organic carbon (Semalulu et al., 2017; Czaban et al., 2014). The application of bentonite can reduce the NO_3^- leaching and increase the water-holding capacity (Abd El-Hady and Eldardiry, 2016). Generally, bentonite has several benefits, and converting it to nanoscale could increase the number of benefits several folds. At the nanoscale, the clay minerals represent a hollow tubular structure and can absorb a significant number of cations and anions (Liu et al., 2012; El-Nagar and Sary, 2021), because

of the presence of negatively charged SiO_2 at the outer surface and the positively charged Al_2O_3 at the inner side. The characterization of nanoscale bentonite revealed that the NPs of bentonite possess a higher surface charge, higher surface area, higher porosity, a greater number of active sites, and tightly bound structure as compared to simple bentonite (Tayebee and Mazruy, 2018). Based on the above-explained properties nano-bentonite can act as a nutrient carrier or a fortified coating material.

1.1. Objectives

Globally we are at a stage where we must make more sustainable decisions to overcome the problem of environmental pollution and climate change. The application of chemical fertilizers without modification leads to more nutrient loss and increased greenhouse gasses from agricultural fields and ultimately exacerbating global warming, climate change, and food insecurity. Nowadays with increasing awareness, farmers are moving towards more sustainable nutrient sources such as controlled-release/slow-release fertilizers. Several researchers already working on different types of slow-release fertilizers but still, there are several organic and inorganic materials that are cost-effective and could be a good source for making slow-release fertilizers. On the other hand, the inclusion of slow-release micronutrient sources along with macronutrients is a plus point to overcoming micronutrient pollution in the environment as well as reducing micronutrient malnutrition in human beings.

This study specifically embarks on the following objectives:

1. Synthesis and characterization of ZnO NPs and Zn-fortified nano-bentonite
2. Development and characterization of Zn fortified nano-bentonite and ZnO NPs coated slow-release urea fertilizer using different binding materials (stearic acid and paraffin wax)
3. Evaluation of Zn and N release characteristics from slow-release macro-micronutrient fertilizer
4. Evaluation of the dissolution of ZnO NPs, and $ZnSO_4$ in two different soils
5. Evaluation of N_2O emission from coated and uncoated urea fertilizer under bare and planted soil conditions
6. Evaluating the comparative effect of coated and uncoated urea on plant growth and development

Figure 2: Sustainable Development Goals connected to this research

2. LITERATURE REVIEW

2.1. Nitrogen fertilization and crop growth in agroecosystem

Nitrogen is one of the major nutrients required by crops for growth and development. It is evident from the previous studies that the application of N significantly increases crop growth and production. Ansari et al. (2022) reported that the application of N in the form of urea increased the growth, yield, and chlorophyll contents of the radish crop. Similarly, an increase in growth, development, photosynthesis, and yield of the soybean crop was also reported by Liao et al. (2022). It was also stated that increasing the rate of N application increased all the growth parameters and specifically the seed yield was increased by 8.9%. Several researchers conducted studies on the role of N in plant growth and production and they supported this argument that the N significantly increases crop growth, development, and increase yield such as in maize (An et al., 2022; Li et al., 2022b), Cotton (Shah et al., 2021), legumes (Bai et al., 2020), barley (Zunfu et al., 2022). Figure 3 showed the amount of N fertilizers used globally. The increase in the growth and development of plants with the application of N occurred because N is one of the major components of plant architecture. It is reported that N affects plant growth by changing plant architecture such as no. of tillers and the size of panicles (Yang et al., 2019; Yi et al., 2019; Wang et al., 2018a, Wu et al., 2020). The uptake of N by plants depends on the growth stages of plants.

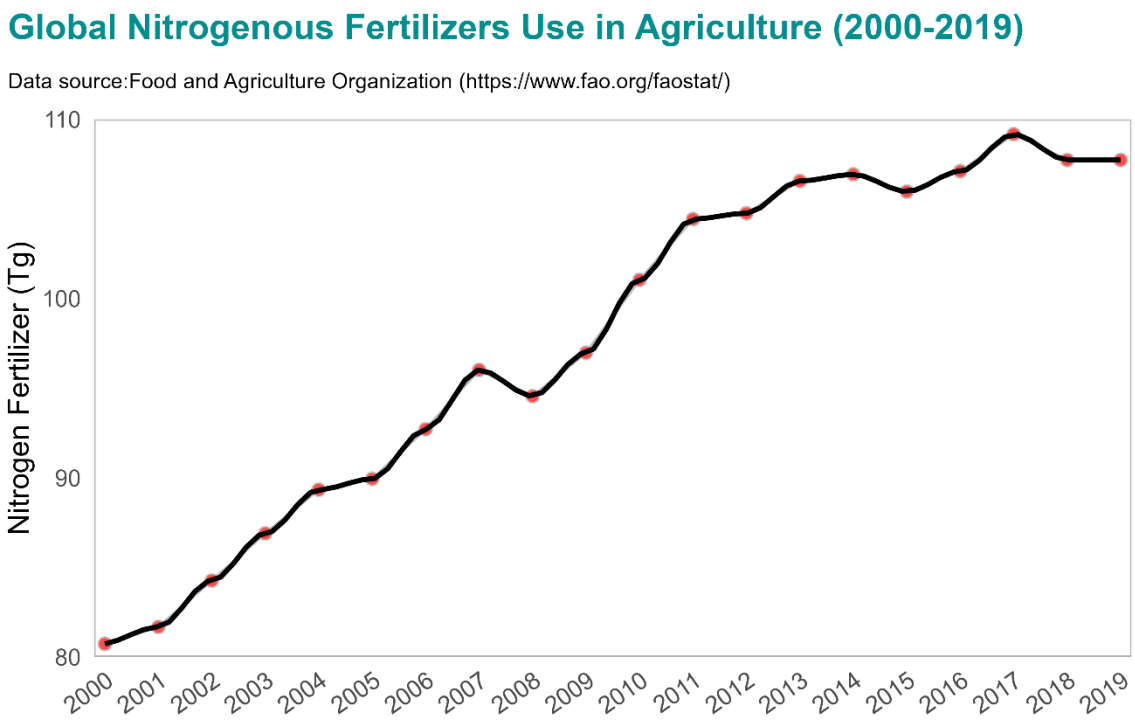

Figure 3: Use of nitrogenous fertilizers in global agriculture from 2000-2019 (FAOSTAT (https://www.fao.org/faostat/en/#data), Data retrieved in July 2022)

It is revealed that in rice the maximum uptake of N takes place at the vegetative stage and just before the start of the reproductive stage and after reaching the maximum stage it starts declining during the grain-filling stage (Hashim et al., 2015). Generally, the effect of the applied rate of N can be predicted on plant height but the estimation of N application rate on other parameters like yield, 1000 grain weight, and no. of grains per panicle is not easy. Researchers reported that the application of N increased the shoot elongation (Wang et al., 2020), whereas the excessive application of N creates a hindrance in cell wall formation and ultimately leads to crop lodging due to weaker crop stand (Wu et al., 2017; Zhang et al., 2017b). An adequate supply of N is necessary because the deficiency and toxicity of N disrupt the metabolic and physiological processes in plants. Haque and Haque (2016) reported that the number of tillers in rice crop increased with the application of an adequate amount of N and can be the opposite case if an excessive amount of N is applied. On the other hand, N deficiency can lead to the suppression of bud elongation (Luo et al., 2017). Nehe et al. (2018) reported that the application of N at the anthesis stage was found beneficial as it helps in increasing the yield and NUE.

2.2. Impact of conventional N fertilization on the environment

The use efficiency of conventional N fertilizers is very low which leads to the emergence of challenges in food production, environmental protection, and ultimately huge economical losses (Rahman et al., 2021). The N use efficiency of conventional N fertilizers ranges from 30-35% which shows that about 65-70% of the applied fertilizer is lost to the environment and failed to reach the targeted site because of the involved process such as microbial degradation and immobilization, photolysis, leaching and hydrolysis (Seleiman et al., 2020). These higher losses of fertilizers and lower uptake by crops force farmers to apply higher amounts of conventional fertilizers to enhance crop production. However, the continuous use of conventional fertilizers in higher amounts leads to environmental pollution by leaching nutrients and the emission of greenhouse gases such as N_2O (Diatta et al., 2020).

2.2.1. NH_3 emission

Apart from N_2O emission, N fertilizer losses are significant in the form of ammonia (NH_3) and molecular nitrogen (N_2). NH_3 is one of the main precursors of particulate matter ($PM_{2.5}$) and hence plays a significant role in deteriorating air quality (Umar et al., 2022). Several factors influence NH_3 emissions such as the pH of the soil, fertilizer application method, soil moisture, and cultivation system (Jiang et al., 2017; Klimczyk et al., 2021). It is confirmed from the results of previous studies that the amount of applied fertilizer and the NH_3 emission level cannot be linear (Jiang et al., 2017). A study was conducted by Liu et al. (2018) to evaluate the influence of different factors (nitrogen source, soil moisture, temperature, and soil type) on NH_3 emission. It was reported that NH_3 emission highly depends on the soil type followed by nitrogen source, soil pH, temperature, and moisture (Liu et al., 2018). Similarly, A field study was conducted to evaluate the loss of urea fertilizer through NH_3 emission from tropical pasture. It was reported that about 16.9% of applied urea was lost through NH_3 emission (da Silva Cardoso et al., 2019). The use of substances like nitrification inhibitors as a coating material on nitrogenous fertilizer could also increase ammonia emissions. It was reported in a study that the use of dicyandiamide (DCD) and N-(n-butyl) thiophosphoric triamide (NBPT) as a coating material on urea significantly increased the NH_3 emission as compared to uncoated urea (Mariano et al., 2019). In a study conducted recently, the researchers used the soil Water Heat Carbon Nitrogen Simulator model (WHCNS) to evaluate the NH_3 losses from different rates and methods of application of urea. Farmer practice, one-time application, and split application of urea was tested, and it was concluded that the losses of NH_3 were highest when urea was applied according to farmers' practice (18.9%), followed by split application (20.6%) and single-dose application (17.8%) (Shi et al., 2022). Most of the time the fertilizers in the granulated form are spread over the surface or injected below

the surface with the help of agrotechnological methods. It is hypothesized that deep injection of urea under the soil surface can reduce NH_3 emissions by 90% (Ministry of Agriculture and Rural Development, 2019). The deep placement of fertilizer grains (3-5 cm) reduced the ammonium ions at the soil surface (Cameron et al., 2013). The application of urea at the soil surface increased the NH_3 emission after a few days of the application. Whereas, the below-surface application of urea significantly reduced the NH_3 emission. By following such methods, the utilization efficiency of nitrogen by plants can be increased several folds. On the other hand, this approach is not suitable in all cases such as in perennial crops where there is a risk of root damage and in crops that leave a huge amount of crop residues after harvesting (Norton and Ouyang, 2019).

2.2.2. Nitrous oxide emission

Based on the IPCC guidelines 1% of applied N is lost in the form of N_2O (IPCC, 2006). However, the literature review showed different results. According to the available literature the emission factor for N_2O ranged from 0.03 to 14% (Walling and Vaneeckhaute, 2020) (Figure 5). Furthermore, in the available literature, it is still confusing that either the emissions increase linearly or non-linearly. There are different schools of thought one of them is supporting the fact of linear increase and the other are supporting the opposite. Several meta-analyses are presenting the linear models for N_2O emission (Wang et al., 2018c; Yi et al., 2017; Liu et al., 2013) while some are presenting the non-linear models (Jiang et al., 2017; Davis et al., 2019; Kim et al., 2013; Shcherbak et al., 2014). But overall, there is no general pattern observed regarding the linear or non-linear dependency of N_2O emission (Kim et al., 2013). Let's move to the basic mechanism of N_2O emission from fertilizers. It is observed that the higher concentration of NH_4^+ and NO_3^- after the application of fertilizer increased the emission of N_2O. According to Davidson (2009), the increased use of synthetic N fertilizers from 1960 is responsible for the increased emission of N_2O. In a recent study, it was reported that in the current fertilization system the concentration of N in the soil-crop system surpassed the required amount of N and the excessive N is then lost to the environment in the form of N_2O (Chen et al., 2017). Similarly, previous studies also reported that N_2O emission increased exponentially with the increased input of N fertilizer (Van Groenigen et al., 2010; Bouwman et al., 2002). This fact is supported by one of the meta-analyses conducted by Sun et al. (2016), they reported a 90% increase in the emission of N_2O from the cropland when the N fertilizer was applied at the rate of 50-100 kg/ha followed by an increase in N_2O emission with N input at the rate of 250-300 kg/ha. The basic processes involved in the emission of N_2O from the soil after the application of fertilizer are given in Figure 4.

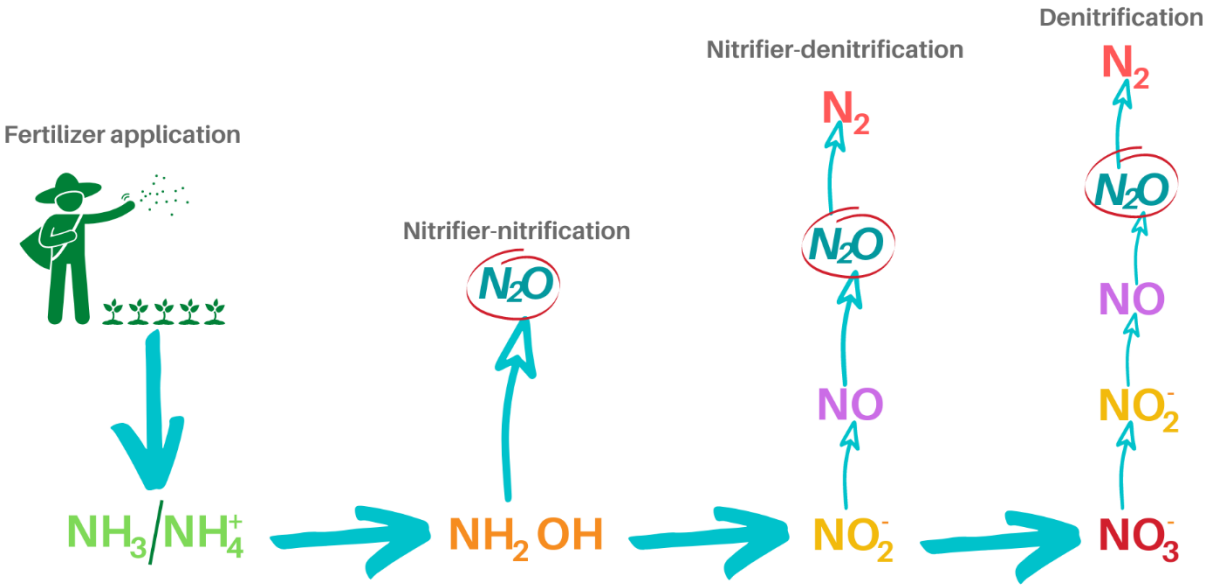

Figure 4: Basic processes of N_2O emission from the soil after fertilization

Another study conducted by Atakora et al. (2019) supported the above-explained results. They stated that the application of N fertilizer at the rate of 120 kg/ha showed higher N_2O emissions as compared to 60 kg/ha N application in maize crop. They reported an average emission factor of 0.10-0.22% throughout the experiment. The application of N fertilizer in a peach orchard in China leads to an N_2O emission factor of 0.81%. The author suggested the linear model fitting as the best model to describe the N_2O emissions (Xu et al., 2022). In a recent study, Glenn et al. (2021) revealed that the site-specific or variable rate application of N based on the plant's needs significantly reduced the emission of N_2O emissions from croplands as compared to conventional N application. Furthermore, a significant emission of N_2O was also observed from the wetlands. The increased emission of N_2O from wetlands could be due to higher N application. The higher concentration of N in the runoff water from crop fields could also increase the N_2O emissions in wetlands and the emission percentage in China increased from 31to 46% (Hou et al., 2018). To overcome the food requirements of the sharply increasing global population, it is obvious that the N fertilizer input will also increase and ultimately increase N_2O emissions (Erisman et al., 2008; Li et al., 2022c). Urgent actions are needed to reduce the emission of N_2O.

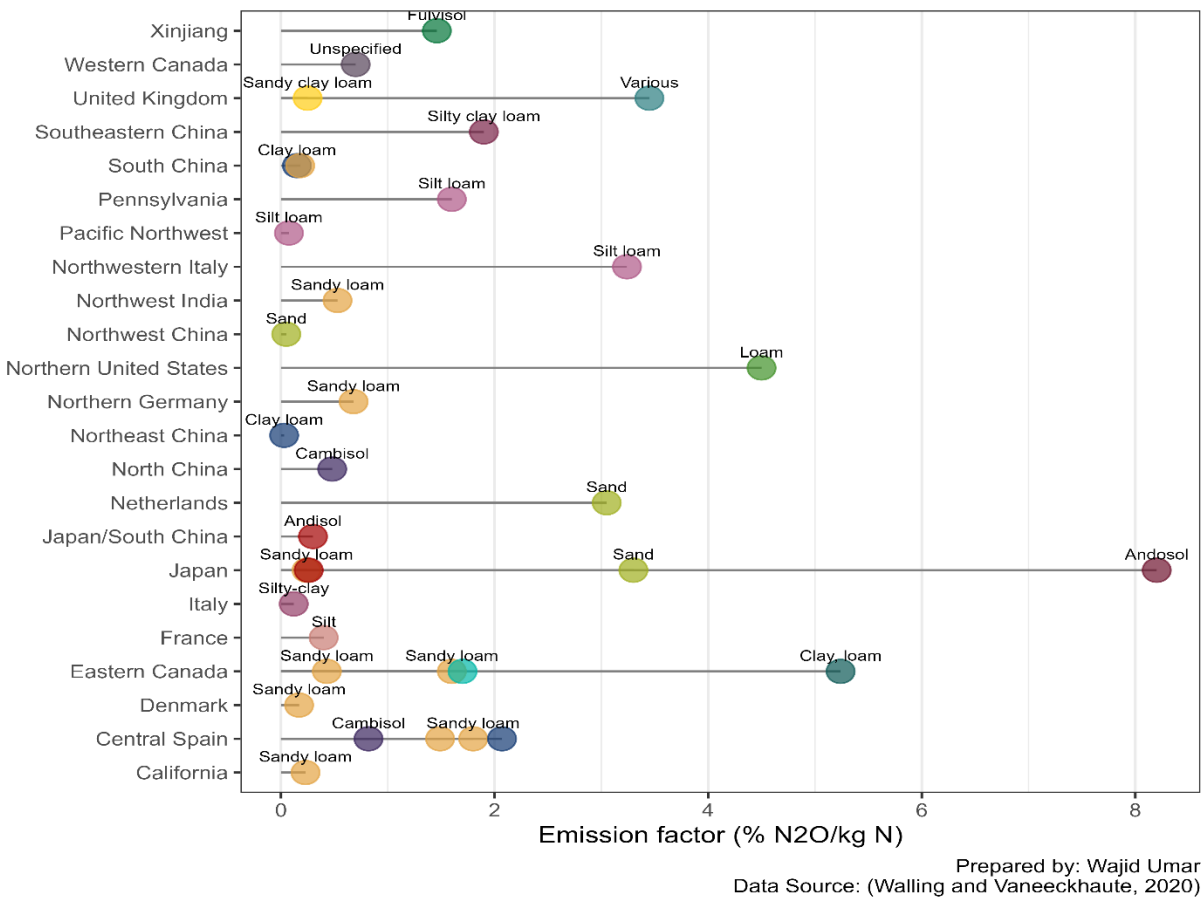

Figure 5:Nitrous oxide emission factors from different countries under different soils, crops, and climatic conditions (Walling and Vaneeckhaute, 2020)

2.3. Role of N_2O in climate change

Nitrous oxide was first discovered in 1772 by Joseph Priestly (Gillman, 2019), while its presence in the atmosphere came to an understanding in 1939. However, the role of N_2O in the environment was realized in the 1970s when scientists discovered that N_2O is released into the atmosphere through the process of denitrification in soil. Later it was discovered that N_2O triggered reactions with the ozone layer in the atmosphere and leads to its degradation (Ussiri and Lal, 2013). Later on, it was also classified as one of the most important greenhouse gases. The concentration of N_2O in the atmosphere is very low as compared to CO_2 (<1200 fold). Even at a low concentration, the contribution of N_2O to global warming is very high because of its very high global warming potential (296 times higher) than CO_2 over 100 years period (Xie et al., 2019). The contribution of N_2O to global warming was estimated at 6% (Nie et al., 2016; Ciais et al., 2014; IPCC, 2014) which is why the emission of N_2O affects the environment for a longer period.

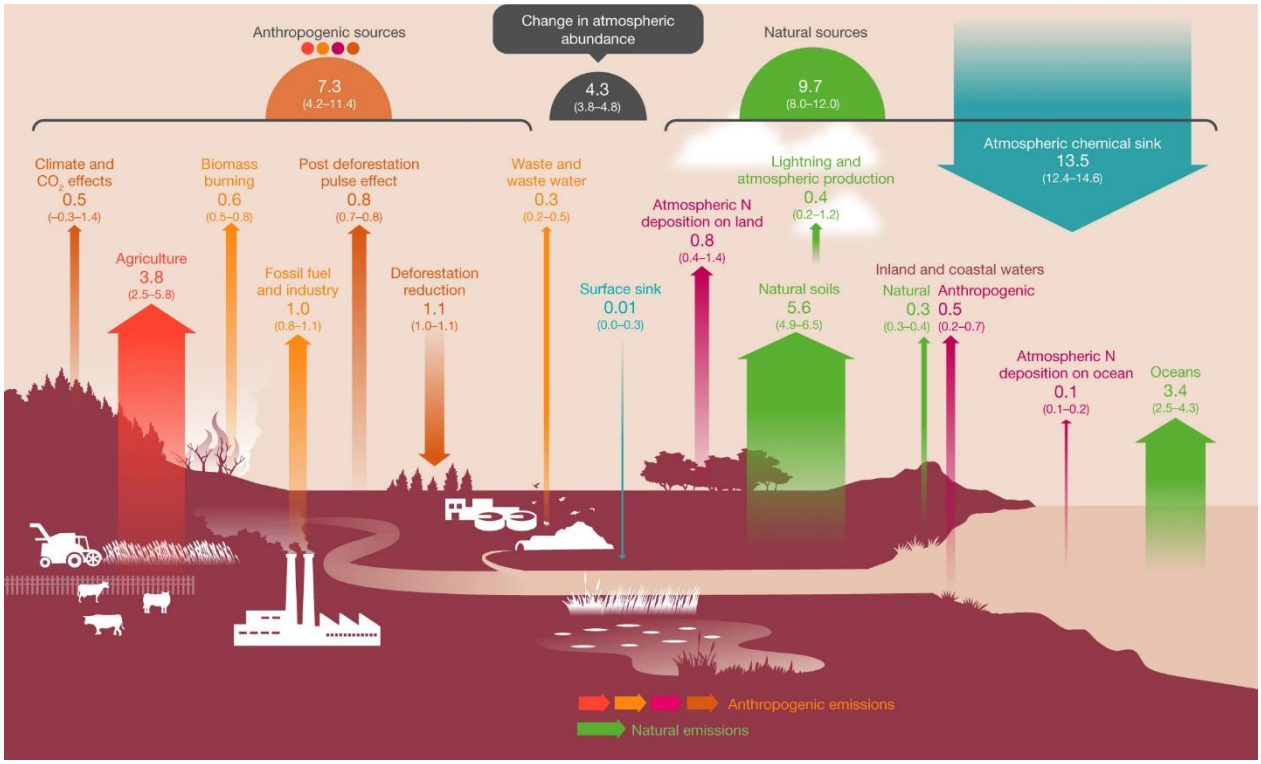

Figure 6:Nitrous oxide fluxes (Tg N yr^{-1}) from 2007-2016. Adapted from Tian et al. (2020) with permission (License no. 5311290631506)

In addition to that, N_2O also causes alterations in atmospheric chemistry. Depletion of N_2O by photochemical processes resulted in the generation of NO_2 and NO which leads to the depletion of the ozone layer (Montzka et al., 2011). The emission of N_2O in the pre-agricultural era was about 6-7 Tg N_2O N per year. The emission of N_2O from the agriculture sector is considered a major contribution to atmospheric N_2O. It is estimated that about 68% of N_2O in the atmosphere is emitted from agricultural soils (Shakoor et al., 2018; Shakoor et al., 2020). Soils receiving nitrogenous fertilizers are emitting about 4.5-6 Tg N_2O annually into the atmosphere (Charles et al., 2017). A summary of N_2O fluxes to the atmosphere from different sources is given in Figure 6.

It was observed that the increase in the emission of N_2O started at the beginning of the industrial era. For the first time, the mixing ratio of N_2O was increased to 280 ppb in 1905 and continued to increase as reported at 300 ppb in the 1970s, 322 ppb in 2010, 328 ppb in 2016, and 331.1 ppb in 2018 (World Meteorological Organization and Global Atmosphere Watch, 2019). This increased mixing ratio of N_2O in 2018 is 1.2 ppb higher as compared to 2017 and in comparison, to the pre-industrial era, this increase is 123% higher (Kudeyarov, 2020). This mixing ratio is increasing every year and the highest increase is noted in the last 10 years with an average increase of 0.95 ppb per year (World Meteorological Organization, 2019). By keeping in mind, the above facts, it is imperative to move

towards sustainable habits to overcome the anthropogenic emission of N_2O. Figure 7 showed the N_2O emission particularly from N fertilizers globally.

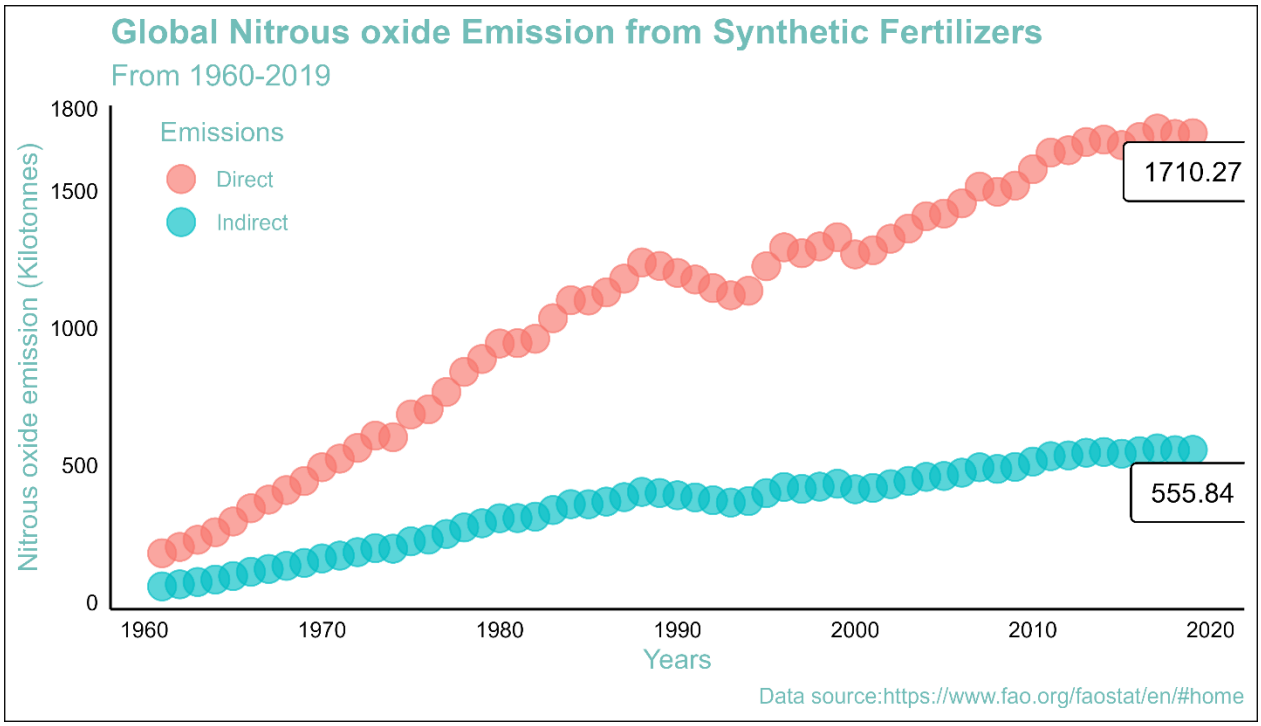

Figure 7: Direct and indirect emission of N_2O from synthetic nitrogen fertilizers applied in soil (FAOSTAT (https://www.fao.org/faostat/en/#data), Data retrieved in June 2022)

2.4. Role of enhanced efficiency fertilizers on NUE

Application of conventional N fertilizer leads to the different fates of the released N as given below:

i. N uptake by plants
ii. N consumed by microbes
iii. Lost in the form of N_2O
iv. Lost in the form of NH_3
v. Lost in the form of N_2
vi. Leached down below the root zone in the form of NO_3^-

In the case of conventional fertilizers, the N is released quickly and most of its portion is lost in different forms due to the inability of the plants to take up all the solubilized N (Umar et al., 2022). The lost N in the form of gases i.e., N_2O, NH_3, and N_2 leads to atmospheric pollution (Chen et al., 2018). NH_3 is the main precursor of particulate matter (PM2.5) and in this way, it deteriorates the air quality. While the N_2O is a potent greenhouse gas and leads to global warming and ultimately climate

change. In addition to that, the N leached below the root zone in the form of NO_3^- polluting the groundwater and causing several disorders in humans drinking the NO_3^- polluted water.

Enhanced efficiency fertilizers (EEFs) are one of the ways to solve these issues and reduce the losses to protect the environment. There are different types of EEFs such as encapsulated nutrients in complex structure materials, and coated granules with natural or synthetic hydrophobic materials to reduce the water penetrability and ultimately reduced solubility and release of nutrients (Rahman et al., 2021). Several studies have been conducted using different EEFs, some of them are highlighted below.

Zhang et al. (2021b) prepared a coated urea for the slow release of N by using bio-based polyurethane obtained from liquified corncob. To further increase the hydrophobicity of the material, polydimethylsiloxane was used for modification. According to the results, a significant slow release of N from the modified polyurethane-coated urea was observed as compared to the un-modified coating. Similarly, Chen et al. (2020) prepared coated urea by using nano-SiO2 and polymer. The water-based polymer was modified by using 1H,1H,2H,2H-perfluorooctyltriethoxysilane, and nano-SiO2. It was observed that the coating of urea with modified polymer reduced the water absorbency up to 150%. The release of urea was reduced significantly as 87.52% of the urea release was noted on the 56th day. Furthermore, Ye et al. (2020) used polyester (biodegradable) for the coating of urea. They used three different polyesters such as poly (propylene succinate), poly (butylene succinate), and poly (ethylene succinate). A significant slow release of urea was noted from the coated fertilizers as compared to uncoated urea. It was explained that the slow release of urea could be due to the crystallizability of the polyesters. Similarly, several other researchers also used different materials for the coating of urea such as carboxymethyl chitosan/Na-alginate hydrogel coated urea (Arafa et al., 2022), triethylenetetramine cured epoxidized vegetable oil-coated urea (Karnakar et al., 2022), lignocellulosic biomass modified with hydroxyapatite (Elhassani et al., 2019), polymer-coated urea (Sun et al., 2019), bio-based coated urea (Li et al., 2018), polyethylene-coated urea (Yang et al., 2018).

Apart from the coated fertilizers several researchers also developed composite materials for the slow release of nutrients. Kenawy et al. (2020) prepared urea-loaded composites of sugarcane bagasse-g-poly(acrylamide)/attapulgite. Results showed that the composite material showed a swelling capacity of 920 g/g in distilled water and significantly reduced the release of urea. It was concluded that the release of urea depends on the amount of composite material. Similarly, Guo et al. (2021) synthesized the biologically originated MIL-100 (Fe)@CNF-SA composite hydrogel material for the slow release

of N. The synthesized composite was used as a carrier material for urea. The composite material can load urea up to 1.47 g/g. It was reported that the slow release of urea was due to the porous structure of the material and higher specific surface area. Several other composite materials are also used by different researchers for example hydrogel-biochar composite (Das and Ghosh, 2022), starch-g-poly (acrylic acid-co-acrylamide) composite (Salimi et al., 2020), nano-zeolite based composites (Khan et al., 2021).

The slow release of N from EEFs increased the NUE and crop growth and production, along with that it also reduces the environmental impact of N by reducing the gaseous losses of N. Cheng et al. (2022) used EEFs in the rice-wheat rotation system. They used different nitrification inhibitors and slow down the process of nitrification. The results showed that NUE increased and emission of N_2O (~30%) and NH_3 (~22%) was reduced significantly. Similarly, Zhou et al. (2021) reported that the use of biochar-based N fertilizer reduced the N_2O emission as compared to conventional fertilizer. Furthermore, Lyu et al. (2021) used slow-release and nitrification inhibitor-based N fertilizers in spring maize and the results reported that the Enhanced efficiency nitrogen fertilizers (EENFs) significantly increased the NUE and reduced the N_2O emission. The N_2O emission was reduced from 49-56% and the NUE was increased from 51-66%. It was reported that the use of nitrification and urease inhibitors can reduce N_2O emissions by 60% in a high-temperature agroecosystem (Recio et al., 2020). There are several studies conducted that proven the fact that the use of EEFs can significantly reduce the emission of N_2O, and NH_3 and can increase the NUE several folds (Wang et al., 2021a; Dawar et al., 2020; Liao et al., 2021; Feng et al., 2016). A summary of recent research related to EEFs is given in Table 1.

Table 1: Recent developments and use of EEFs in agriculture and their role in plant growth, NUE, and environmental impact of N

EEFs	**Material used**	**Results**	**References**
Nanocomposite of Urea-Fe_3O_4	Fe_3O_4 NPs, Urea	NUE increased significantly. Rice yield was increased 1.45 times with a 50% fertilizer application	Guha et al., 2022
Nitrification and urease inhibitors-urea	NBPT, DMPSA, Urea	Decreased the NH_3 and N_2O emissions by 21.7 and 29.9%	Cheng et al., 2022

Slow-release NPK	NPK	N_2O emission was reduced (0.16 kg N_2O/ha) compared to control (0.31 kg N_2O/ha)	Lyu et al., 2021
Composite-Urea	Urea, Gluconite/smectite	Increase the longevity of N release	Rudmin et al., 2020
SBC-urea	Sugarcane bagasse, polyacrylamide, attapulgite	Released urea slowly	Kenawy et al., 2020
Wheat straw+ CRF-N	CRF, wheat straw	Little effect on GHGs but improve the NUE and crop yield	Sun et al., 2020b
Polymer-coated urea	Hydrophobic polymer, nano-SiO_2, perfluorooctyltriethoxysilane	Release N slowly	Chen et al., 2020
Polymer network N fertilizer	Ammonium polyphosphate, PVA-APP/MSP-g-AA	Slow-release of N and P and increase the crop growth	Wang et al., 2021b
Nanohybrid fertilizer	Urea, Silica	Reduced the release of N	De Silva et al., 2020
Rubber-based fertilizer	Natural rubber, poly-acrylic acid	Controlled release of NPK	Cui et al., 2020b
Coated urea	Urea, polyesters	10-1000 times reduced release of N	Ye et al., 2020
Composite urea	Urea, bagasse, cassava starch	Increase NUE and reduce environmental impact	Versino et al., 2019
Coated urea-polymer	Urea, polymer	Increase N recovery efficiency and crop yield	Sun et al., 2019
Coated urea	Bio-based epoxy, urea	Slow-release of N 12 times	Li et al., 2018
Urea-formaldehyde	Formaldehyde, urea	Significantly reduced the release of N, reduced soil pH, and increased microbial activity	Nardi et al., 2018
Coated urea	Polyethylene, urea	Slowly released N	Yang et al., 2018
Inhibitor coated urea	Urea, DMPSA, NBPT	60% decrease in NO_x emissions	Recio et al., 2020

CRNFs	Inhibitors, commercial CRNFs	Reduced N_2O emission	Gurung et al., 2021
Commercial CR urea (Green UreaNV®)	Commercial CRNFs	Reduced NH_3 emission by 45-55%	Lam et al., 2019
NBPT and S-coated urea	NBPT, sulfur, urea	Reduced NH_3 losses	Mariano et al., 2019
DCD, NBPT, Urea	DCD, NBPT, Urea	Increased sugarcane yield and reduced NH_3 emission by 60%	Barth et al., 2020
Rubber coated urea	Nature rubber, urea, epoxy resin	Increased the yield and reduced the NH_3 emission and NO_3^- leaching by 20% and 26% respectively	Qi et al., 2021

2.5. Importance of Zn in plants and humans

2.5.1. Plants

After iron (Fe) and manganese (Mn), Zn is the 3rd important metal and one of the essential plant nutrients. Several physiological, metabolic, and biochemical reactions depend on Zn (Sturikova et al., 2018; Sadeghzadeh, 2013). Hence, for better metabolic functioning it is necessary to supply Zn in adequate amounts to plants. Being the main component of enzymes such as ligases, isomerases, oxidoreductases, transferases, lyases, and hydrolases makes Zn a unique plant nutrient (Broadly et al., 2007; Natasha et al., 2022). Zn is mostly present in the plant body as a Zn ion (Zn^{+2}). In addition to the structural part of the enzymes, Zn is also present at the catalytic and co-catalytic sites, this makes Zn essential for the functioning of the enzymes (Sousa et al., 2009). Although, Zn activates more than 300 enzymes the most important enzymes that depend on Zn for their functioning are Copper-Zn-SOD, alcohol dehydrogenase, and carbonic anhydrase (Castillo-Gonzalez et al., 2018). Production of alcohol from acetaldehyde is mediated by alcohol dehydrogenase in plants. Apart from enzymes, biosynthesis, and functioning in plants also depend on Zn availability (Castillo-Gonzalez et al., 2018). Lower levels of proteins have been reported in plants with Zn deficiency and it was also reported that with the application of Zn the biosynthesis of proteins in the plant body increased immediately (Alloway, 2008). The reduction in protein biosynthesis is because Zn is an integral part of ribosomes and its deficiency leads to the disintegration of the ribosomes and ultimately reduced protein

metabolism (Castillo-Gonzalez et al., 2018). Another important function of Zn in plants is membrane stability. Zn availability increased the membrane stability by nullifying the impact of $O_2^{\cdot -}$ with the help of Copper-Zn-SOD (Castillo-Gonzalez et al., 2018; Natasha et al., 2022). Production of ROS under oxidative stress causes lipid membrane oxidation (Rehman et al., 2019), while Zn as a main component of Copper-Zn-SOD enhances plant tolerance against $O_2^{\cdot -}$ and help plant convert it to fewer toxic products (Shabbir et al., 2020; Shahid et al., 2014).

The deficiency of Zn in plants resulted in several symptoms such as leaf bronzing, chlorosis, spikelet sterility, stunted growth, thin stem, necrosis, small leaves and shoot dieback, etc. (Nakayama et al., 2020; Akhter et al., 2020; Lilay et al., 2020). The low mobility of Zn in the plant body resulted in the appearance of deficiency symptoms in the younger plant parts such as meristems and younger leaves (Mattiello et al., 2015). According to Coffin and Slaton (2020), a deficiency of Zn leads to lower grain yield, late maturity of crops, and even plant mortality (Figure 8). Generally, the deficiency symptoms appear on plant leaves when the Zn concentration is below 15-20 mg/kg of plant dry mass (Broadley et al., 2007). The reduced pollen fertility due to Zn deficiency leads to more effect on crop yield rather than dry matter production (Natasha et al., 2022). Plant tolerance to Zn deficiency depends on the genotypes, the crops such as maize, tomato, and rice are sensitive to Zn deficiency (Khatun et al., 2018). Zn deficiency also reduced the photosynthetic efficiency of the plants by reducing pigment production (Souza et al., 2020; Sidhu et al., 2020; Umar et al., 2021). According to the study conducted by Salama et al. (2006), the activity of PS II was reduced by 56% and 37% in maize and chickpea because of Zn deficiency. Zn deficiency also induces oxidative stress in the plant body (Marreiro et al., 2017). Lower levels of Copper-Zn-SOD enzyme in plant body due to Zn deficiency resulted in higher production of ROS (Marreiro et al., 2017). Furthermore, the activity of antioxidant enzymes such as POD, SOD, APX, GPX, CAT, and GR is reduced due to Zn deficiency (Natasha et al., 2022).

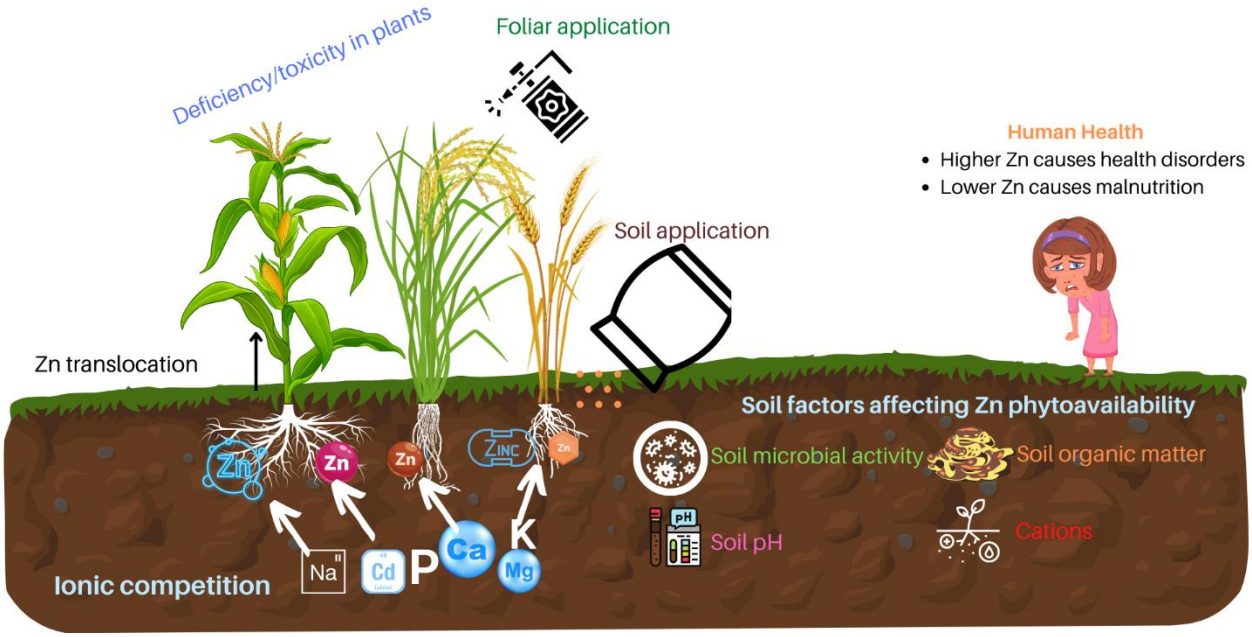

Figure 8:Zinc cycling in soil and its role in plants and humans

From the above discussion, it is clear that Zn is highly important for plant functioning. On the other hand, higher concentrations of Zn can also cause Zn toxicity in plants. In a healthy plant, the optimum level of Zn is 20-60 mg/kg of dry weight (DW) (de Almeida et al., 2020). The higher Zn levels may lead to a reduction in enzyme activity, reduced growth, and damage to pigment contents (Yusefi-Tanha et al., 2020; Sidhu et al., 2020; Bankaji et al., 2019). At toxic levels, Zn competes with Mg and reduced the activity of Rubisco, ultimately reducing photosynthetic activity (Mateos-Naranjo et al., 2018). Furthermore, the excessive presence of Zn replaces the Mn in the thylakoid membrane (Scmidt and Husted, 2019) and lowers the PS II efficiency. On the other hand, the toxicity of Zn also leads to the deficiency of other nutrients such as P, Mg, and Fe (Chakreborty and Mishra, 2020).

2.5.2. Humans

For reproduction and proper growth human body also need Zn in an adequate amount (Figure 8). Similar to plants Zn is also involved in the enzyme activities in the human body (Nriagu, 2019). Zn is also involved in cell division, DNA synthesis, immune function, protein synthesis, and wound healing (Nriagu, 2019). Zn deficiency is affecting about 1/3rd of the population of the world. The lower concentration of Zn in edible plant parts can aggravate Zn deficiency in humans (Sharma et al., 2013). Crop cultivation on soil with Zn deficiency can lead to Zn malnutrition in humans (Zia et al., 2020). Even though the daily intake requirement is not much clear, as a reference it is recommended about

4-17 mg for children and 15 mg for adults on daily basis (Natasha et al., 2022). Despite being an essential nutrient for humans the daily intake should not surpass 40 mg for adults. The toxicity of Zn can lead to headaches, poor appetite, nausea, vomiting, and diarrhea (Nriagu, 2019). Furthermore, the impairment of immune response can be caused by Zn toxicity. The plant parts with higher Zn levels can cause Zn toxicity in humans. The compartmentalization of Zn in different plant parts controls the health hazard linked with Zn.

2.6. ZnO NPs as a fertilizer

The demand for a higher food supply is increasing day by day to overcome global hunger. To meet crop growth challenges, chemical synthetic fertilizers are the first choice (Feregrino-Perez et al., 2018). However, the applied amount of nutrients is hardly utilized by the crops and the excessive nutrients leached into the groundwater and lead to environmental pollution (Liu and Lal, 2015). The repeated application of such nutrients worsened the nutrient loss problem and reduced the utilization efficiency of fertilizers. To overcome this problem, it is necessary to formulate slow-release high-efficiency fertilizers (NDABA et al., 2022). The nano-sized materials which help in plant growth promotion are known as nano-fertilizers. It is proved by previous studies that the application of metallic NPs increased crop growth (Shang et al., 2019; Raliya et al., 2015). Based on the novel properties that NPs possess such as slow-release ability, higher surface-to-volume ratio, adsorption characteristics, and higher reactivity they can be considered a useful material for fertilization (Zulfiqar et al., 2019; Tapan et al., 2010).

Zn is an important micronutrient for plant growth and development as explained in the above section. The efficiency of conventional Zn fertilizers such as $ZnSO_4$, ZnO, and others is very low due to several factors. Soil factors are the major contributor to the reduced efficiency of conventional Zn fertilizers such as soil pH, organic matter, $CaCO_3$, and the nutrients like P. According to the literature, the use of ZnO NPs as a fertilizer significantly improved the plant growth, development, yield, and utilization efficiency of Zn. Khalid et al. (2022) conducted a study to evaluate the effect of Zn nano-fertilizer on the growth and development of *Caesalpinia bonducella* as compared to conventional Zn fertilizer. The Zn was applied at a concentration of 25,50,75 and 100 ppm. The results showed that the morphological parameters and chlorophyll contents of the plants were improved by 50-93% and 30-80% by nano-fertilizers as compared to conventional fertilizers which showed an improvement of 28-50% and 5-28% respectively. In another study, Yang et al. (2021) evaluated the effect of ZnO NPs on rice yield, productivity, and Zn biofortification as compared to conventional $ZnSO_4$. Both sources were applied at two concentrations (25 and 100 mg/kg) and at three different stages of the rice crop

(basal stage, tillering, and panicle stage). The results showed that the application of ZnO NPs significantly improved the yield-related parameters such as a 3.8-10% increased number of panicles, a 2.2-4.7% increase in spikelet per panicle, and a 6.8-7.6% increase in biomass production. Most importantly it was reported that the ZnO NPs increased the grain Zn concentration up to 13.5-39.4%. In another report, Almendros et al. (2022) evaluated the Zn biofortification potential of ZnO NPs in cherry tomatoes. The ZnO NPs were applied in two soils, one with low pH (5.5) and the other with pH (8.5). Results reported that the application of ZnO NPs increased the concentration of boron and decreased the concentration of Mn and Cu in fruits. While it was noted that the Zn concentration in tomato fruit ranged from 2.5-3.5 mg/kg in high-pH soil and 4.5-4.8 mg/kg in low-pH soil. Similarly, Prakash et al. (2022) reported that the application of ZnO NPs @25 µM in rice grown under chromium toxicity improved the growth and development and reduce the toxicity of chromium. They reported that ZnO NPs increased the activity of DHAR, APX, GR, and MDHAR. It also reduced the H_2O_2 and SOR levels. Furthermore, Azam et al. (2022) evaluated the impact of soil and foliar-applied ZnO NPs on maize. ZnO NPs were applied at different concentrations such as 40, 80, 120, and 160 mg/kg. The results showed that the plant growth, antioxidant activity, and photosynthetic pigments were increased by 61%, 49.25%, and 51.8% respectively by soil application and with the foliar application, 59.28%, 52.91%, and 48.19% increase was reported respectively as compared to control.

Many studies are reporting the beneficial effects of ZnO NPs in different crops regarding yield, growth, and grain Zn improvement Such as in Pea and beet (Garcia-Gomez et al., 2018), green gram (Sahoo et al., 2021), Rice and mung bean (Cyriac et al., 2020), wheat (Rai-Kalal et al., 2021) and many more (Table 2).

Table 2: Use of ZnO NPs as a fertilizer and its role in plant growth and Zn biofortification

Size of NPs	**Application method**	**Crop**	**Results**	**References**
65-80 nm	Soil application	Fenugreek	Increased seed germination and plant growth	Shaik et al., 2020
11 nm	Coating of seed	Indian mustard	Seed germination increased with a 20 µg/mL concentration	Mazumder et al., 2020
11.9 nm	Seed priming	Maize	Increased the protein contents	Sabir et al., 2020
20 ± 5 nm	Foliar application	Wheat	Increased grain Zn contents	Zhang et al., 2017b
≤ 30 nm	Foliar	Saffron	Increased flower yield	Rostami et al., 2019

18 nm	Foliar and soil	Sorghum	Increased yield and translocation of Zn, N, and K in grain	Dimkpa et al., 2017
10-30 nm	Suspension application	Lemon balm	Increased accumulation of K, Zn, and Fe	Babajani et al., 2019
22.4 ± 1.8	Foliar	Mung bean	Increased stem and root length and increased chlorophyll and protein content	Raliya et al., 2016
20-30 nm	Foliar	Wheat	Increased growth and yield. Decrease Cd uptake	Hussain et al., 2018
≤ 20 nm	Foliar	Foxtail millet	Increased N and oil contents in grain	Kolencik et al., 2019
21.3 nm	Seed soaking	Lupine	Increased growth and reduce the effect of salinity	Abdel Latif et al., 2017
18 nm	Powder application	Winter wheat	Reduced the drought stress	Dimkpa et al., 2020
Not given	Foliar	Tomato	Reduced the salt stress, increased the protein contents, and increased the activity of antioxidant enzymes	Faizan et al., 2021
30 nm	Foliar	Rice	Increased yield, grain accumulation of Zn and NPK	Yang et al., 2021
30 nm	Soil	Sweet sorghum	Increased growth, and yield and reduced the Cd stress and uptake	Wang et al., 2018b
9 nm	Seedling treatment	Maize	NPs transformed into Zn^{+2} in the plant body after the entrance	Lv et al., 2021
30-70 nm	Foliar and Soil	Maize	Increased the growth yield and grain Zn contents	Umar et al., 2021
20 nm	Foliar	Wheat	Increased Zn accumulation in the endosperm	Sun et al., 2020a
20-50 nm	Soil	Rice	Increased growth yield, dry matter, and Zn accumulation	Zhang et al., 2021a
17.3 nm	Foliar	Lentil	Increased 1000 seed weight, no. of seeds per pod	Kolencik et al., 2022

2.7. Bentonite clay as a nutrient carrier

Clay minerals are naturally occurring materials and have the potential to be used in several ways (Ruiz-Hitzky et al., 2019). There are different clay minerals such as kaolinite, chlorite, brucite, illite,

montmorillonite, sepiolite, zeolite, and bentonite (Zhang et al., 2022). Bentonite comes under the category of smectite clays, and these are most often used in industrial adsorption processes (Almahri, 2022). A huge number of negative charges are present in the octahedral and tetrahedral layers of bentonite (Khan and Ajlouni, 2020; Kantesaria and Sharma, 2020). The characteristics of bentonite such as high CEC, high specific surface area, higher swelling ability, cost-effectiveness, easy availability, and non-toxic behavior make it an ideal adsorptive material (Shokouh et al., 2019). Montmorillonite is the main part of bentonite composition and most of the ideal characteristics are due to the presence of montmorillonite. Montmorillonite shows higher adsorption and desorption potential for polar and ionic compounds (Peng et al., 2020). Based on the above-explained characteristics bentonite can be used as a nutrient carrier and can be applied as a slow-release fertilizer in the agriculture sector.

Liu et al. (2021) conducted a study to evaluate the effect of bentonite on the growth of *V. spiralis* and the results showed that the application of bentonite in a ratio of 1:1(bentonite: sediments) improved the growth of *V. spiralis* by 18.78%. The authors explained that this improvement in growth could be due to the release of nutrients from bentonite. Recently, we used nano-bentonite fortified with Zn as a coating material on urea and the results showed that nano-bentonite released a significantly higher amount of Zn, and the release pattern was notably slow as compared to conventional Zn fertilizers (Umar et al., 2022). In another study, El-Nagar and Sary (2021), used micro-bentonite and nano-bentonite to evaluate their effect on soil properties and plant growth. They applied micro-bentonite at the rate of 5, 10 tons/ha and nano-bentonite at the rate of 250 and 500 kg/ha. The results showed that the application of nano-bentonite at 500 kg/ha significantly increase the water holding capacity and available water. They also stated that it also increased the biological and grain yield of wheat. In another report, Chu et al. (2020) reported that the application of bentonite hydrochar in rice crops significantly improved the NUE and reduced the NH3 emission. Furthermore, Iskander et al. (2011) evaluated the adsorption potential of zeolite and bentonite for Zn and Mn, and they reported that bentonite adsorb a significantly higher amount of Zn and Mn as compared to zeolite. Apart from the cations, bentonite can also be used as a carrier for microorganisms. In a study conducted by He et al. (2015), they encapsulated *Raoultella planticola* RS-2 in a composite of Na-bentonite and alginate. It was reported that the biofertilizer was released slowly from the capsules significantly. There are several other studies in which bentonite is used as an efficient slow-release carrier for drugs in the medical industry.

3. MATERIALS AND METHODS

3.1. Soil sampling

Soil samples were collected from two sites (Figure 9). The first site was Atkár, located in the north of Hungary in the Gyöngyös district (47°42'24.5"N 19°54'35.6"E). It lies between the right bank of the river Tisza and the Mátra and Bükk mountains. The average rainfall in the area is about 40.75 mm with the highest rainfall in June (76 mm) and the driest month in October (26 mm). The average high temperature in the region is 15.43 °C with the warmest month being August (28.3 °C) and the average low temperature in the region is 6.8 °C with the coolest month being January (-3.5 °C). The reference soil group in the region is vertisols with high clay contents and shrinking and swelling characteristics (WRB, 2014).

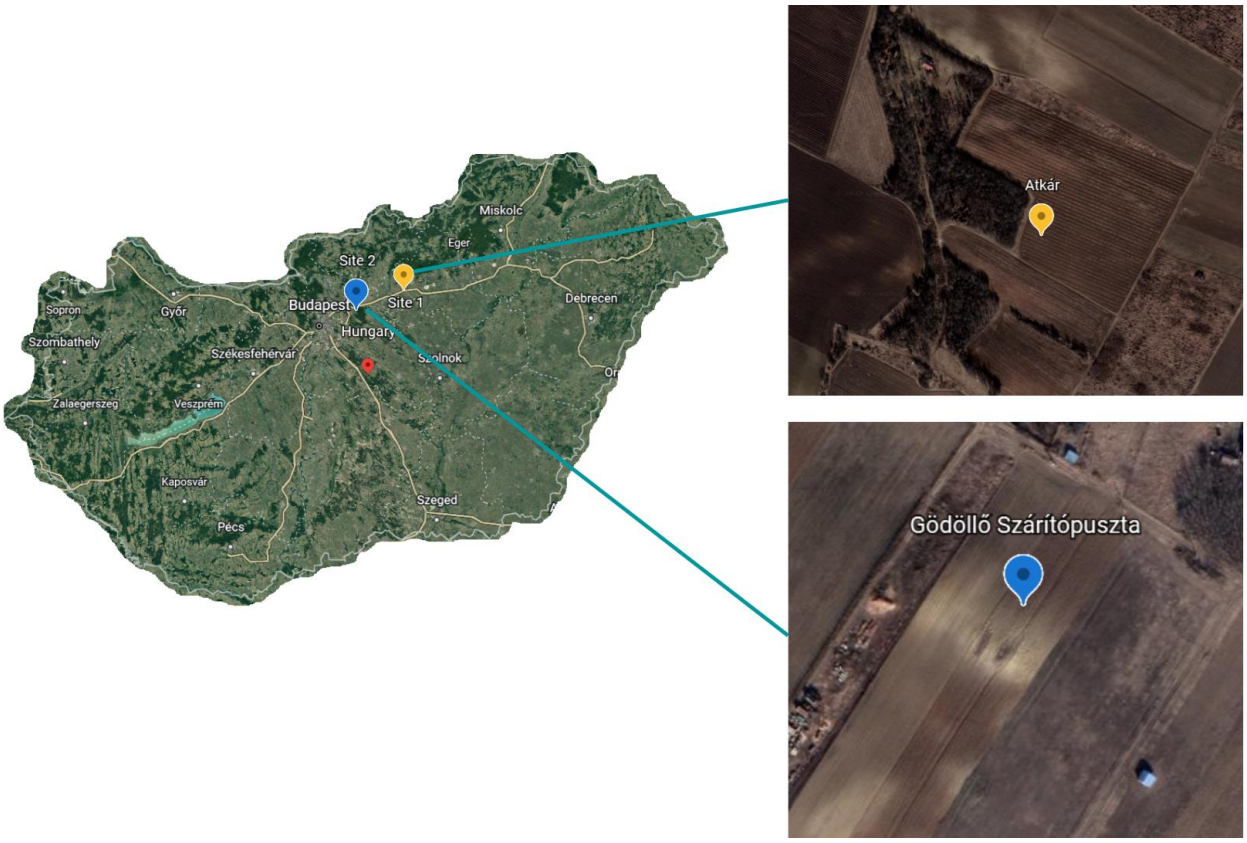

Figure 9:Sampling site description

The second sampling site was Gödöllő Szárítópuszta located in the central part of Hungary in Pest county (47°34'41.8"N 19°24'11.6"E). The average elevation of the region is 207 m from the sea level. The average rainfall in the area is about 28.25 mm with the highest rainfall in May (39 mm) and the driest month being September (17 mm). The average high temperature in the region is 15.87 °C with the warmest month being August (28.8 °C) and the average low temperature in the region is 7.71 °C

with the coolest month being January (-2.7 °C). The Physico-chemical characteristics of both soils are given below in Table 3.

Table 3: Physico-chemical characteristics of sandy loam and silty clay soils

Elements	Silty clay	Sandy loam	Units
pH	8.80	7.10	----
EC	0.095	0.0634	dS/m
CEC	40.1	14.6	$cmol^+/kg$
Exch. Ca	26.75	----	$cmol^+/kg$
$CaCO_3$	----	7.76	%
OM	3.67	1.36	%
Sand	3	65	%
Silt	45.05	25	%
Clay	51.95	10	%
Textural class	Silty Clay	Sandy loam	----
P	23.75	170	$mg\ kg^{-1}$
Zn	3.16	2.85	$mg\ kg^{-1}$

3.2. Chemicals and materials used

All the chemicals used in the study were of analytical grade. $ZnSO_4.7H_2O$, Urea (46% N), potassium hydroxide (KOH), ethylene diamine tetraacetic acid (EDTA 99.9%), and ethanol (96%) were bought from REANAL laboratory chemicals in Budapest, Hungary. Nano-bentonite was obtained from Bentonite-KFT Budapest, Hungary. Hydrochloric acid (HCl), calcium hydroxide ($Ca(OH)_2$), and nitric acid (HNO_3) were obtained from Molar chemicals in Budapest, Hungary.

3.3. Preparation of ZnO NPs

A method presented by He et al. (2019) was adopted with modifications for the preparation of ZnO NPs (Figure 10). KOH and $ZnSO_4$ were used as a precipitating agent and Zn source respectively. Equal concentration (0.2 M) solutions were prepared of KOH and $ZnSO_4$ in 200 mL beakers. In the

next step, the KOH solution was added to a 500 mL beaker and the beaker was placed on a magnetic stirrer. The solution of $ZnSO_4$ was added dropwise in KOH solution using a burette during vigorous stirring. The shaking was continued for 3 hours after the complete mixing of the $ZnSO_4$ solution in the KOH solution. After stirring the suspension was left for settling. The filtration was carried out using filter paper followed by washing of precipitates using distilled water and in the end with ethanol to remove all the impurities. The washed precipitates were then dried in an oven at 80 °C until the moisture was removed completely. The dried precipitates were ground into powder form using mortar and pastels. The ground powder was calcined in the furnace for 2 hours at 250 °C. The calcined powder was ground again into a fine powder and stored in an airtight box for further use and characterization.

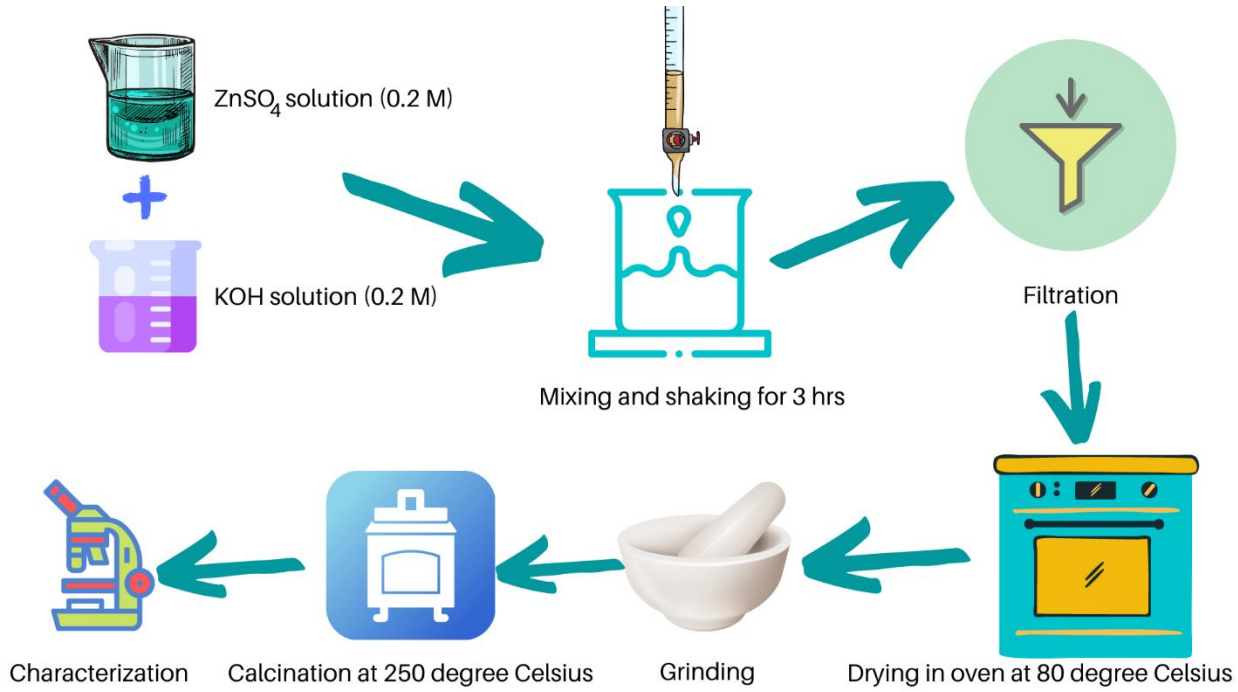

Figure 10:Basic steps in preparation of ZnO NPs by precipitation method

3.4. Evaluation of Zn adsorption properties of nano-bentonite

The batch adsorption method was used to evaluate the Zn sorption characteristics of nano-bentonite. $ZnSO_4.7H_2O$ was used to prepare Zn solutions of different concentrations (0-640 ppm with a difference of 40 ppm). Briefly, 1g of nano-bentonite was taken in 50 mL centrifuge tubes and 40 mL of Zn solution of different concentrations was added to the tubes. The tubes were then shaken on a rotary shaker for 2 hours followed by centrifugation at 5000 rpm for 20 minutes. The supernatant was then filtered using Whatman No.42 filter paper (0.25 µm). The filtrate was analyzed on atomic absorption spectrophotometer (AAS) (PERKIN-ELMER, 303, USA) at 213.9 nm wavelength with a

slit width of 1.0 nm for Zn concentration. Standard reference material was used to calibrate the instrument. The Zn adsorption potential of nano-bentonite was evaluated by fitting different adsorption isotherms such as the Langmuir model, the Freundlich model, and the newly developed model for multilayer adsorption. The following equation was used to calculate the Zn adsorption on nano-bentonite:

Equation 1

$$q_e = (C_i - C_e)\, {}^{v}/_{m}$$

In the above equation C_i represents the initial concentration, C_e is the equilibrium concentration, v is the volume, m is the mass of nano-bentonite taken and q_e is the adsorbed amount of Zn.

The non-linear form of the Langmuir model was fitted (Langmuir, 1916). The model equation is given below:

Equation 2

$$q_e = q_{max} K_L\, C_e / 1 + K_L C_e$$

In this equation, q_e is the adsorption amount of Zn, q_{max} and K_L are Langmuir constants. The Freundlich model was used to evaluate the multilayer adsorption of Zn onto nano-bentonite (Freundlich, 1907). The Freundlich model was based on the following equation:

Equation 3

$$q_e = K_F C_e^n$$

In the above equation q_e and n are known as empirical constants and represent the adsorption capacity and adsorption intensity respectively. To further understand the multilayer adsorption of Zn on nano-bentonite a newly developed model based on the Sips and Gapon equation was used. The new model was recently developed by Czinkota et al. (2021). The model equation is given below:

Equation 4

$$Q = \sum_{i=1}^{s} \left(\frac{\left(A_i \times K_i \times C_i^{ni}\right)}{1 + K_i \times C_i^{ni}} \right)$$

Where s is the isotherm steps, A_i is the adsorption capacity, n_i is the n values and the K_i is the equilibrium constant.

3.5. Preparation of Zn-fortified nano-bentonite

For the fortification of nano-bentonite with Zn, a method presented by Yuvaraj and Subramanian (2018) was adopted with slight modifications (Figure 11). A Zn solution was prepared in a 250 mL beaker by dissolving 30 g $ZnSO_4.7H_2O$. In another 250 mL, beaker nano-bentonite was homogenized using distilled water. The Zn solution and the homogenized nano-bentonite were then transferred to a 500 mL beaker and the walls of the other two beakers were rinsed with distilled water. The material of both beakers was mixed in a 500 mL beaker and a 1-2 cm layer of distilled water was maintained on the surface. The sonication of the mixture was carried out for 3 hours in a sonication bath. After sonication, the extra solution was removed with the help of a vacuum pump. The remaining clay was dried in an oven at 35 ℃ until all the moisture was lost. The dried clay was ground into powder form and stored in an airtight container for further use and characterization. The composition of Zn-fortified nano-bentonite is given in Table 4.

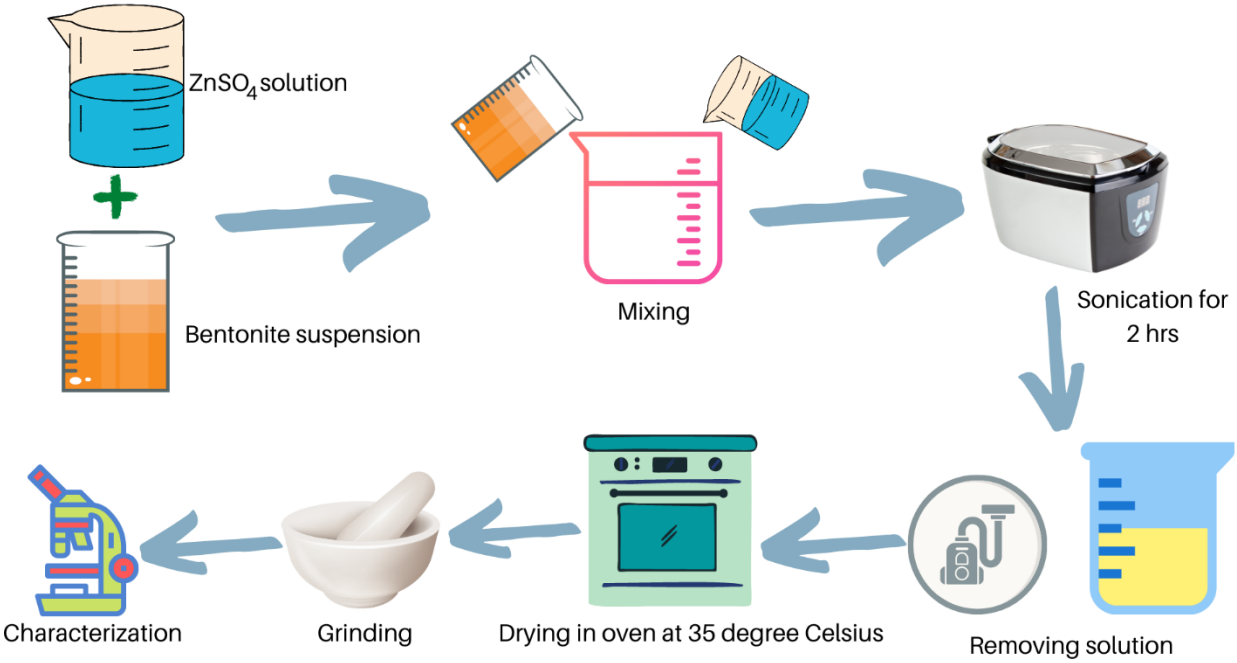

Figure 11:Steps involved in the Zn fortification process of nano-bentonite

3.6. Preparation of Zn-coated slow-release urea

The slow-release urea was prepared using two methods. In the first method, urea was coated with stearic acid, paraffin wax, and Zn-fortified nano-bentonite (or) ZnO NPs (Figure 12). The process was as follows, in the first step approximately 9 g of stearic acid was melted in a wide-mouth glass bottle and then the botel was let to cool down till ~50 ℃, and then 50 g of urea and 3 g of Ca $(OH)_2$ was

added and mixed until the free-flowing granules were obtained. The stearic acid-coated urea granules were left for 24 hours and then coated with paraffin wax. For paraffin wax coating 3g of wax was melted and mixed with urea along with Ca $(OH)_2$. In the last step Zn-fortified, nano-bentonite/ZnO NPs were coated on stearic acid+paraffin wax-coated urea granules by using paraffin oil as a binding material. Approximately 2 g of Zn-fortified nano-bentonite or 1 g of ZnO NPs were used for the coating on 50 g of urea granules making it a coating of 4% Zn-fortified nano-bentonite and 2% ZnO NPs. In the end, the bottle consisting of coated granules was placed on a rotating shaker for 2 hours. The coated granules were then dried in a vacuum dryer for 48 hours.

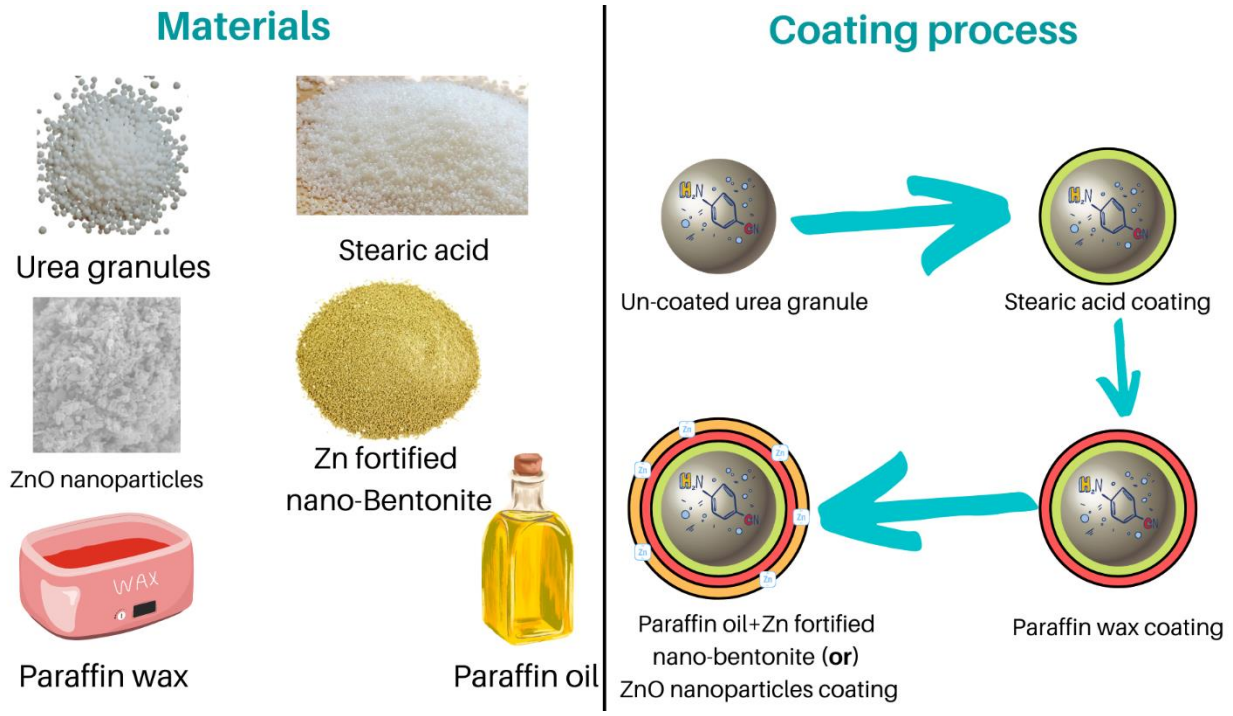

Figure 12:Required materials and the process of coating urea

The second coating method was adopted by Dimkpa et al. (2020a) with slight modifications. In this method, 50 g of urea granules were mixed with approximately 1 mL of vegetable oil. After that 2 g of Zn fortified nano-bentonite (or) 1 g of ZnO NPs were mixed with urea granules along with 3 g Ca $(OH)_2$ and mixed properly and placed on a rotating shaker for 2 hours until the free-flowing granules were obtained.

Table 4: Composition of Zn fortified nano-bentonite, Zn fortified nano-bentonite coated urea and ZnO NPs coated urea

Elements	Zn fortified nano-bentonite	Zn-fortified nano-bentonite-coated urea	ZnO NPs coated urea

Zn	24.97%	1.03%	2.1%
S	17.09%	0.18%	0.57%
Si	12.67%	0.44%	0.75%
Al	4.05%	0.23%	0.27%
K	1.045%	---	0.05%
Fe	0.56%	0.05%	0.096%
P	190 ppm	---	---
Cu	70 ppm	---	---
Co	58 ppm	---	---
Mn	101 ppm	---	---
Ca	---	0.7%	0.82%
N	---	42.3%	41.8%

3.7. Characterization

3.7.1. Characterization of ZnO NPs, Zn fortified nano-bentonite, and Coated urea

Analysis for the characterization of ZnO NPs, nano-bentonite, and the coated urea granules was performed in the Department of Mineralogy, Geochemistry, and Petrology at the University of Szeged (http://www.asvanytan.hu/language/en). X-ray powder diffraction technique was used to determine the size of the crystals of ZnO NPs and nano-bentonite. For this purpose, an X-ray diffractometer (Rigaku Ultima IV) was used which was equipped with Bragg-Brentano geometry, CuKα radiation, graphite monochromator, proportional counter, divergence, and detector slits of 2/3° were used to measure the samples. The specimens were scanned at 50 kV/40 mA from 3 to 80° 2θ with a goniometer step rate of 1°/min and data acquisition steps of 0.02°. Instrumental line broadening was determined by using an in-house silicon standard. The sharpest reflection measured for these bulk powder samples was 0.100° and the narrowest FWHM value measured on the silicon standard was 0.040°. Match! 3 software was used to evaluate the XRPD spectra.

The above-mentioned software evaluates the crystallite size based on the Scherrer equation given as follows:

Equation 5

$$L = \frac{K\lambda}{\beta cos\Theta}$$

where K is a constant (Scherrer constant) which generally takes a value of 0.89–0.94 depending on the function used to fit the given peak, L is the main crystallite dimension (in Ångström or nanometer) along a line normal to the reflecting plane, β is the width of a peak at half-height expressed in radians of 2Θ (the Bragg angle) and λ is the applied wavelength.

The external standard method was used to correct the peak width to obtain higher accuracy in measuring crystallite size value. In that method, Standard and test samples were measured separately. The width of test sample peaks was corrected by calculating the full width at half the maximum correction curve using the measured standard sample peak width as the instrumental broadening.

Scanning electron microscopy (SEM) was used to examine the morphology of nano-bentonite clay, ZnO NPs, and coated urea granules (HITACHI S-4700 Field emission-SEM). Before analysis, the samples were prepared in an ion-sputtering device and urea grains were coated with Au-Pd. The nutrient composition of coated urea granules was determined using X-ray fluorescence (XRF) (IP55 VENTATM, C series). The XRF was performed using a silicon drift detector and a 40 kV X-ray tube with tungsten or rhodium anode.

3.8. Evaluation of the N and Zn release characteristics from slow-release Zn-coated urea

Nitrogen and Zn release characteristics from slow-release Zn-coated urea was evaluated through an incubation experiment. The experiment was set up using sandy loam soil. The soil's Physico-chemical characteristics are given in Table 3. Briefly, 50 g of soil was weighed in 150 mL plastic cups. The equal size (2 mm) urea granules (0.5 g) coated with Zn-fortified nano-bentonite and ZnO NPs were placed in the cups below a 5 cm layer of soil. The urea granules without coating were used as a control treatment. Treatments were applied following a completely randomized design (CRD). The soil was moistened using distilled water and the moisture contents were maintained at 60% of the field capacity throughout the experiment. After applying the water, the weight of the cups was noted, and the moisture was maintained by weighing the pots every second day. To minimize the soil disturbance and to make the sampling process easy separate cups were used for each time sampling. The samples were collected every 5th day (0, 5, 10, 15, 20, 25, and 30 days). During the sampling process, the undissolved urea granules were removed carefully with the help of a spatula, and the remaining soil was mixed thoroughly and used for further analysis.

3.8.1. Extraction of Zn from the soil

To extract the released amount of Zn from the soil, the extraction method was used. 0.05 M EDTA was used as an extractant. Briefly, 5 g of soil was extracted with 40 mL of 0.05M EDTA. The suspension was shaken for 2 hours followed by centrifugation for 15 min at 5000 rpm. The centrifuged samples were filtered using Whatman No. 42 filter paper. The filtrate was analyzed for Zn on AAS. The Zn concentration obtained from blank samples was subtracted from the treated soil Zn concentration.

3.8.2. Analyzing N contents in soil

Soil extraction by using 2M KCl was carried out to evaluate the released N in the soil. 10 g of soil was extracted by using 20 mL of 2 M KCl. The shaking was carried out for 1 hour followed by centrifugation for 15 min at 5000 rpm. The samples were then filtered using Whatman No. 42 filter paper. The filtrate was stored at 4 °C before analysis. GALLERY automated analyzer was used to analyze N contents in extractants. The values from blank samples were subtracted from the treatment samples. Based on the previous studies the treatments which released about 80% of the N were considered as completely released (Ellison et al., 2013; Ransom et al., 2020).

3.9. Release kinetics of N and Zn

Release kinetics of N and Zn from slow-release Zn-coated urea were evaluated by using kinetic models such as the Higuchi model and the Korsmeyer Peppas model. The Higuchi model was based on the following equation:

Equation 6

$$f_1 = M_t = K_H\sqrt{t}$$

In this equation, K_H represents the Higuchi constant.

It is assumed that the diffusion region of the planer system was under a “pseudo steady state” (Higuchi, 1961; Eghbali Babadi et al., 2021).

The Korsmeyer Peppas model used was based on the following equation:

Equation 7

$$M_i/M_\infty = kt^n$$

Where, k is the rate constant and M_t/M_∞ is the N or Zn released fraction at time t.

It was stated that the Higuchi model best explains the release kinetics of chemicals from water-soluble coated materials (Higuchi, 1961). For the Korsmeyer-Peppas model, it was stated that best described the release kinetics of chemicals where there was more than one release mechanism involved (Ritger and Peppas, 1987; Korsmeyer et el., 1983).

3.10. Effect of NPs size, soil types, and incubation time on the solubility of ZnO NPs

Evaluation of solubility of ZnO NPs under different soil conditions using different size NPs incubated for different periods was carried out through an incubation experiment. Two types of soils (Silty clay and Sandy loam) sampled from different locations in Hungary were used in this experiment.

3.10.1. Soil spiking with ZnO NPs and $ZnSO_4$

Approximately, 200 g of air-dried soil was weighed in plastic pots. ZnO NPs of two sizes (small size and large size) were used. ZnO NPs were added in the form of suspension at a concentration of 500 mg L^{-1}. While the $ZnSO_4$ was added in the form of a solution at the same concentration. 30 mL volume of suspension and solution was added to each pot. The experiment was replicated thrice. The CRD-factorial design was followed. The suspension of NPs was prepared by sonicating the required amount of ZnO NPs in distilled water for 10 min using a sonication bath. The added amount of suspension and solution were mixed completely with the soil using a spatula. After mixing the weight of every pot was noted and the moisture contents were maintained at 80% of the field capacity. The moisture loss was compensated every second day by adding distilled water. The aluminum foil was used to cover the samples with perforation to allow air exchange. The incubation was carried out for 7 days and 14 days. The soil samples without Zn spiking were used as a control treatment. At the end of the incubation period, soil samples were crushed and homogenized for leaching.

3.10.2. Leaching of the soil

To evaluate the solubility of ZnO NPs and $ZnSO_4$ in water, column leaching of the soil was carried out. For this purpose isocratic pump (ECOM, KAPPA 10, Czech Republic) attached to a steel, the column was used. The specifications of the column were as follows: the volume of the column was 91 mL, the width was 2.2 cm and the length of the column was 24 cm. The setup of the leaching system is given in Figure 13.

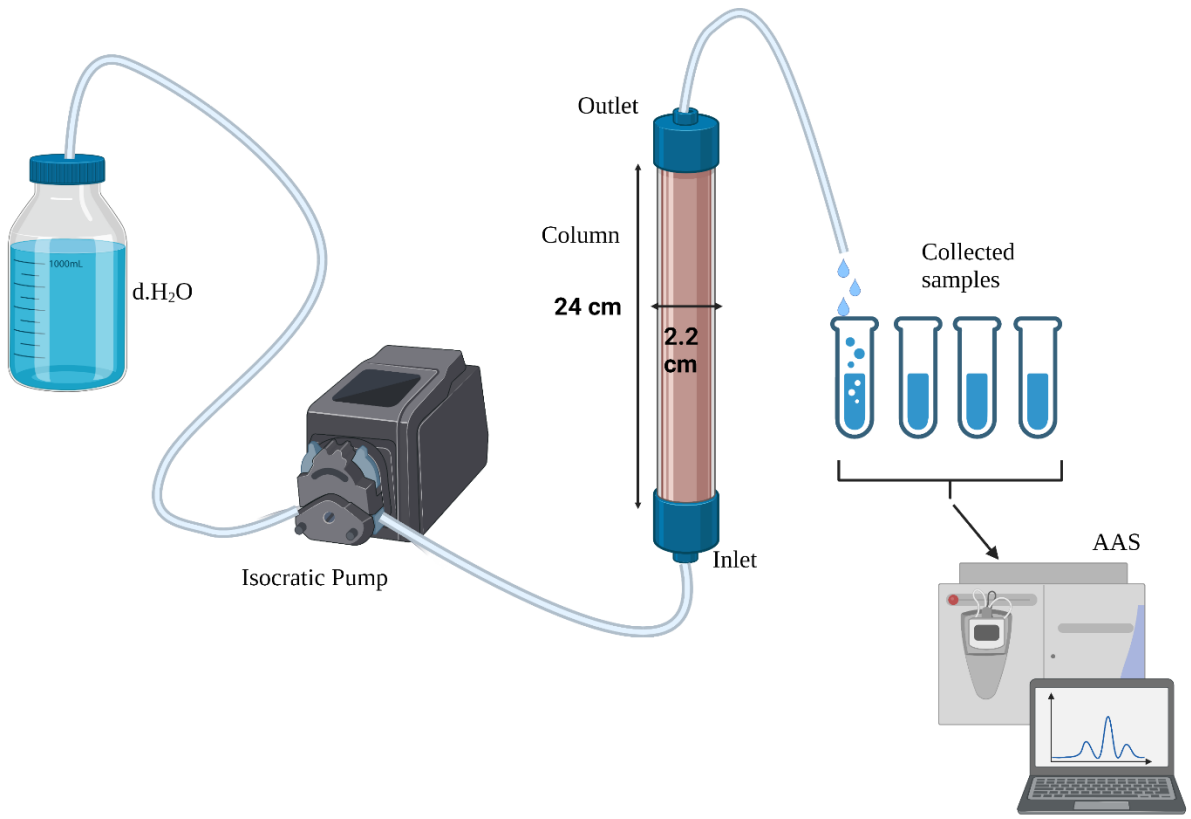

Figure 13: Instrumentation and leaching process of incubated soil

The eluent volume for leaching was pre-optimized. To perform the leaching the column was filled with Zn-spiked soil and the upper and bottom caps were tightened. The upper cap of the column includes an inbuilt filter and both sides of the column also contain the spacer. The flow rate of the water was set at 1 mL per minute and the water was pumped from the bottom of the column to achieve the full saturation of the soil. The elute was collected from the upper part of the column and in each cycle, 5 mL of the volume was collected and around 40 mL of total elute was collected for each sample. The collected elute was centrifuged for 35 min at 5000 rpm at room temperature for the separation of leached ZnO NPs. The samples were filtered using 0.20 µm syringe filters and a few drops of concentrated HNO_3 were added to each sample. The samples were then analyzed for Zn concentration on AAS. The leaching was repeated three times per treatment.

3.10.3. Zn extraction from the soil matrix

After the leaching of the soil, the retained Zn on the soil matrix was extracted by using 0.05 M EDTA. A weight-to-volume ratio of 1:10 was followed during extraction (Cruz et al., 2021). Briefly, 3g of soil was weighed in a 50 mL centrifuge tube and 30 mL of 0.05 M EDTA solution was added to it.

The mixture was shaken for 2 hours followed by centrifugation for 10 min at 5000 rpm. The samples were then filtered using filter paper. The extraction was replicated thrice. The extractant was analyzed on AAS for Zn concentration.

3.11. Nitrous oxide emission potential of conventional and coated urea from unplanted soils

The nitrous oxide emission potential of uncoated and coated urea from unplanted soils was evaluated through a laboratory experiment. Two types of soil silty clay and sandy loam were used in this experiment. Open-ended plastic tubes were used to incubate the soil. The tubes contain the lids on both the lower and upper sides. The diameter, length, and volume of the tube were 10.2 cm, 15 cm, and 1225 cm^3 respectively. Approximately 2 kg of soil was used in each tube. The uncoated urea, Zn-fortified nano-bentonite coated urea, and ZnO NPs coated urea was applied at the rate of 250 kg N per ha. The fertilizer was completely mixed with the soil and the soil was then filled in the tubes. The soil without fertilizer was used as a control treatment. The tubes were arranged following a CRD-factorial design. The moisture contents in the soil were calculated. The added amount of water was calculated on a volumetric basis and the moisture contents already present in the soil were subtracted from the added amount of water. The water contents were calculated to achieve the 80% of the field capacity of the soils. After adding water, the weight of each tube was noted. The moisture contents were maintained by weighing the tubes on daily basis after flux measurement.

3.11.1. N_2O flux measurement

Nitrous oxide flux measurement was started right after adding water to the tubes. A nitrous oxide analyzer was used to measure the flux. The instrument worked on a principle of infrared correlation (NDIR). The flux measurement was carried out for 20 min for each sample. To calculate the flux the measurement data points were plotted using time on one axis and N_2O concentration on the other axis and a linear regression line was fitted to get the slope value. The N_2O emission flux (µg N m^{-2} hr^{-1}) was calculated using the following equation:

Equation 8

$$F = {\Delta N_2O \times 2 \times AN \times Vch \times f}/{Vm \times Ach \times t}$$

Where F is the flux, ΔN_2O is the slope of the N_2O mixing ratio during sampling, AN is the atomic weight of N, Vch is the chamber volume (m^3), f is the factor, Vm is the molar volume (L), Ach is the soil surface covered by the chamber, t is sampling time.

The cumulative N_2O emission (kg N ha^{-1} yr^{-1}) was calculated using the following equation:

Equation 9

$$T = \sum_{i=1}^{n}[(X_i + X_{i+1})/2 \times (t_{i+1} - t_i) \times 24 \times 365 \times 10000/1000000000]$$

Where, T is the cumulative N_2O emission (kg N ha^{-1} yr^{-1}), X is the daily average flux rate (µg N m^{-2} h^{-1}), i is the ith measurement, and $(t_{i+1}-t_i)$ is the days between two adjacent measurements.

The emission factor of N_2O was also calculated using the following equation:

Equation 10

$$EF = \left\{\frac{(Cumulative\ N_2O{-}N_{fert} - Cumulative\ N_2O{-}N_{control})}{Total\ N\ added}\right\} \times 100$$

Where, EF is the emission factor for N_2O (% of added N), $Cumulative\ N_2O\text{-}N_{fert}$ is the cumulative N_2O emission from fertilized treatment, and $Cumulative\ N_2O\text{-}N_{control}$ is the cumulative N_2O emission from unfertilized treatment.

3.12. Nitrous oxide emission potential of conventional and coated urea from planted soils

3.12.1. Soil sampling and preparation

The soils were sampled from two locations in Hungary as explained above. The sampled soil was brought to the laboratory on the same day. The soil was spread on a sheet for air drying. All the external materials such as plat residues, roots, and stones were removed. After drying the soil was ground by using a mechanical grinder equipped with a 2 mm sieve. After that, the pre-sowing Physico-chemical analysis of the soil was carried out.

3.12.2. Experimentation

The nitrous oxide emission potential of uncoated and coated urea from planted soils was evaluated through a laboratory experiment. Two types of soil silty clay and sandy loam were used in this experiment. Wheat was used as a test crop. The crop was planted in trapezoidal plastic pots. The dimensions of the pots were as follows: length 16 cm, width 15.5 cm, and volume 3968 cm^3. Around 6 kg of ground and sieved soil was added to each pot. A plastic tube chamber was placed in the center of the pot and two rows of the wheat crop were planted on both sides of the chamber. Nitrogen treatments were applied at the rate of 250 kg N per ha in two split doses. The first dose was applied at the time of sowing and the second dose of N fertilizers was applied at the 5th leave stage of the crop. The potassium (MOP) and phosphorus (Superphosphate) were applied at the time of sowing at a

recommended rate. The experiment was carried out following the Completely Randomized Design with factorial treatments. The soil moisture contents were maintained at 80% of the field capacity. The moisture loss was compensated by adding distilled water daily. Day and night conditions (12 hours) were maintained by using growing lamps (Mars Hydro, MH-150MA-41B, LG LED Solutions Ltd, China). The weeds were removed manually.

3.12.3. N_2O flux measurement

Nitrous oxide flux measurement was started right after adding water to the tubes. A nitrous oxide analyzer was used to measure the flux. The instrument worked on a principle of infrared correlation (NDIR). The flux measurement was carried out for 20 min for each sample. To calculate the flux the measurement data points were plotted using time on one axis and N_2O concentration on the other axis and a linear regression line was fitted to get the slope value. The N_2O emission flux (μg N m^{-2} hr^{-1}) was calculated using the following equation:

$$F = \Delta N_2O \times 2 \times AN \times Vch \times f \Big/ Vm \times Ach \times t$$

Where F is the flux, ΔN_2O is the slope of the N_2O mixing ratio during sampling, AN is the atomic weight of N, Vch is the chamber volume (m^3), f is the factor, Vm is the molar volume (L), Ach is the soil surface covered by the chamber, t is sampling time.

The cumulative N_2O emission (kg N ha^{-1} yr^{-1}) was calculated using the following equation:

$$T = \frac{\sum_{i=1}^{n}(X_i + X_{i+1})}{2(t_{i+1} - t_i)} \times 24 \times 360 \times \frac{10000}{1000000000}$$

Where, T is the cumulative N_2O emission (kg N ha^{-1} yr^{-1}), X is the daily average flux rate (μg N m^{-2} h^{-1}), i is the ith measurement, and $(t_{i+1}-t_i)$ is the days between two adjacent measurements.

The emission factor of N_2O was also calculated using the following equation:

$$EF = \left\{\frac{(Cumulative\ N_2O - N_{fert} - Cumulative\ N_2O - N_{control})}{Total\ N\ added}\right\} \times 100$$

Where, EF is the emission factor for N_2O (% of added N), $Cumulative\ N_2O\text{-}N_{fert}$ is the cumulative N_2O emission from fertilized treatment, and $Cumulative\ N_2O\text{-}N_{control}$ is the cumulative N_2O emission from unfertilized treatment.

3.12.4. Crop growth evaluation

For crop growth evaluation I measured the fresh and dry weight of the plants and chlorophyll contents at the end of the experiment.

The fresh weight of the plants was calculated after harvesting plants from the pots at the soil surface. For dry weight, the harvested plants were air-dried for one week and then placed in an oven at 65 °C until the constant weight was achieved. The dried plants were then used for the calculation of the oven-dry weight of the plants. In the end, the average of the fresh and dry weight was calculated.

To analyze the chlorophyll contents of the plants the fresh healthy leaves were collected and stored at -16°C. About 0.5 g of leave sample was taken in the form of discs from the middle part of the leaves. The sample was then ground using mortar and pestle in the presence of 1 mL 100% pure acetone and the mixture of $CaCO_3$ and sand to facilitate the grinding. The ground mixture was then poured into a 2 mL vial, the mortar was washed with the help of another 1 mL acetone and the volume of the vial was set at 2 mL. The vials were then transferred to the centrifuge machine. The centrifugation was done for 5 min. at 10000 rpm. Throughout this process, the temperature of the acetone used for grinding and the centrifuge machine was maintained at 4 °C. After centrifugation, the supernatant was analyzed on UV Visible Spectrophotometer at wavelengths 470, 520, 644.8, 661.6, and 750 nm. The chlorophyll a and b were calculated using the equations given below:

Equation 11

$$Chl\ a\ (\mu g/cm^2) = [11.24(A661.6) - 2.04(A644.8)] \times \frac{V}{W}$$

Equation 12

$$Chl\ b\ (\mu g/cm^2) = [20.13(A644.8) - 4.19(A661.6)] \times V/W$$

3.12.5. Nitrogen in soil and plant samples

To measure the total N contents in soil and plant samples CNS analyzer (Vario MAX cube, Germany) was used. The instrument was equipped with a thermal conductivity detector and an infrared detector for sulfur. The furnace temperature can reach a maximum of up to 1200 °C but in our analysis, we used a max temperature of up to 1140 °C. High-purity helium and oxygen were used as carrier gases. Sulfadiazine was used to standardize the instrument. The composition of sulfadiazine was 22.37% nitrogen, 47.99% carbon, and 12.81% sulfur. Before running the standard samples 3 blank samples were set for cleaning the instrument path. For plant sample analysis, 120-140 mg of dried and ground plant samples were weighed in ceramic boats. The samples were placed in the autosampler plate for

analysis. During plant sample analysis the oxygen flow was maintained at 200 mL/min and the oxygen dose time was set at 60 seconds.

For soil samples analysis we used two different operating conditions because we had soil samples from two different locations and both soils have different characteristics. For the analysis of sandy loam soil, we used the oxygen flow rate of 80 mL/min and the oxygen flow time was maintained at 120 seconds. While in the case of silty clay soil we used the oxygen flow rate of 100 mL/min with a flow time of 120 seconds. The process of instrument standardization was the same as that used in plant sample analysis. The soil sample weight used was in the range of 0.8-1.0 g.

3.12.6. Zn concentration in plant samples

For analyzing Zn contents in plant samples, the plants were dried and ground into a fine homogenous powder. The powdered samples were then digested using a microwave digester (CEM MARS 6, USA). About 0.5 g of plant samples were weighed and put into the washed and clean Teflon tubes directly to the base of the tube. After that 5 mL of concentrated HNO_3 was added into the tubes and gently swirled to mix the plant material with the acid and kept for a while. Then 2 mL of H_2O_2 30% was added to the tubes and mixed with the contents. In the end, the walls of the tubes were washed with a small amount of Milli Q water. The caps of the tubes were placed and locked with the key. The tubes were then placed inside the microwave digester and the program was started. The ramping time was 18 minutes to reach the temperature of 160 °C. Then the standby time was 38 min and then the cooling cycle was started. After cooling down the tubes were removed from the digester and the caps were opened and a small amount of Milli Q water was added to stop the fumes. The digested samples were then filtered in 25 mL volumetric flasks and the final volume was made by using Milli Q water. The filtrate was analyzed on AAS for Zn contents.

3.12.7. Zn concentration in soil samples

To evaluate the bioavailable concentration of Zn in the soil, about 2 g of air-dried, ground, and sieved soil samples were taken in the 50 mL centrifuge tubes and 20 mL of 0.05 M EDTA solution was added in each tube. The samples were shaken for 5 hours followed by centrifugation at 5000 rpm for 10 minutes and then filtration. The filtered solutions were then analyzed on atomic absorption spectrophotometer for Zn concentration. The instrument was calibrated using Zn standards before analysis.

3.13. Methods of Data Analysis

To achieve the stated objectives, the appropriate data was analyzed using different statistical methods. The data from different experiments were recorded and stored in *Microsoft Excel* sheets. For further analysis, *R programming* was used. Before using any statistical method on the data, the pre-processing of the data was carried out using *R studio* as an IDE for R programming. The packages used for data pre-processing/wrangling were *Tidyverse, Tidyr, and dplyr*. First, the outlier and missing values were handled using the appropriate techniques. The interquartile range method was used to remove the outlier values (Vinutha et al., 2018). In the next step, data distribution was evaluated (normal or not normal), where possible the data was normalized otherwise the statistical tests were implied based on the data distribution. For the comparison of the means of more than two variables and a higher number of factors, appropriate forms of ANOVA (one-way, two-way, or multifactor-ANOVA) were used (Kim, 2014). *TukeyHSD* function of base R was used for mean comparison and *lm* function was implied for linear model fitting. To compare the one or two means, *t-test* was used for normal distributed data (Kim and Park, 2019), and *Wilcoxon test* was used for non-normal distributed data (Wadgave, 2019). The *multcompview* package was used for extracting the letters of significance. In the end, the data visualization was carried out using the *ggplot2* package of R programming along with several additional extension packages.

4. RESULTS

4.1. Characterization

The crystal size analysis of ZnO NPs by XRD is presented in Figure 14. Some strong peaks were noted in XRD spectra. The peaks at planes (201), (101), (100), (102), (002), (110), (112), and (103) confirmed the presence of ZnO in the NPs form. The size of NPs calculated by using the Scherrer equation ranged from 21-41 nm and the average size was noted as about 31 nm. The crystal size analysis of nano-bentonite is given in Figure 15.

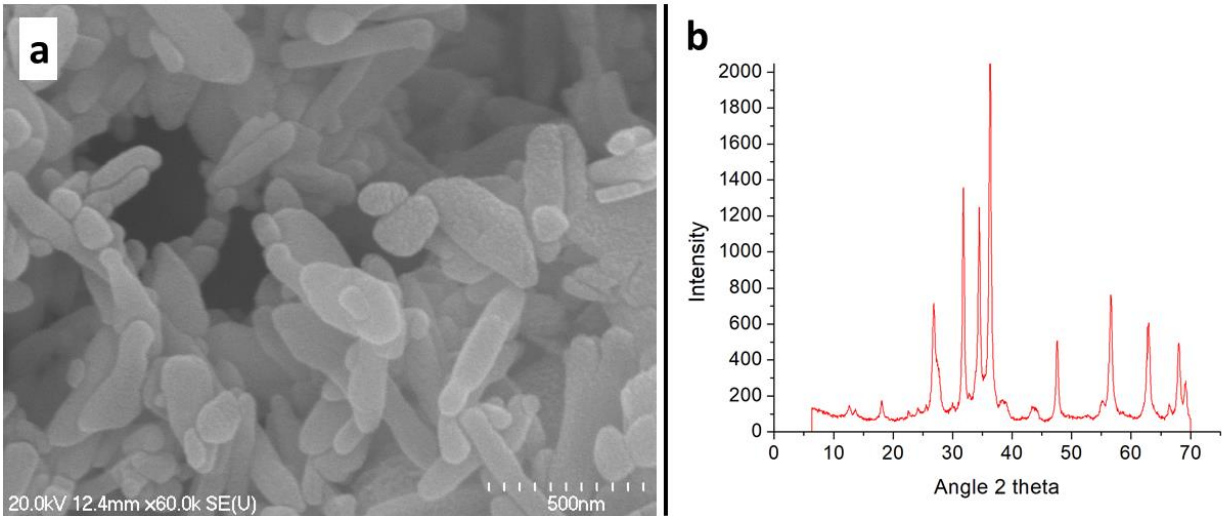

Figure 14: Characterization of ZnO NPs a) SEM, b) XRD

The presence of quartz and montmorillonite was confirmed by the peaks at planes (005), (001), and (004). Based on the Scherrer equation the crystal size of nano-bentonite ranged from 6-50 nm and the mean crystal size was reported about 32 nm. The scanning electron microscope was used to carry out morphological analysis of ZnO NPs, nano-bentonite, and coated urea granules. The SEM images showed that the ZnO NPs appeared in the form of rectangles and the particles are a little bit aggregated Figure 14. The SEM images of nano-bentonite showed a sheet-like structure. The sheet-like structure is the characteristic of montmorillonite. The coated granules of urea fertilizer were also tested using SEM for the morphology and coating characteristics. The morphological representation of coated urea granules is given in Figure 16.

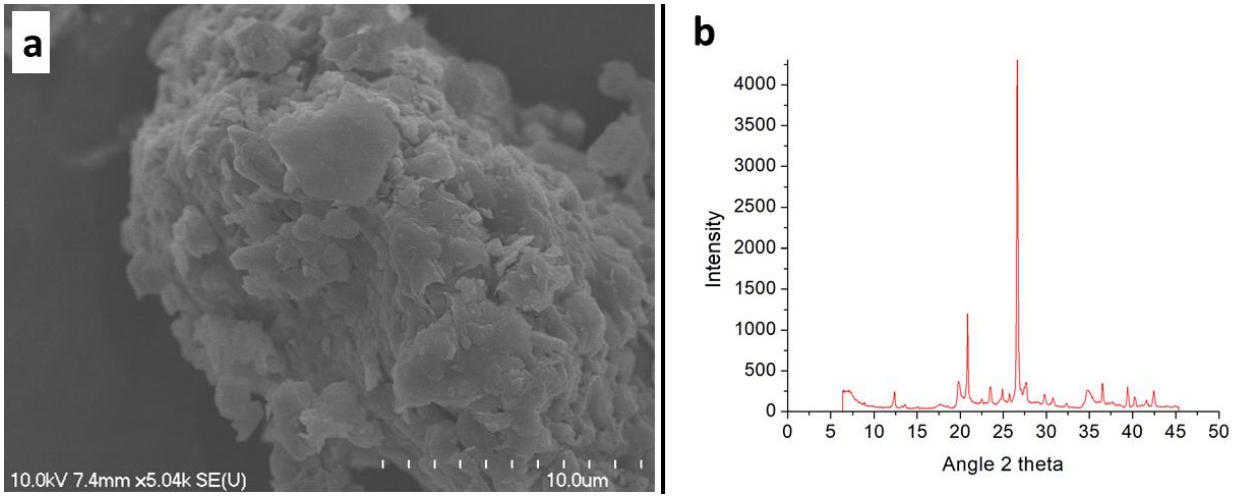

Figure 15: Characterization of nano-bentonite a) SEM, b) XRD

It was observed that urea granules appeared uniformly coated in all treatments except ZU2. The appearance of cracks can be seen in the SEM images of ZU2. It was also observed that the coating on ZU1 was also not uniform as compared to ZU3 and ZU4 treatments. The coating on ZU1 and ZU2 was carried out by using vegetable oil as a binder. The images showed that the ZU3 and ZU4 appeared uniformly coated. In the case of both ZU3 and ZU4, the coating was carried out by using stearic acid, paraffin oil, and paraffin wax as binding material.

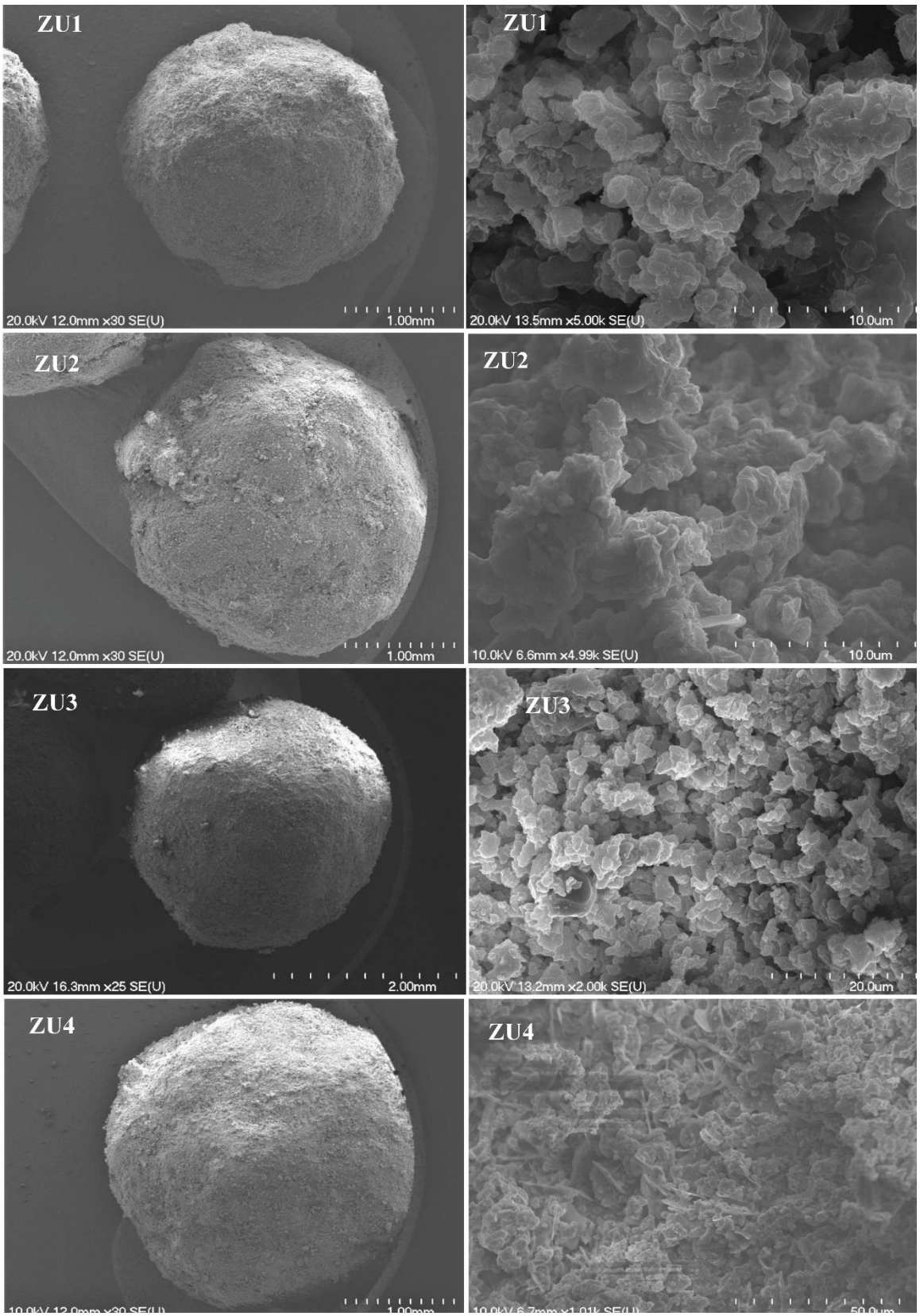

Figure 16: Characterization of coated urea granules using SEM

4.2. Zn sorption potential of nano-bentonite

The Freundlich, Langmuir, and new multilayer adsorption models were used to evaluate the Zn adsorption potential of nano-bentonite. Results showed that the new multilayer adsorption model was the best fit model (Figure 17), which explained the Zn adsorption in a better way. The model fit indices ($R^2 = 0.992$) showed that the new model is fitted to the data very well.

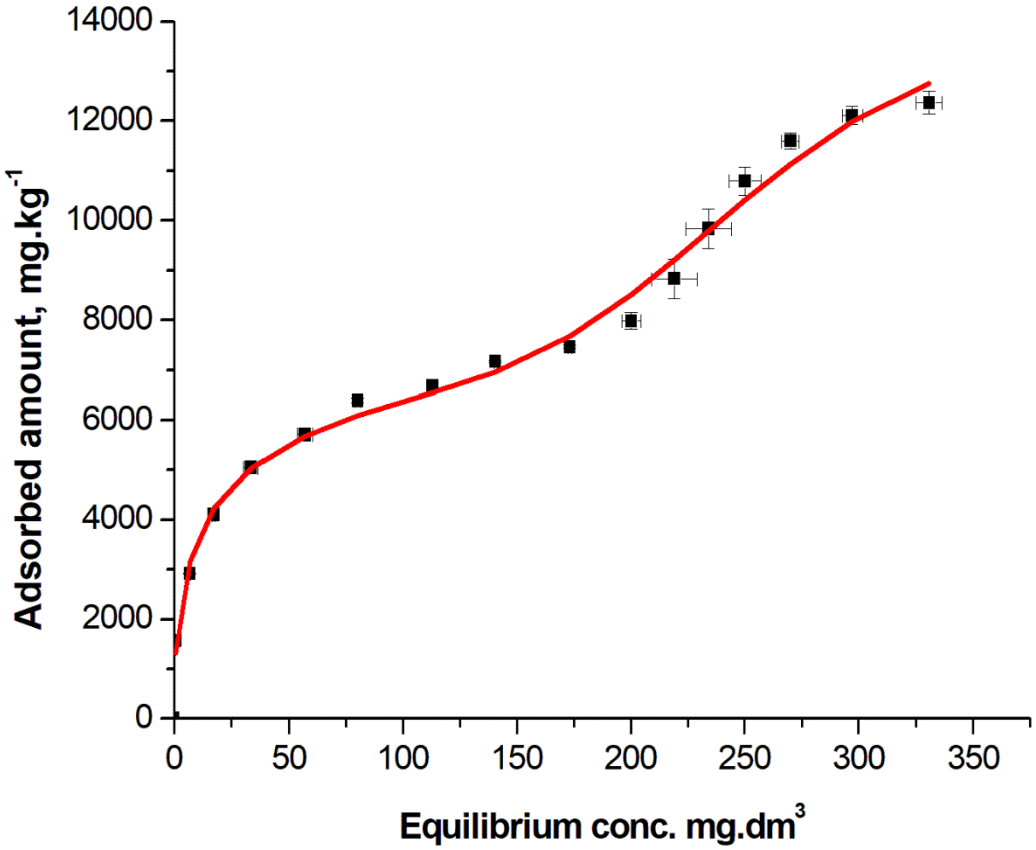

Figure 17: Evaluation of Zn adsorption potential of nano-bentonite using new multilayer adsorption model

According to the new model, the maximum adsorption of Zn onto nano-bentonite was 16.3 mg g^{-1}. It was observed that the adsorption of Zn in the first cycle was higher (9.8 mg g^{-1}) as compared to the second cycle (6.5 mg g^{-1}). The maximum adsorption capacity of bentonite according to the Langmuir model was 13.96 mg g^{-1} while the adsorption constant of the Freundlich model (Kfr) was 1.0 (Table 5).

Table 5: Parameters of adsorption models used to evaluate the Zn adsorption potential of nano-bentonite

Constant values of adsorption Isotherm models									
Langmuir constants			Freundlich constants			New model constants			
q_e	Kl	R^2	Kfr	nfr	R^2	a_i	k	n	R^2
13.96	0.01	0.859	1.0	2.37	0.94	16.272	0.181	5.85	0.992

Based on the model fit indices Freundlich model ($R^2 = 0.94$) was fitted better to the data as compared to the Langmuir model ($R^2 = 0.86$) (Figure 18). The overall model fitness trend was as follows: new multilayer model> Freundlich model >Langmuir model.

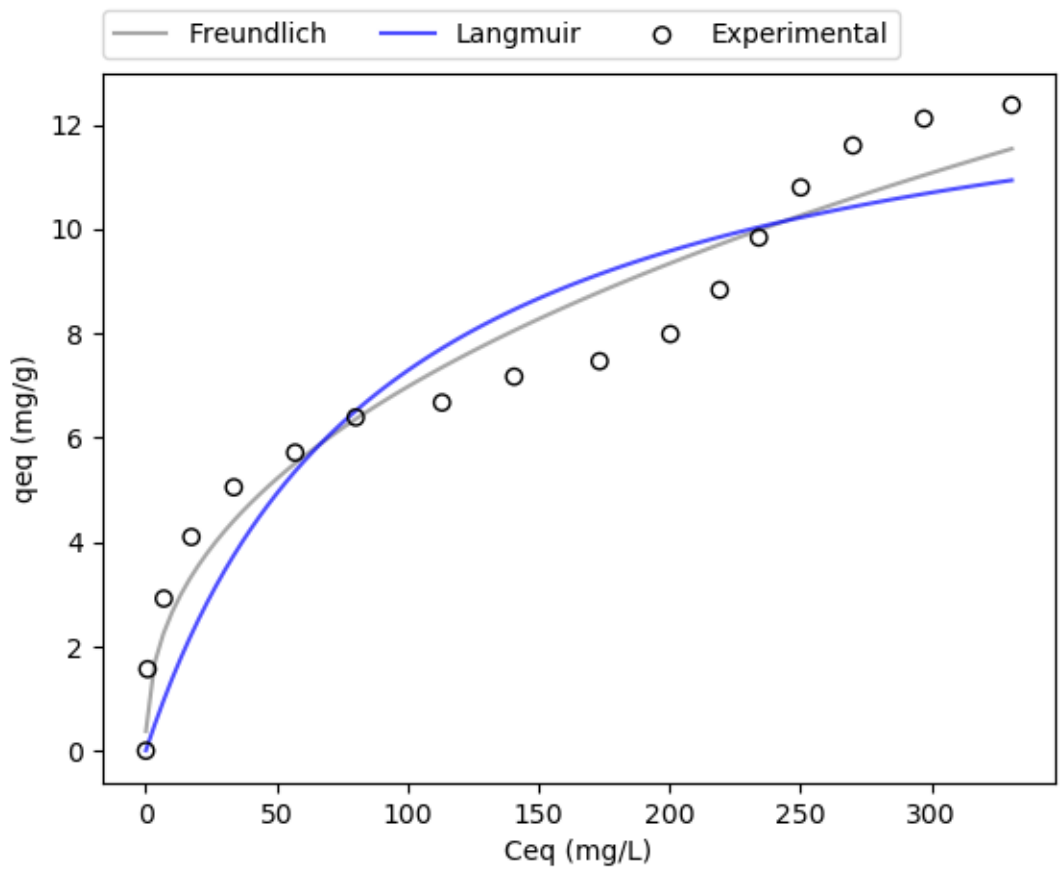

Figure 18: Evaluation of Zn adsorption potential of nano-bentonite using Langmuir and Freundlich adsorption isotherms

4.3. Release kinetics of Zn from ZnO NPs and Zn fortified nano-bentonite coated urea

Results showed that the amount of Zn released was significantly higher in the case of ZnO NPs coated urea (ZU2 and ZU4) as compared to the Zn-fortified nano-bentonite coated urea (ZU1 and ZU3)

(Figure 19). It was also observed that there was no significant difference among the treatments of ZnO NPs coated urea and Zn-fortified nano-bentonite-coated urea in terms of the released amount of Zn. The release of Zn from ZU3 and ZU4 showed a continuously increasing trend even on the 30th day of the experiment, while the maximum release of Zn from ZU1 and ZU2 was noted on the 15th day of the experiment and after that it become stagnant.

To evaluate the Zn release behavior from the coated urea, Korsmeyer-Peppas and Higuchi kinetic models were used. The fitted kinetic model results showed that the Zn-fortified nano-bentonite released Zn slowly as compared to ZnO NPs (Figures 39 & 40). The dissolution rate constants of both models were significantly lower in the case of Zn-fortified nano-bentonite-coated urea as compared to ZnO NPs-coated urea.

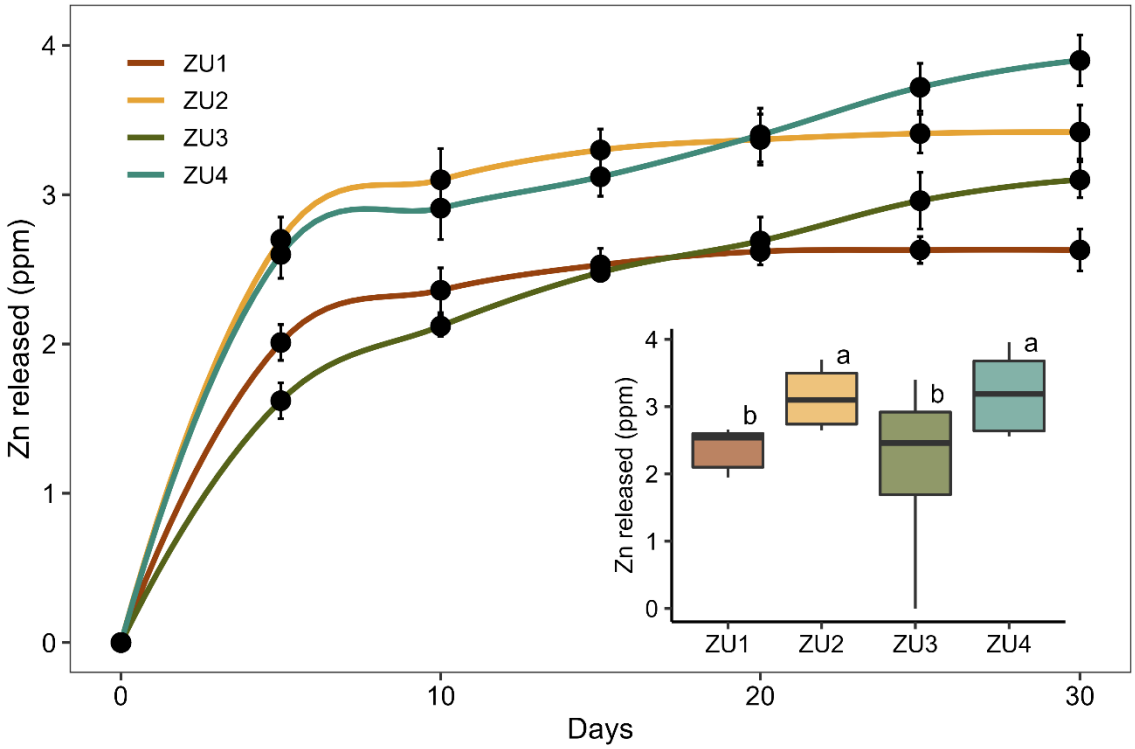

Figure 19: Zinc release behavior from Zn-fortified nano-bentonite and ZnO NPs coated urea. Letters of significance were presented based on the confidence interval of 0.05. The different letters showed a significant difference between treatments at α=0.05, n=3.

4.4. Release kinetics of N from ZnO NPs and Zn fortified nano-bentonite coated urea

Results showed that the urea granules which were coated by using stearic acid and paraffin wax (ZU3 and ZU4) released N slowly as compared to the vegetable oil-coated (ZU1 and ZU2) and uncoated urea granules (Figure 20). It was noted that the uncoated urea and ZU1 and ZU2 released complete N within 5 days of the experiment. While in the case of ZU4 and ZU3 only 28% and 35% of N were

released in the first 5 days respectively. The 80% release of N from ZU3 and ZU4 was noted on the 15th day of the experiment. On the 15th day, both treatments were considered completely released. Kinetic models such as Korsmeyer-Peppas and Higuchi models were fitted very well to the data (Figures 41 & 42). Model fit indices for Korsmeyer-Peppas and Higuchi models were $R^2 = 0.96$ and $R^2 = 0.94$ respectively in the case of both ZU3 and ZU4 treatments. The dissolution constants of both models confirmed the slow release of N from ZU3 and ZU4 as compared to ZU1, ZU2, and uncoated urea.

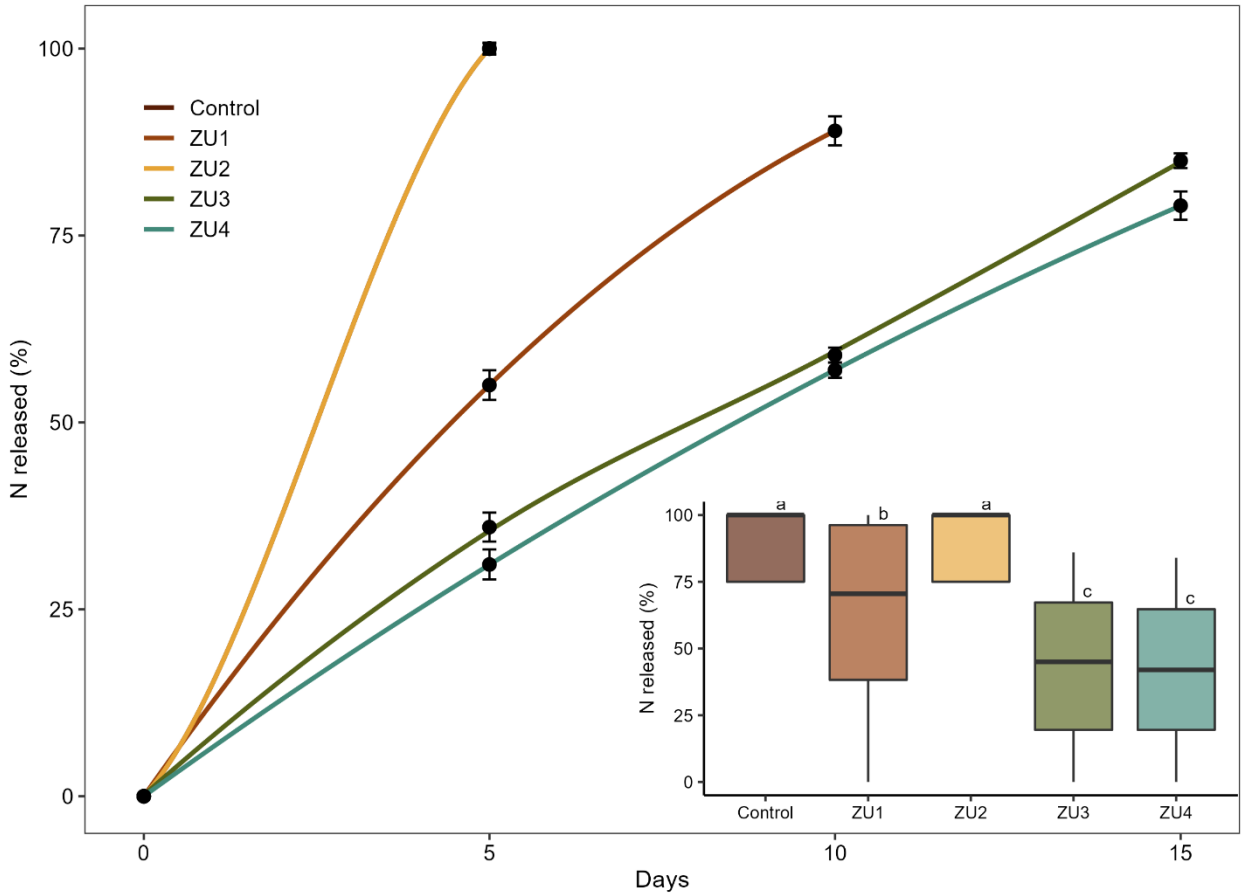

Figure 20: Nitrogen release behavior from coated urea granules. Letters of significance were presented based on the confidence interval of 0.05. The different letters showed a significant difference between treatments at α=0.05, n=3.

4.5. Effect of NPs size, soil types, and incubation time on the solubility of ZnO NPs

The dissolution of ZnO NPs was evaluated by incubating the soil for 7 and 14 days using different soil types and sizes of NPs. After leaching the soil, the leachate was analyzed for Zn concentration on AAS.

4.5.1. Zn concentration in leachate

After analyzing the leachate on AAS, the results were presented in the form of elution curves for both soils used in the experiment (Figure 21 (a & b)). The Zn concentration obtained in the control treatment was subtracted from the Zn concentration in treated soils. The figure showed a clear reduction in the Zn concentration with time. A maximum amount of Zn was noted in the first 5 mL elute volume after that a continuous reduction was noted as the elute volume increased.

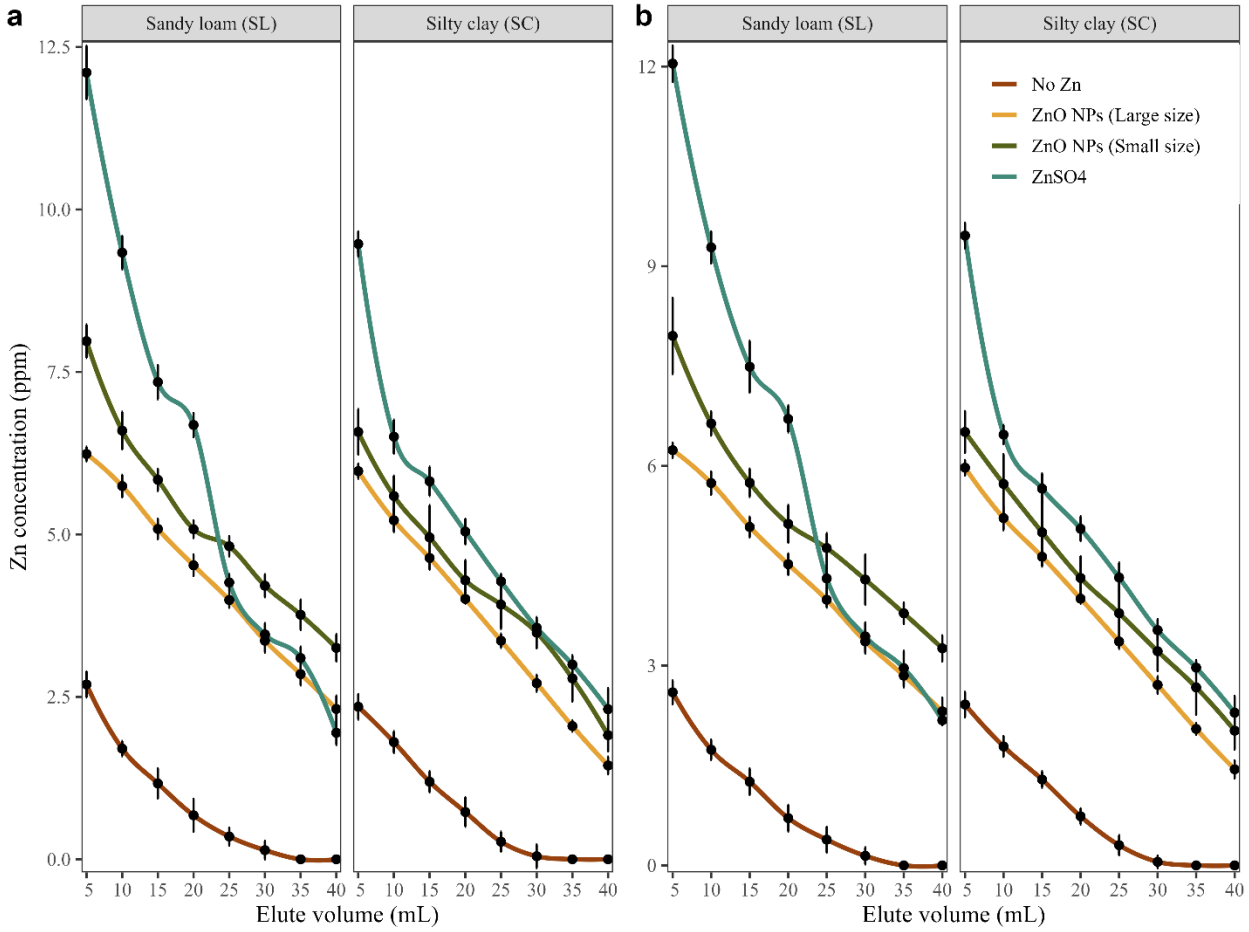

Figure 21: Pore water Zn concentration in soil leachates of sandy loam and silty clay soils a) 7 days of incubation b) 14 days of incubation

It was also noted that maximum Zn in elute was observed when the soil was spiked with $ZnSO_4$ followed by NPs spiked soil. A minimum concentration of Zn was observed in control soil without

Zn spiking. The results showed that the size of NPs significantly influences the dissolution of ZnO NPs ($p<0.05$). It was noted that pore water Zn concentration was significantly higher in both soils when soils were spiked with small-size NPs as compared to large-size NPs. Cumulatively, 21-23% of higher Zn concentration was noted in SL soil spiked with small-size NPs, and about 10-13% higher Zn was observed in SC soil as compared to large-size NPs. Along with the size of NPs, soil texture also influences the dissolution of ZnO NPs. In this study, the pore water Zn concentration was lower in SC soil as compared to SL soil. It was noted that 20.6%, 26.5%, and 14.5% higher pore water Zn were analyzed in SL soil as compared to SC soil when spiked with $ZnSO_4$, NPs (small size), and NPs (large size) respectively.

4.5.2. Bioavailability of retained Zn on soil matrix

To evaluate the bioavailability potential of Zn retained on the soil matrix EDTA (0.05 M) solution was used for the extraction (Figure 22). A significant amount of Zn was extracted from both soils using EDTA as an extractant. The extraction efficiency of EDTA was 54-57% in SC soil and 48-53% was noted in SL soil. All the Zn spiked soil treatments showed significantly higher Zn extraction as compared to the control treatment without Zn spiking. It was noted that extracted Zn concentration from SC soil was significantly higher (40.7 mg kg^{-1}) as compared to SL soil (34.3 mg kg^{-1}) when spiked with small-size NPs. While there was no significant difference between other treatments.

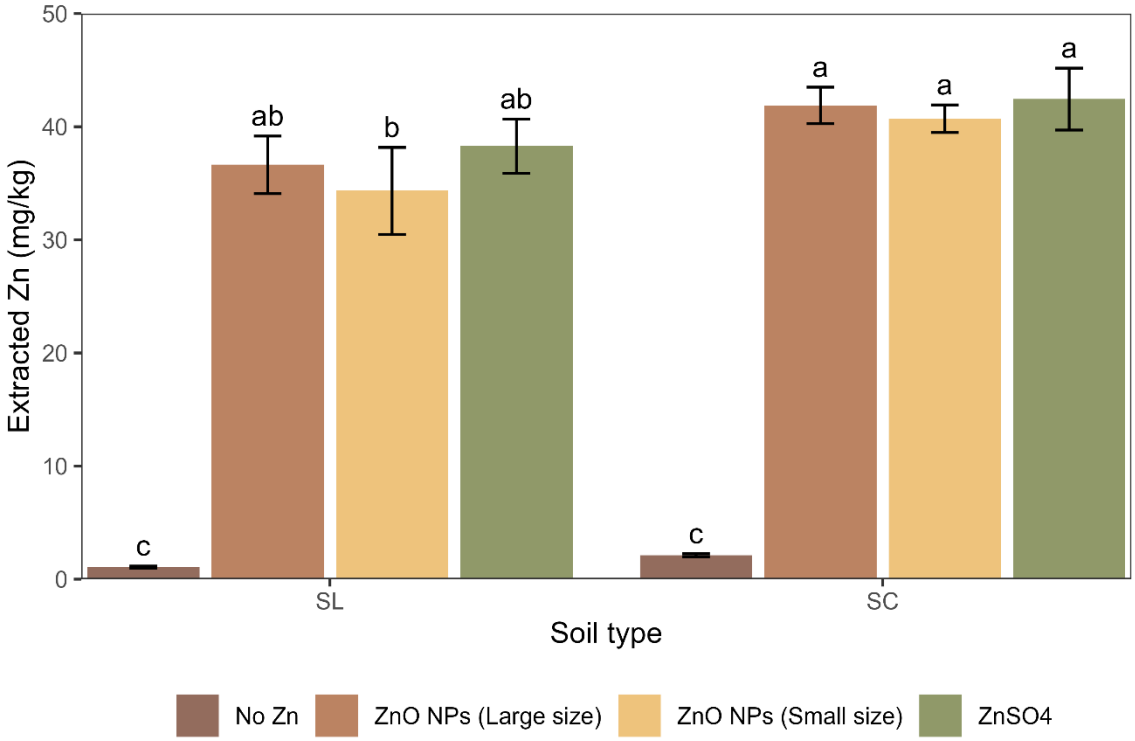

Figure 22: The extracted amount of Zn from sandy loam and silty clay soil by using EDTA (0.05M) solution as an extractant. The different letters showed a significant difference between treatments at α=0.05, n=3.

4.6. Nitrous oxide emission potential of conventional and coated urea from unplanted soils

After continuous measurement of N_2O flux in the laboratory for 15 days, the flux was calculated and visualized. The flux for sandy loam soil is presented in Figures (23 & 24). It was noted that the flux points were distributed in a wide range. From the results, it was observed that during the first week of flux measurement maximum average flux (µg N m^{-2} h^{-1}) was noted for uncoated urea (55.3±6.4) followed by nano-bentonite coated urea (34.3±4.28). The minimum flux from the treated samples was shown by ZnO NPs coated urea (32.9±4.48). The overall minimum flux was reported in the case of control treatment without fertilizer application (21.6±1.90).

In the second week of the flux measurement, uncoated urea again showed the maximum N_2O flux (44.41±4.08) like in the first week. The nano-bentonite and ZnO NPs coated urea showed similar flux values (30.6±3.01 and 30.3±2.07) respectively during the second week. It was noted that the flux calculated for the control treatment during the second week was the minimum (12.97±1.92).

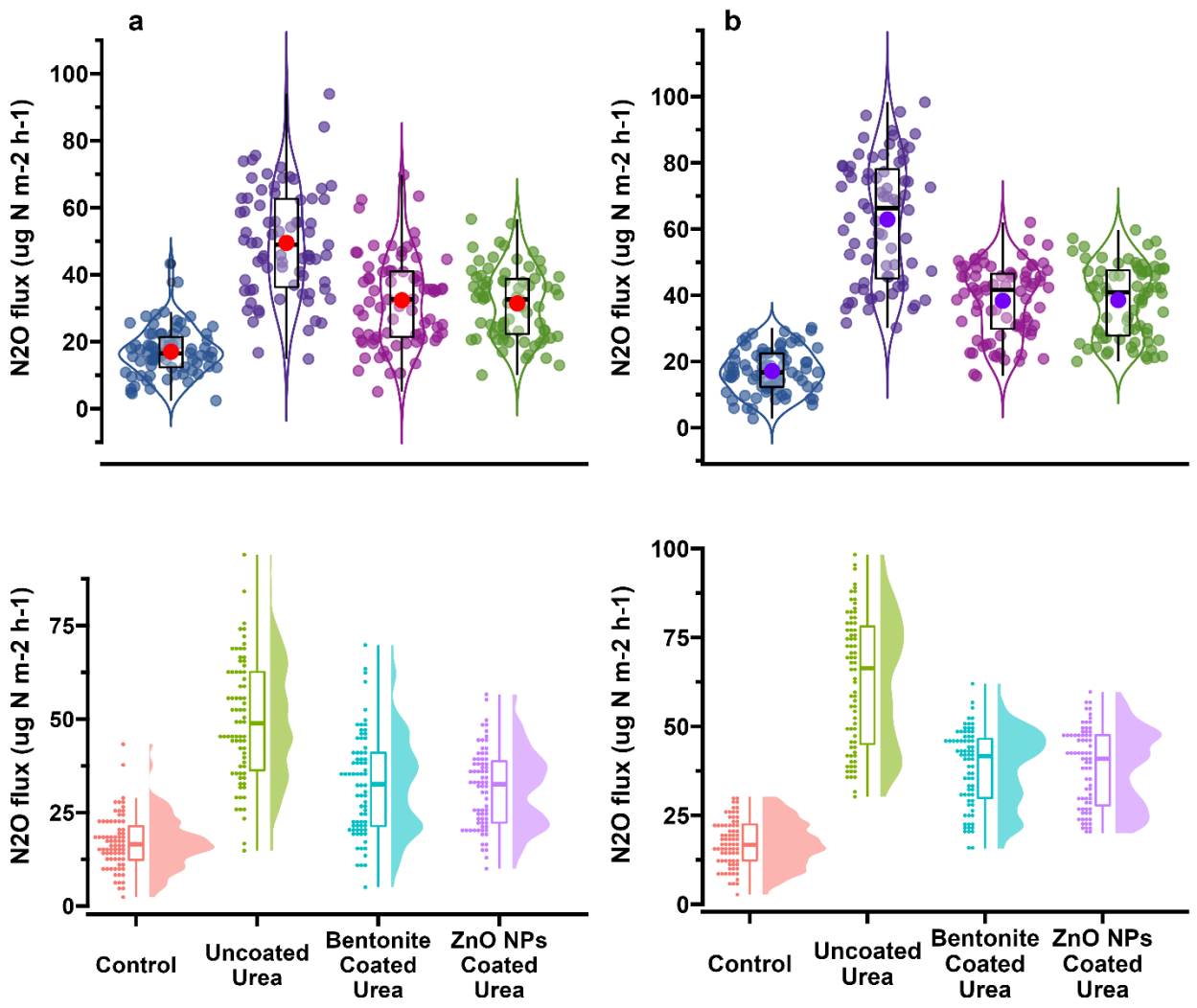

Figure 23: Distribution of nitrous oxide flux points (µg N m^{-2} h^{-1}) from a) sandy loam soil b) silty clay soil fertilized with coated and un-coated urea (15 days measurement)

Overall, the average flux during the 15 days measurement was highest for uncoated urea which was around 35% higher than nano-bentonite coated urea and ZnO NPs coated urea. The minimum flux was noted in the case of the control treatment (17.28±1.91 µg N m^{-2} h^{-1}).

The calculated flux for silty clay soil is presented in Figures (23 & 24). Flux points were distributed in a wide range. In the case of control treatment majority of the points lay close to zero, while for uncoated urea the maximum points are measured between 20-40 µg N m^{-2} h^{-1}. The points distribution for nano-bentonite coated and ZnO NPs coated urea are distributed in a range of 10-20 µg N m^{-2} h^{-1}. The average flux calculation (µg N m^{-2} h^{-1}) during the first week showed that the maximum flux value was noted for uncoated urea (70.38±3.53) followed by nano-bentonite coated urea (35.26±3.61). The ZnO NPs coated urea showed the lowest flux values from the treatments (35.91±2.34), while overall

minimum flux was recorded in the case of the control treatment (21.66±2.21) respectively. In the second week of flux measurement the calculated flux was in the order of uncoated urea > nano-bentonite coated urea > ZnO NPs coated urea >Control with the values 56.34±7.4 >41.03±2.73 >40.07±3.40>13.04±1.70 respectively.

Figure 24: Average daily N_2O flux (µg N m^{-2} hr^{-1}) from a) sandy loam soil b) silty clay soil fertilized with conventional and Zn-coated urea

The overall, average flux during 15 days was recorded as maximum for uncoated urea which was approximately 40% higher than nano-bentonite coated urea and ZnO NPs coated urea. The minimum was recorded for the control treatment (17.35±1.96 µg N m^{-2} h^{-1}).

4.6.1. Cumulative N_2O emission

The cumulative N_2O emission (kg N ha^{-1} yr^{-1}) was calculated for both soils using equation (9). The results showed that the uncoated urea emitted maximum cumulative N_2O in both soils (Silty clay and Sandy loam) at 82.6 and 64.14 kg N ha^{-1} yr^{-1} respectively followed by nano-bentonite coated urea (50.4 and 41.94 kg N ha^{-1} yr^{-1}) and ZnO NPs coated urea (50.6 and 40.88 kg N ha^{-1} yr^{-1}) (Figure 25).

The minimum cumulative emission was noted in the case of the control treatment (22.4 and 22.02 kg N ha^{-1} yr^{-1}) in silty clay and sandy loam soils respectively.

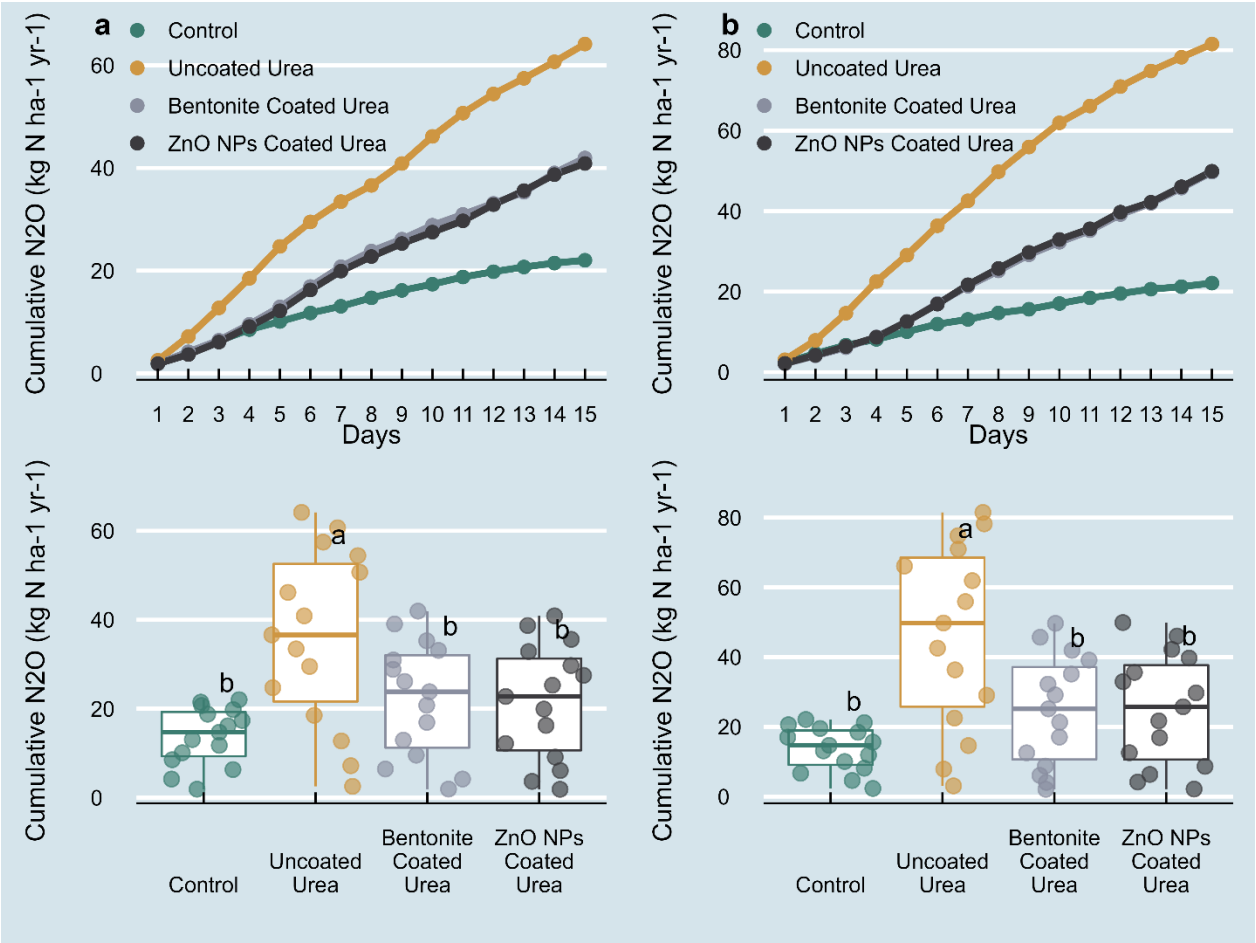

Figure 25: Cumulative N_2O emission (kg N ha^{-1} yr^{-1}) from a) sandy loam soil and b) silty clay soil fertilized with coated and un-coated urea. The different letters showed a significant difference between treatments at α=0.05, n=5.

4.6.2. N_2O emission factor

The N_2O emission factors were calculated using equation (10). The results showed that the N_2O emission factors for coated and uncoated fertilizers were significantly ($p \leq 0.03$) higher in silty clay soil as compared to sandy loam soil (Table 7). The N_2O emission factor values for uncoated urea, nano-bentonite coated urea, and ZnO NPs coated urea in silty clay soil were 1.0, 0.46, and 0.46 respectively. While the emission factor values in sandy loam soil were as follows 0.7, 0.33, and 0.31 for uncoated urea, nano-bentonite coated urea, and ZnO NPs coated urea respectively. Based on the emission factor values it was clear that the maximum applied N was lost in the case of uncoated urea as compared to coated urea in both soils.

Table 6: Nitrous oxide emission factors from conventional and Zn-coated urea applied in bare and planted soil conditions

			Sandy loam soil			Silty clay soil		
			Uncoated Urea	Bentonite coated urea	ZnO NPs coated urea	Uncoated Urea	Bentonite coated urea	ZnO NPs coated urea
Emission factors (% of applied N lost in the form of N_2O)	Planted soil	Surface Placement	5.3	3.3	3.4	6.1	3.65	3.62
		Deep Placement	5.33	3.2	2.95	4.44	2.7	3.6
	Bare soil		0.7	0.33	0.31	1.0	0.46	0.46

4.7. Nitrous oxide emission potential of conventional and coated urea from planted soils

4.7.1. Effect of Coated urea fertilizer on plant growth

To evaluate the effect of slow-release coated urea on plant growth, shoot fresh weight (FW), dry weight (DW), and chlorophyll contents were measured. Maximum FW was recorded from the pots where coated urea was applied followed by conventional urea and the minimum FW was recorded in the control treatment (Figure 26).

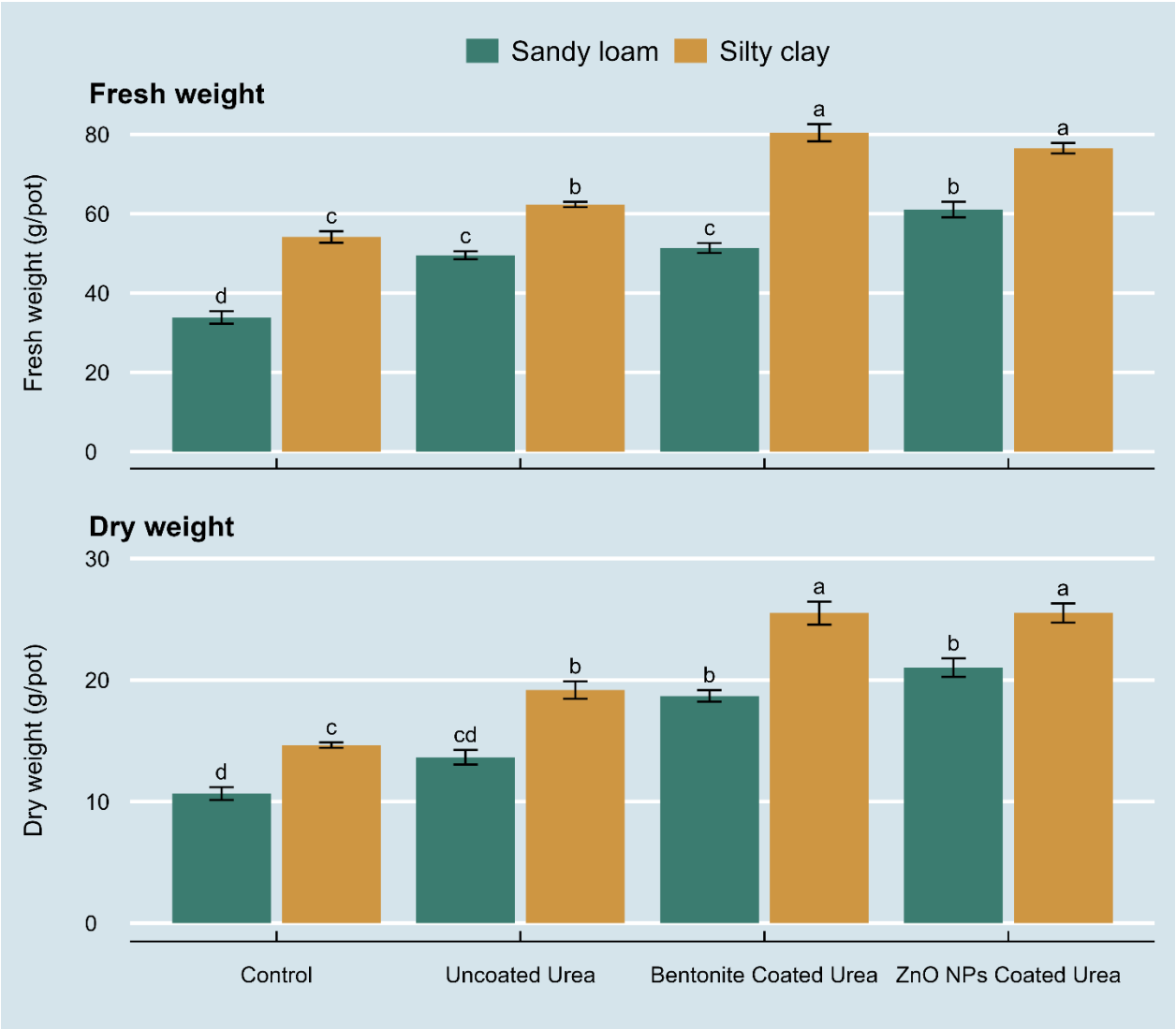

Figure 26: Fresh and dry weight of wheat plants in sandy loam and silty clay soil fertilized with conventional and Zn-coated urea. The different letters showed a significant difference between treatments at α=0.05, n=3.

Both coated urea treatments have no significant effect ($p \geq 0.05$) concerning each other but showed significantly higher ($p \leq 0.001$) FW as compared to conventional urea and control. Apart from the treatments soil type also affect the FW significantly. It was observed that the silty clay soil significantly ($p \leq 0.001$) showed higher FW as compared to sandy loam soil. The interaction effect of treatments and soil type on FW was also significant. Results depicted that the application method of fertilizer had no significant ($p \geq 0.05$) effect on FW.

A similar trend was also observed in the case of DW, where the coated urea application showed a significant increase ($p \leq 0.001$) in DW as compared to conventional urea and control treatment (Figure 26). Like FW, soil type also affects the DW significantly ($p \leq 0.001$), while the method of application

has no significant ($p \geq 0.05$) effect on DW. It was observed that in sandy loam soil the conventional urea application has no significant effect ($p \geq 0.05$) as compared to the control treatment. Higher crop growth and vigor under the application of coated urea as compared to conventional urea can be seen in Figure 27.

Figure 27: Visual crop growth comparison based on different fertilizer treatments

Chlorophyll *a* contents were significantly affected by the treatments ($p \leq 0.001$) and soil type ($p \leq 0.0035$) (Figure 28). Maximum chlorophyll *a* was observed under coated urea application (~42.5 µg cm^{-2}) in both soil types followed by conventional urea 38.1 µg cm^{-2} in silty clay soil and 34.3 µg cm^{-2} in sandy loam soil. Minimum chlorophyll *a* was detected in control treatment 31 and 27.6 µg cm^{-2} in silty clay and sandy loam soil respectively. It was observed that the method of application has no significant effect on chlorophyll *a*.

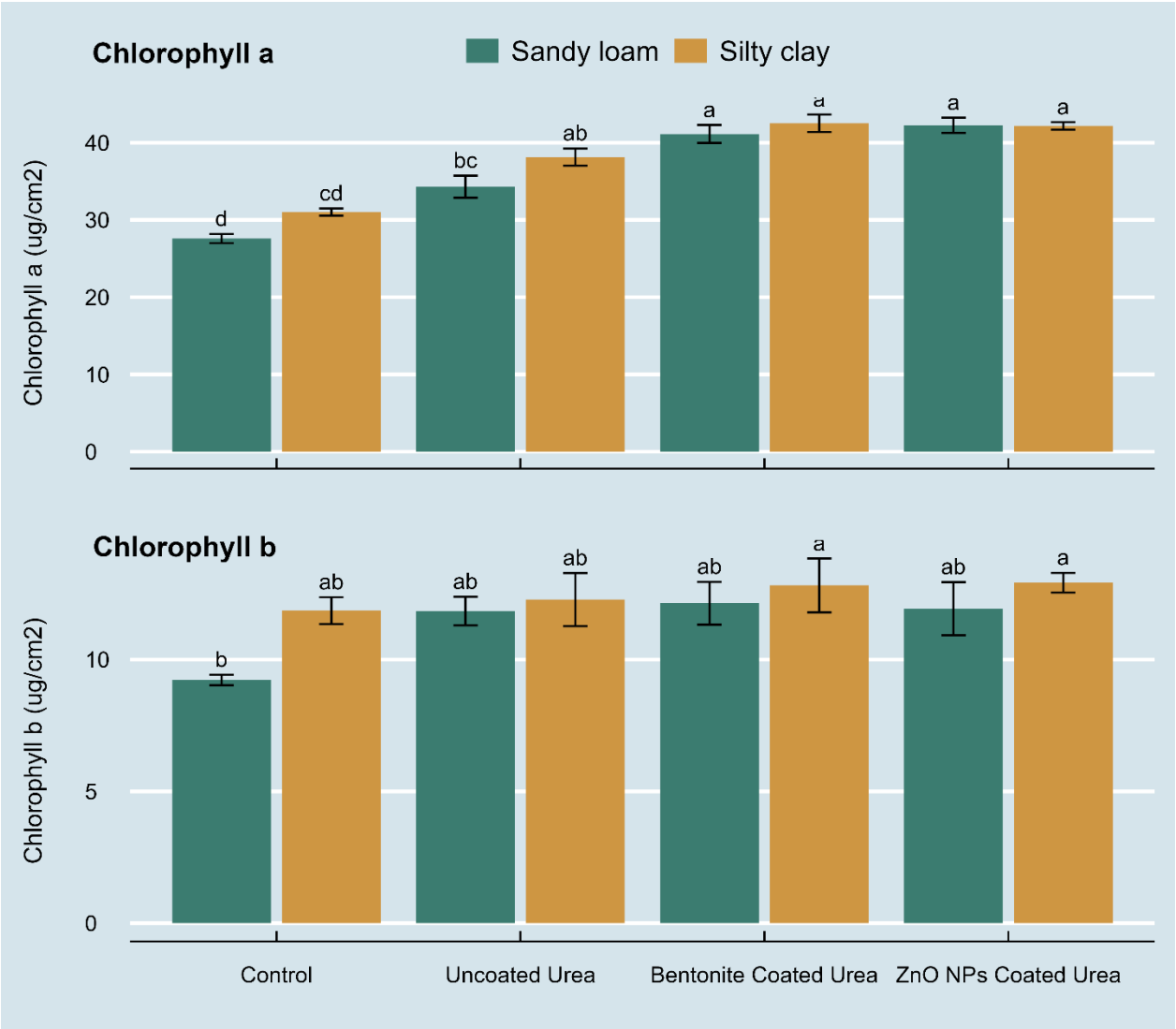

Figure 28: Chlorophyll *a* and *b* contents in plant leaves in sandy loam and silty clay soil fertilized with conventional and Zn-coated urea. The different letters showed a significant difference between treatments at α=0.05, n=3.

Like chlorophyll *a*, a similar trend was also observed in chlorophyll *b* (Figure 28), where coated urea application significantly improved the chlorophyll *b* contents as compared to conventional urea. In the case of soil type, higher chlorophyll *b* was observed in plant leaves grown in silty clay soil as compared to sandy loam soil. The method of application has no significant effect on chlorophyll *b*. Based on the trends in chlorophyll *a* and *b* the total chlorophyll also showed similar results depicting the higher total chlorophyll contents in plants where coated urea was applied as compared to conventional urea and control treatment. The chlorophyll *a:b* ratio ranged from 2.63-3.72. The chlorophyll *a:b* ration was higher in coated urea treatments as compared to other treatments (Figure 29).

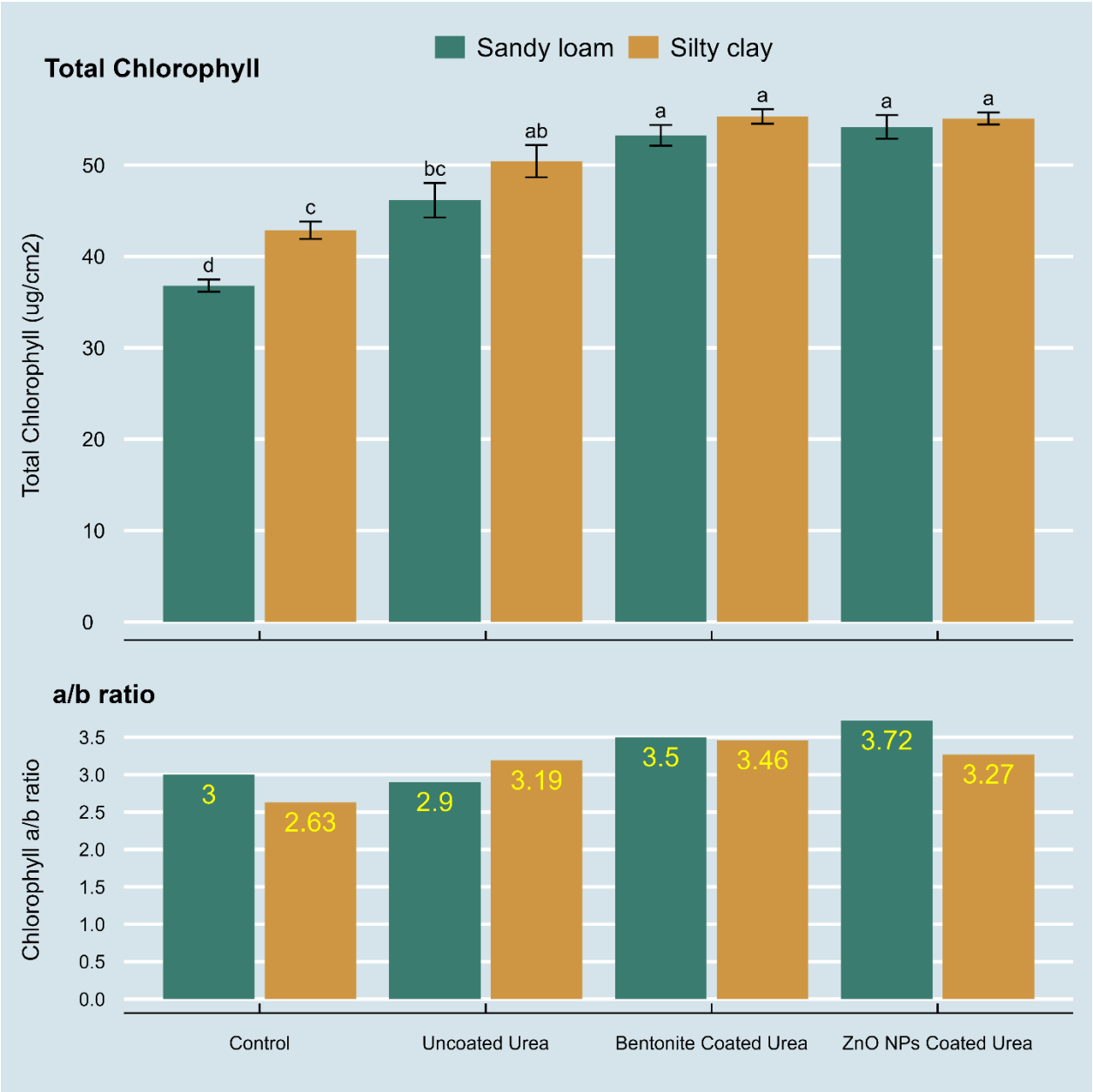

Figure 29: Total chlorophyll and chlorophyll *a:b* ratio in sandy loam and silty clay soil fertilized with conventional and Zn-coated urea. The different letters showed a significant difference between treatments at α=0.05, n=3.

4.7.2. Zn concentration in plants and soil

Analysis of the digested plant samples showed that the application of Zn-coated urea significantly ($p \leq 0.0001$) affect the plant Zn contents (Figure 30). The Highest Zn concentration in plants was reported with the application of ZnO NPs coated urea (53.76 mg kg^{-1}) and (60 mg kg^{-1}) in both sandy loam and silty clay soils respectively. The maximum Zn concentration with the application of Zn-fortified nano-bentonite coated urea was reported at 48.5 and 55.2 mg kg^{-1} in sandy loam and silty

clay soil respectively. Minimum Zn concentration in plants was reported in control treatments in both sandy loam and silty clay soils (24.8 and 32.2 mg kg^{-1}) respectively. In comparison to the control, the Zn concentration in plants was increased up to 46.3% and 53.8% with the application of ZnO NPs coated urea in both soils respectively. While about 48.8% and 41.6% higher Zn concentration was observed with the Zn-fortified nano-bentonite coated urea application in both soils respectively.

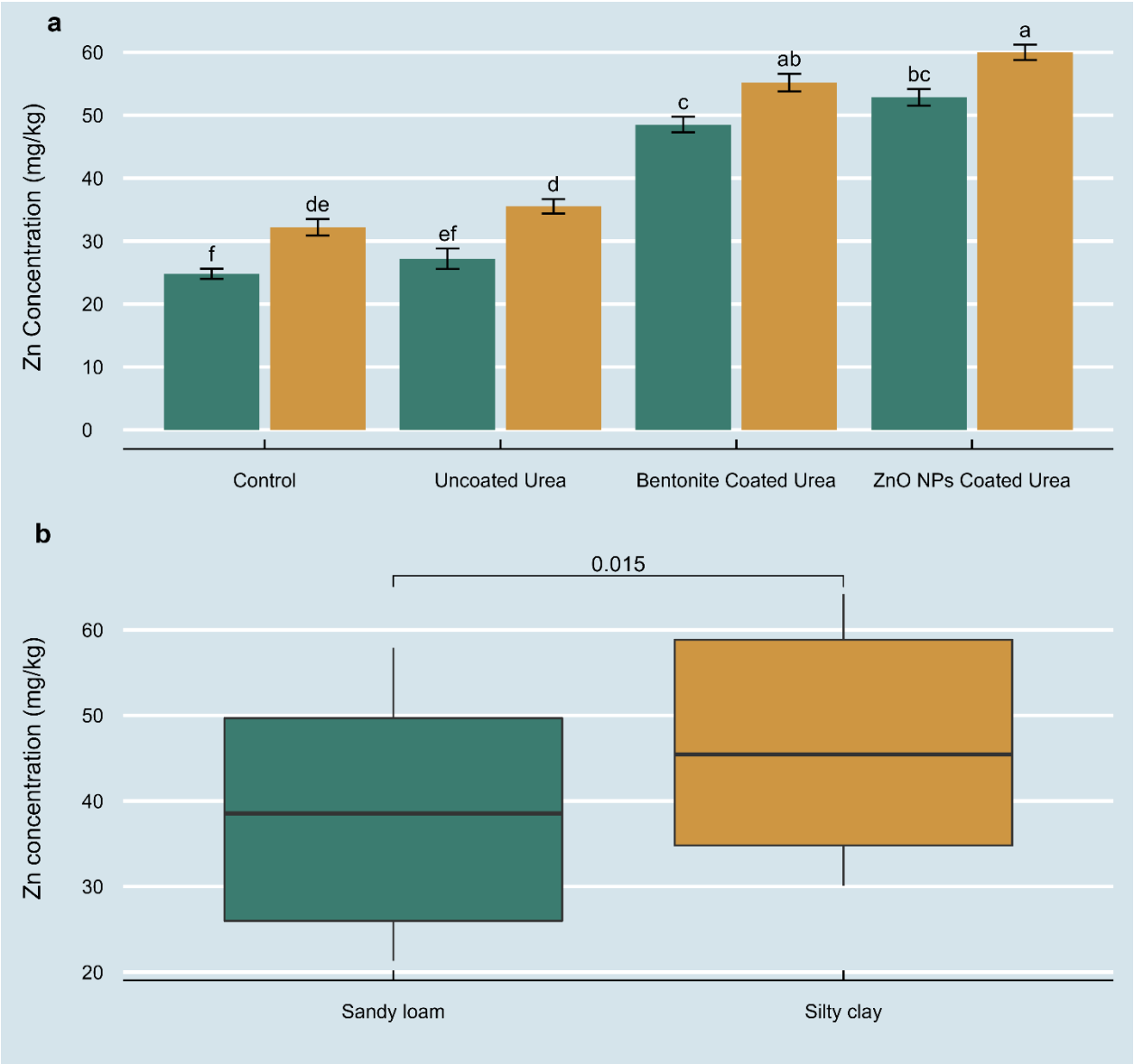

Figure 30: Zn concentration in plants a) Zn in above-ground plant parts in sandy loam and silty clay soil under conventional and Zn coated urea treatments b) Effect of soil type on plant Zn concentration. The different letters showed a significant difference between treatments at α=0.05, n=3.

The comparative analysis of soil types showed that Zn concentration in plants was significantly ($p \leq 0.015$) higher in silty clay soil as compared to sandy loam soil. While it was noted that the method

of fertilizer application (surface placement and deep placement) has no significant ($p \geq 0.274$) effect on the plant Zn concentration. Similarly, the interaction effects of fertilizer type, soil type, and application method were also non-significant ($p \geq 0.929$).

The analysis of soil extracts showed that the application of Zn-coated urea significantly (≤ 0.001) affected the soil Zn contents (Figure 31). Pre-experiment Zn analysis of silty clay soil showed that it contains ~3.16 mg kg^{-1} of Zn. While the post-harvest soil Zn analysis showed that these contents in the control treatment were reduced to ~1-1.5 mg kg^{-1}. It was noted that the application of ZnO NPs coated urea significantly increased the Zn contents in the soil (3.42 mg kg^{-1}) followed by Zn-fortified nano-bentonite (2.19 mg kg^{-1}).

Similarly, the sandy loam soil analysis showed that before the start of the experiment it contains ~2.86 mg kg^{-1} of Zn contents. These Zn contents were reduced to ~1.73 mg kg^{-1} in the control treatment after the experiment. Like silty clay soil in sandy loam soil, the application of Zn-coated urea significantly ($p \leq 0.00143$) increased the Zn contents, recorded maximum with ZnO NPs coated urea (3.18 mg kg^{-1}) followed by Zn fortified nano-bentonite coated urea (2.37 mg kg^{-1}). The comparative analysis of soil type and method of application showed that there was no significant difference in soil Zn contents in both soil types ($p \geq 0.296$) with both application methods ($p \geq 0.7504$).

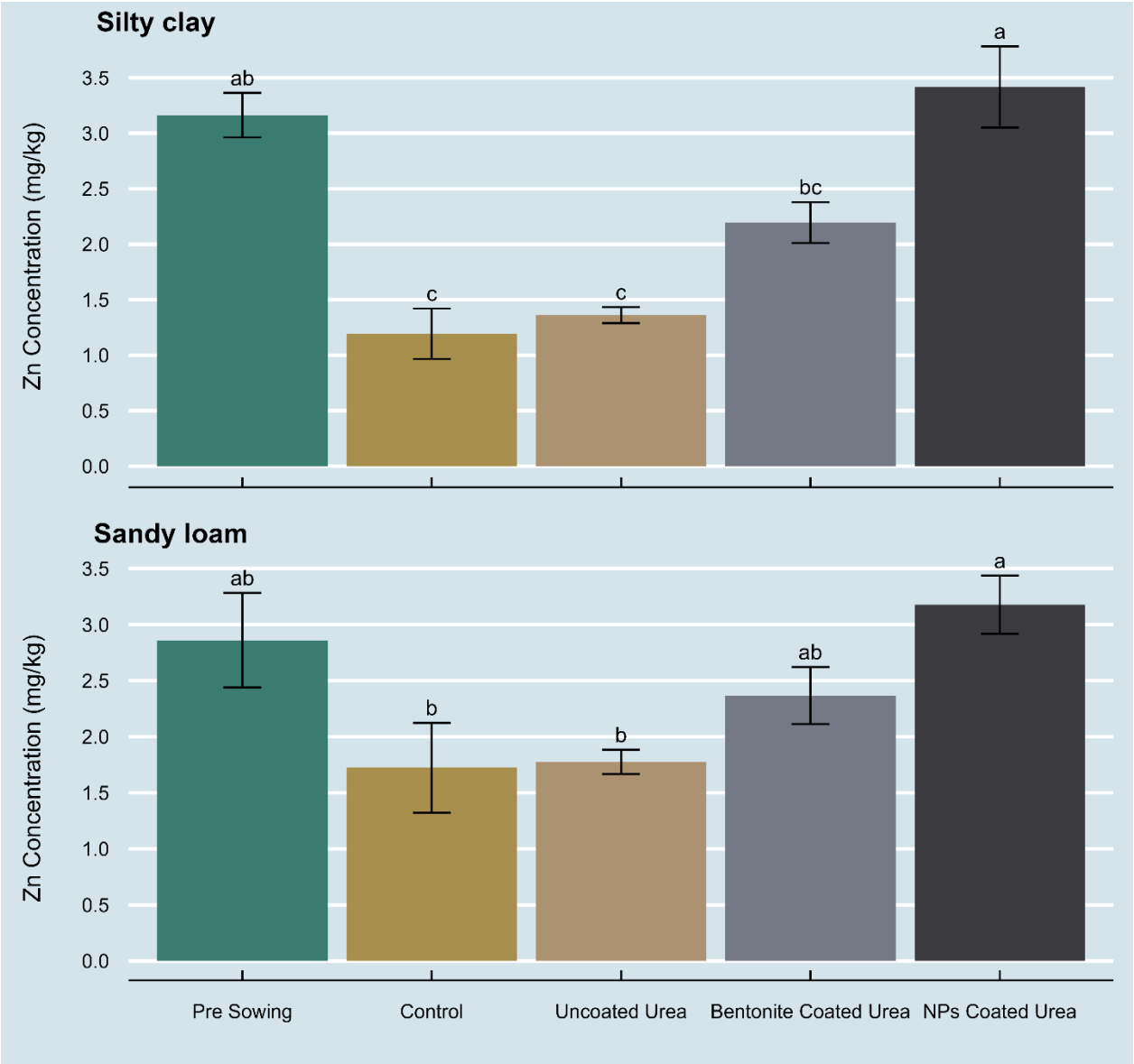

Figure 31: Pre and post-harvesting Zn concentration in sandy loam and silty clay soil under conventional and Zn-coated urea treatments. The different letters showed a significant difference between treatments at α=0.05, n=3.

4.7.3. Nitrogen concentration in plants and soils

The dried and ground plant samples were analyzed on a CNS analyzer for total N contents in the plant body. The results showed that the maximum N contents in plants were measured in the treatments where coated urea was applied (> 40 g N kg^{-1}) in both soils, followed by uncoated urea and control (Figure 32 a & b). It was observed that the N contents were higher in the case of silty clay soil as compared to sandy loam soil, but the difference was not significant statistically ($p \geq 0.05$) between coated urea treatments. On the other hand, N contents in plants were significantly ($p \leq 0.001$) higher in silty clay soil with the control treatments and where conventional urea was applied. The effect of

application methods on the plant N contents was also compared using the Wilcoxon t-test and it was concluded that the application method of fertilizers has no significant ($p \geq 0.05$) effect on plant N contents.

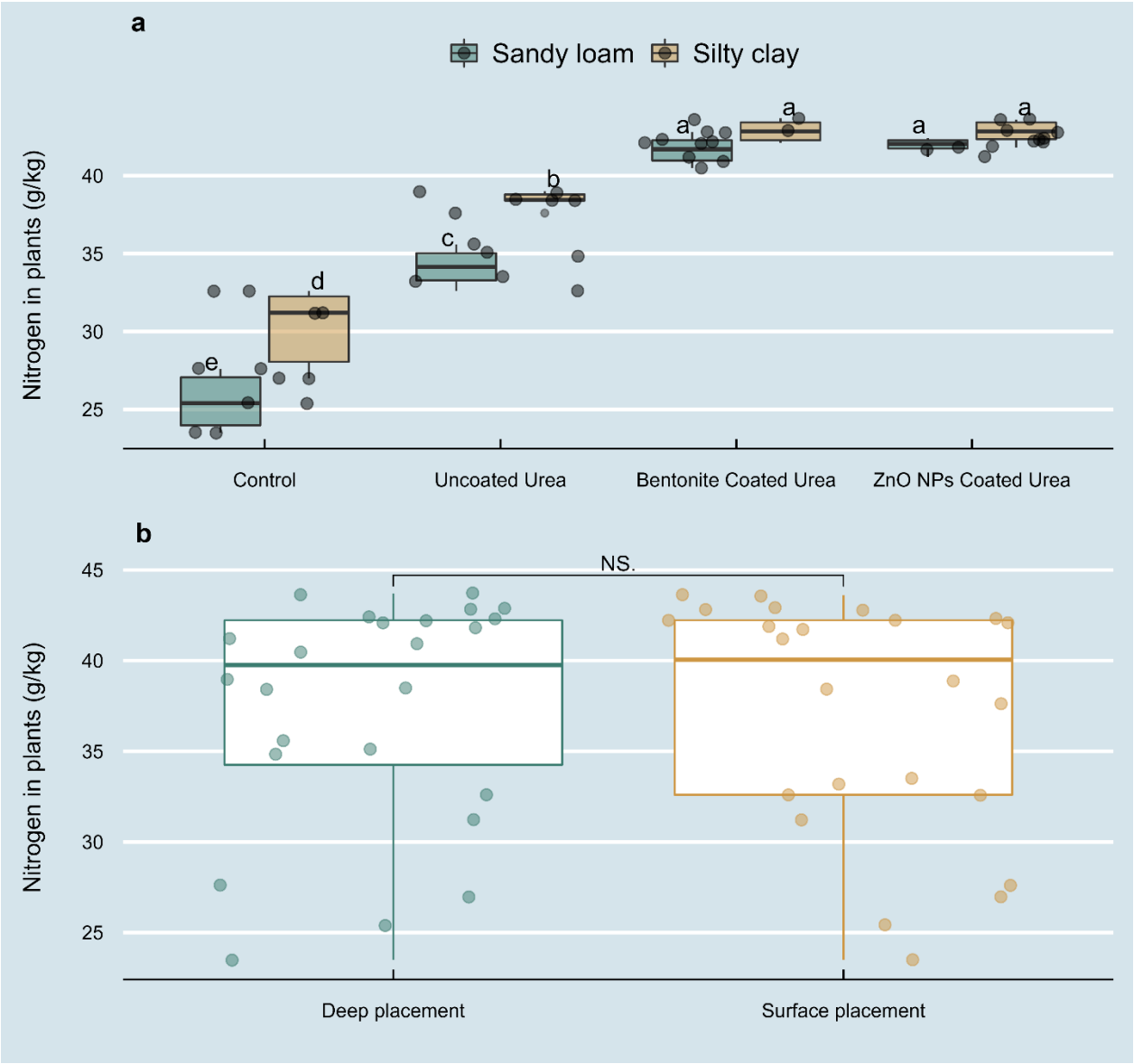

Figure 32: Nitrogen concentration in plants a) Effect of conventional and Zn coated urea treatments on plant N in sandy loam and silty clay soil b) Effect of soil type on plant N concentration. The different letters showed a significant difference between treatments at $\alpha=0.05$, n=3.

Soil analysis for N contents showed that N contents in the soil before the start of the experiment were significantly ($p \leq 0.001$) higher in silty clay soil (1.8 g N kg^{-1}) as compared to sandy loam soil (0.8 g N kg^{-1}) (Figure 33 a & b). Overall, it was noted that silty clay soil had higher N contents as compared to sandy loam soil. The N contents were higher in the soil where N was applied as compared to the control but the difference between the treatments was non-significant ($p \geq 0.05$). The comparison of

the application method showed that there was no significant ($p \geq 0.75$) difference in N contents in soils with surface or deep placement of the fertilizers.

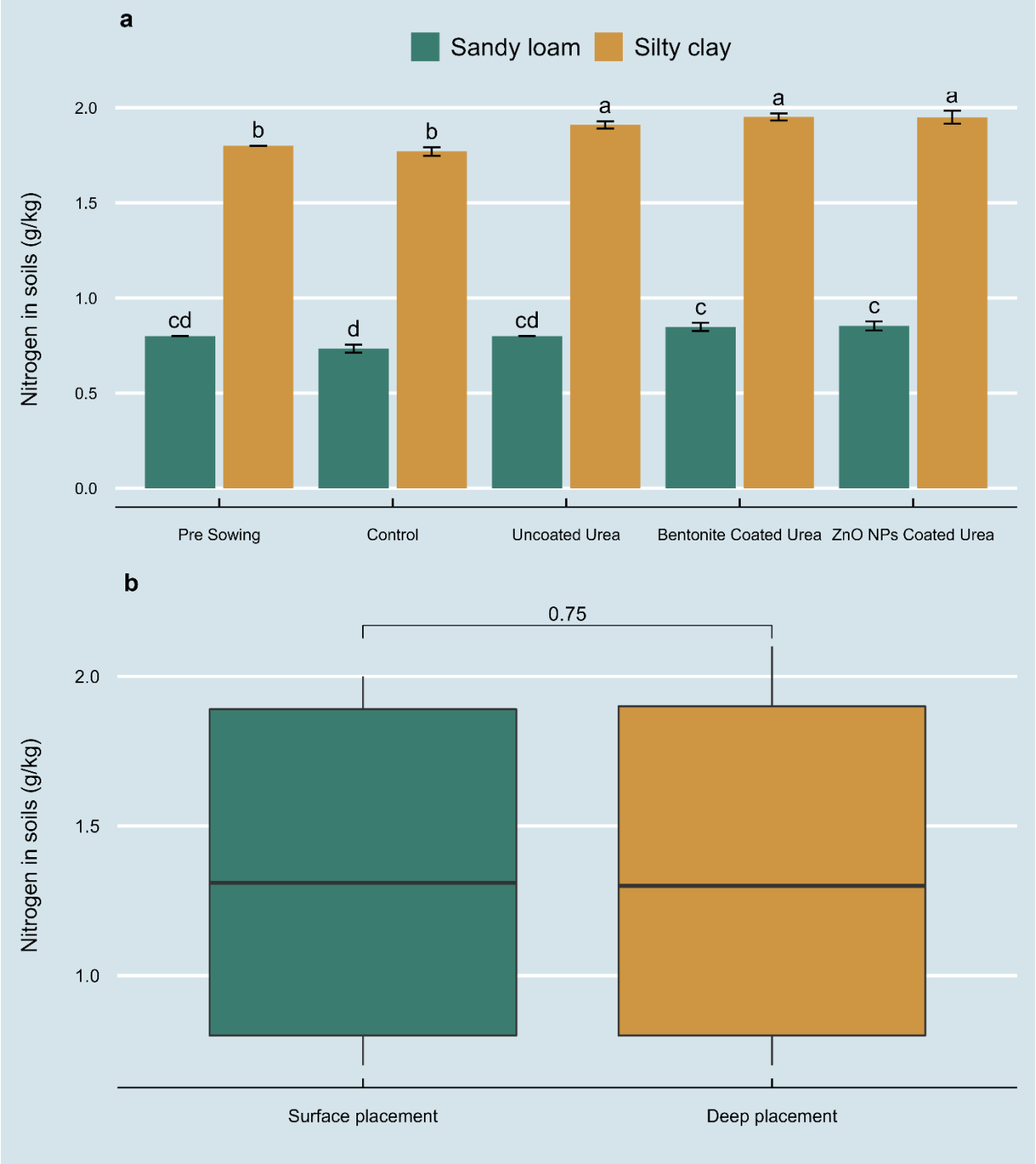

Figure 33: Pre and post-harvesting N concentration in sandy loam and silty clay soil a) Effect of treatments b) Effect of soil type. The different letters showed a significant difference between treatments at $\alpha=0.05$, $n=3$.

4.7.4. Nitrous oxide emission from planted soil

Nitrous oxide emission from two different soils under wheat plantation was measured over 48 days.

4.7.4.1. N_2O Flux measurement from sandy loam and silty clay soil

After data analysis, it was observed that the daily flux intensity was higher in silty clay soil as compared to sandy loam soil (Figure 34, & Figure 35).

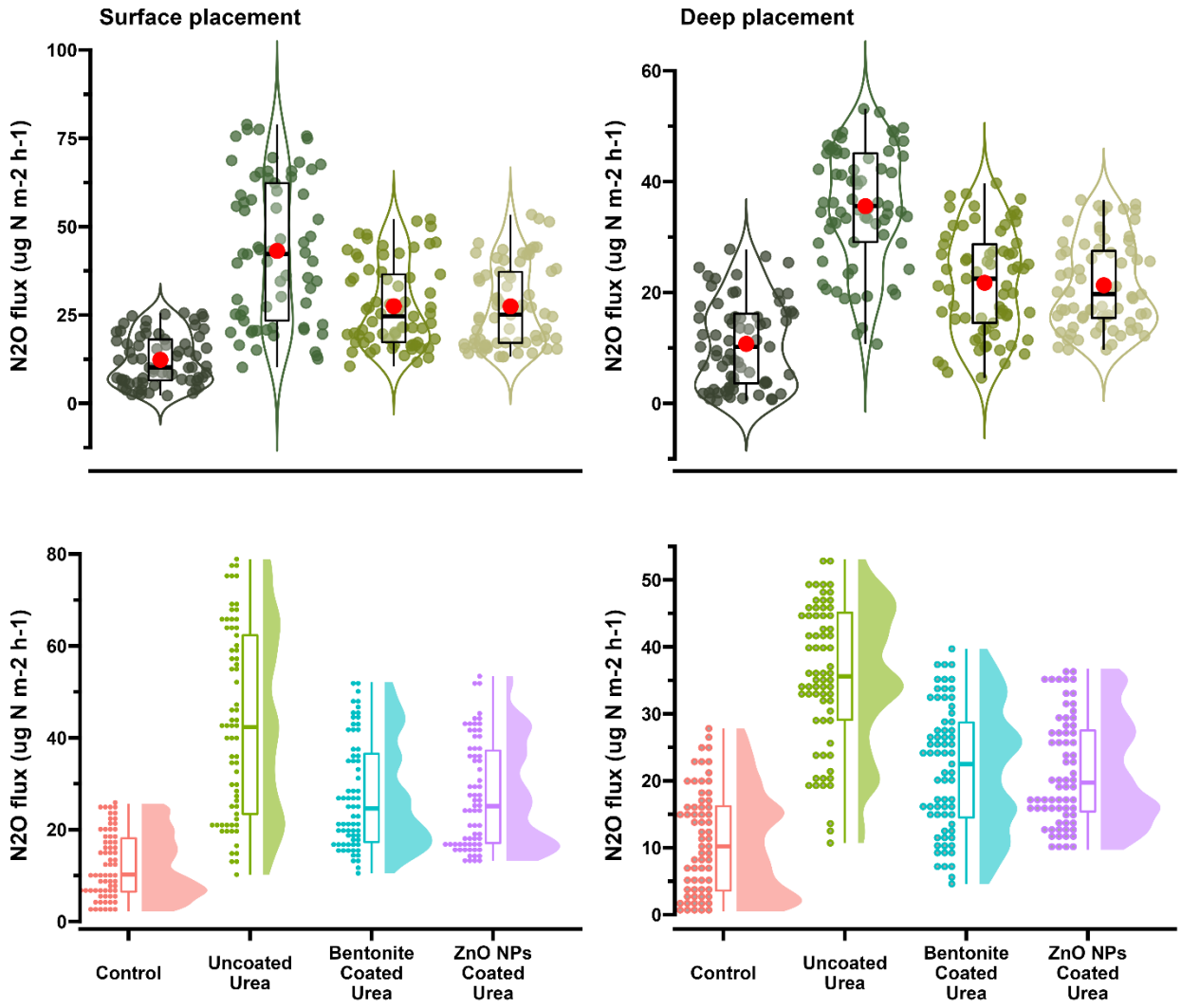

Figure 34: Distribution of N_2O flux points in sandy loam soil fertilized with conventional and Zn-coated urea using surface and deep placement methods

The maximum average daily flux from silty cay soil was 77.3 µg N m^{-2} h^{-1} recorded from the treatment where conventional urea was applied on the 4th day after the application of the first dose of fertilizer. While the maximum daily average flux value from sandy loam soil was 66.4 µg N m^{-2} h^{-1} from conventional urea on the 10th day of the first dose of fertilizer.

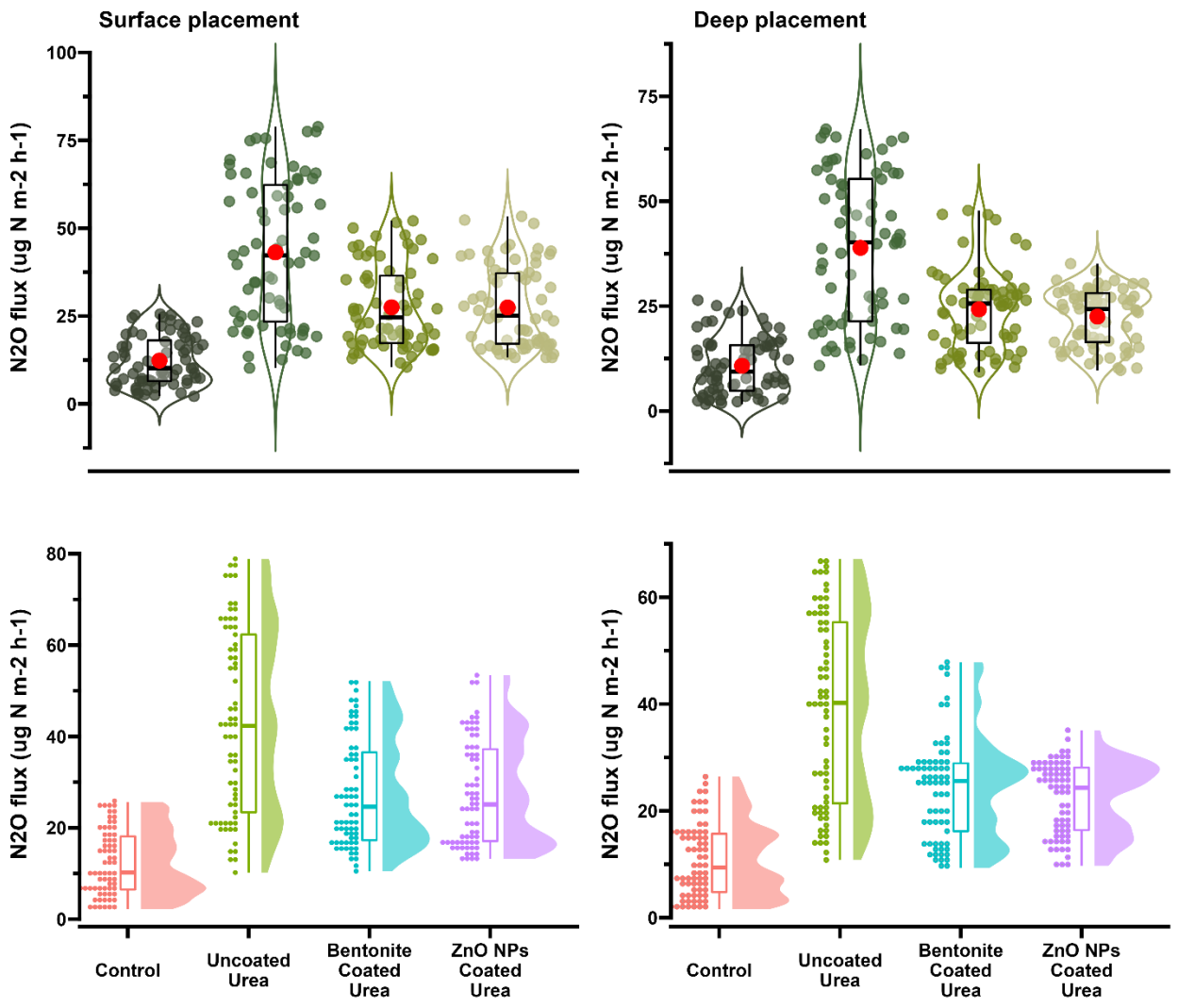

Figure 35:Distribution of N_2O flux points in silty clay soil fertilized with conventional and Zn coated urea using surface and deep placement methods

It was observed that the flux was higher during the first 15 days in both soils and after the application of a second dose of fertilizer on the 20th day the flux values were not as much higher as recorded during the first 15 days. The coated urea significantly delayed the N_2O emission and overall, the emission of N_2O from coated urea was lower ($p \leq 0.05$) as compared to the conventional urea (Figure 36 & Figure 37).

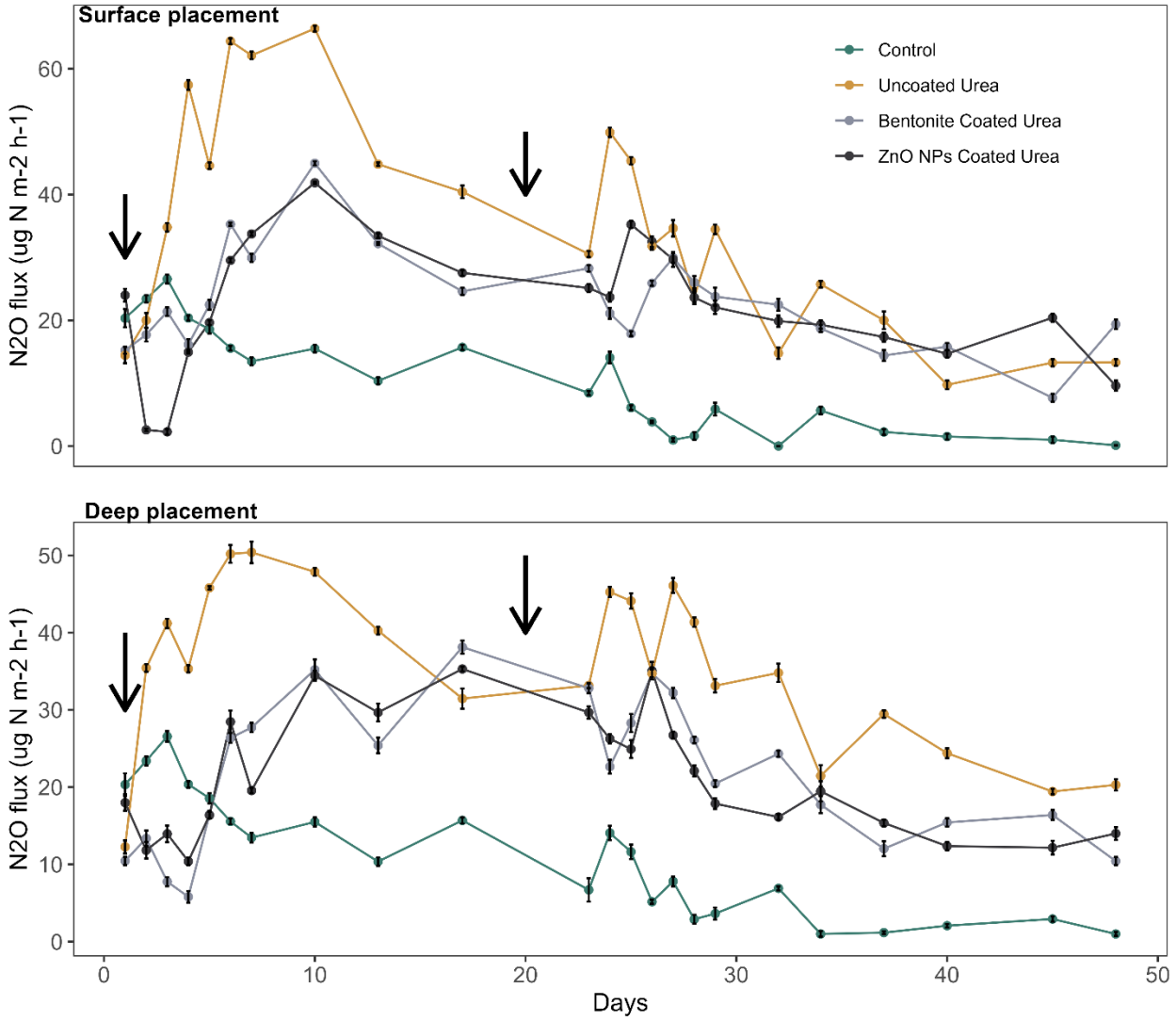

Figure 36: Daily average N_2O flux from sandy loam soil fertilized with conventional and Zn-coated urea using surface and deep placement methods. Arrows are indicating the time of fertilizer application.

The comparison of fertilizer application methods showed that the surface or deep placement of fertilizer have no significant effect ($p \geq 0.05$) on N_2O emission in sandy loam soil, while it was noted that the deep placement of the fertilizer significantly reduced the emission of the N_2O from silty clay soil (Figure 38 c & d).

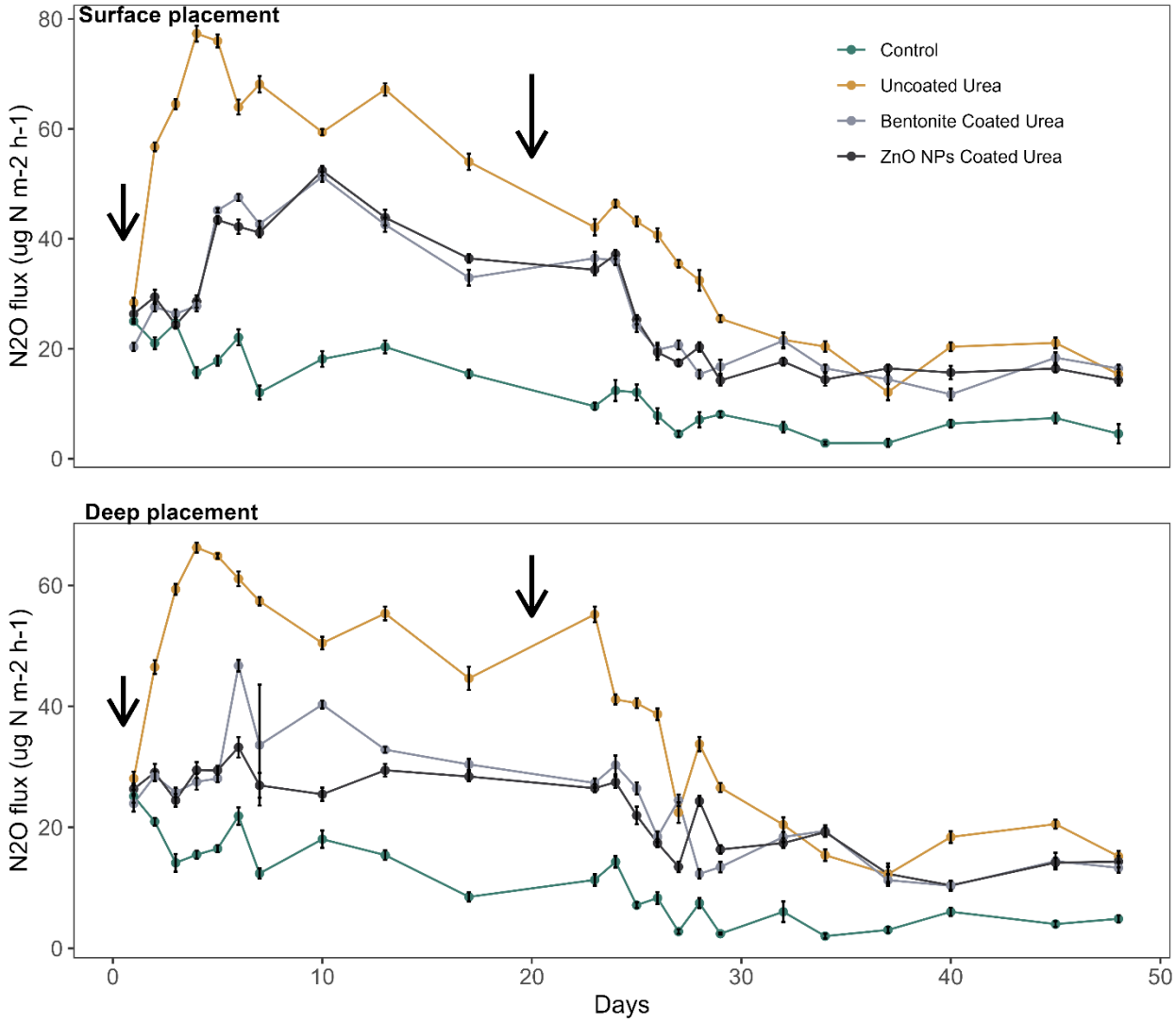

Figure 37:Daily average N_2O flux from silty clay soil fertilized with conventional and Zn coated urea using surface and deep placement methods. Arrows are an indication of the time of fertilizer application.

4.7.4.2. Cumulative N_2O emission

After the calculation of cumulative N_2O emission, it was noted that the cumulative emission of N_2O was significantly higher ($p \leq 0.0001$) in both soils where conventional urea was applied (Figure 38). While it was observed that there was no significant difference in cumulative N_2O emission between ZnO NPs coated urea and Zn-fortified nano-bentonite-coated urea. The cumulative N_2O emission in silty clay soil under conventional urea application was 14.3% higher as compared to sandy loam soil. The minimum cumulative N_2O emission was measured in control treatments where no fertilizer was applied. Even though the emission of N_2O from silty clay was higher as compared to sandy loam soil but the difference was statistically not significant ($p \geq 0.06$) (Figure 39).

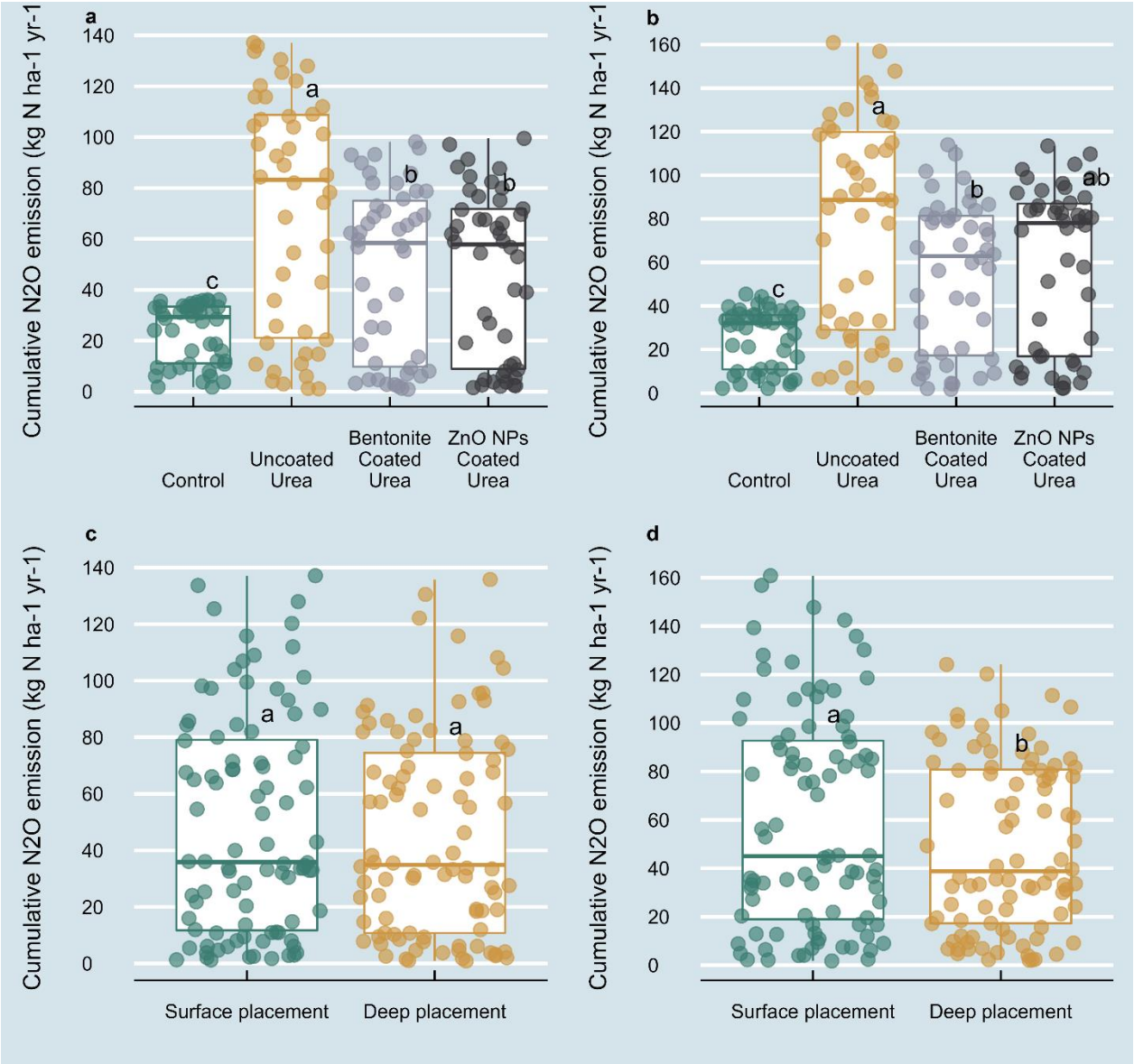

Figure 38: Cumulative N_2O emission from planted soils a) sandy loam soil b) silty clay soil c) Effect of application method on cumulative N_2O emission in sandy loam soil d) Effect of application method on cumulative N_2O emission in silty clay soil. The different letters showed a significant difference between treatments at α=0.05, n=3.

After cumulative N_2O emission, the emission factors were calculated for applied treatments in both soils (Table 7). Results showed that the EF for conventional urea in sandy loam soil was 5.3% in both surface placement and deep placement methods. The EFs for both coated urea (Bentonite coated and ZnO NPs coated) were significantly lower in sandy loam and silty clay soil (3.3% and 3.4%) and (3.2% and 2.95%) respectively. Similarly, the EF for conventional urea in silty clay soil was 6.1% when applied on the surface, while a significant reduction in EF (4.4%) was noted when applied deeper in the soil. The EFs for bentonite-coated urea in sandy loam, and silty clay soil were (3.3%, 3.65%,

and 3.2%, 2.7%) when applied at the surface and deep in the soil respectively. Similarly, the EFs for ZnO NPs coated urea in sandy loam, silty clay soil were (3.4%, 3.62% and 2.95%, 3.6%) when applied at the surface and deep in the soil respectively The EFs for coated urea was slightly higher in silty clay soil as compared to sandy loam soil. The application method has no significant effect on the EFs for coated urea in silty clay soil.

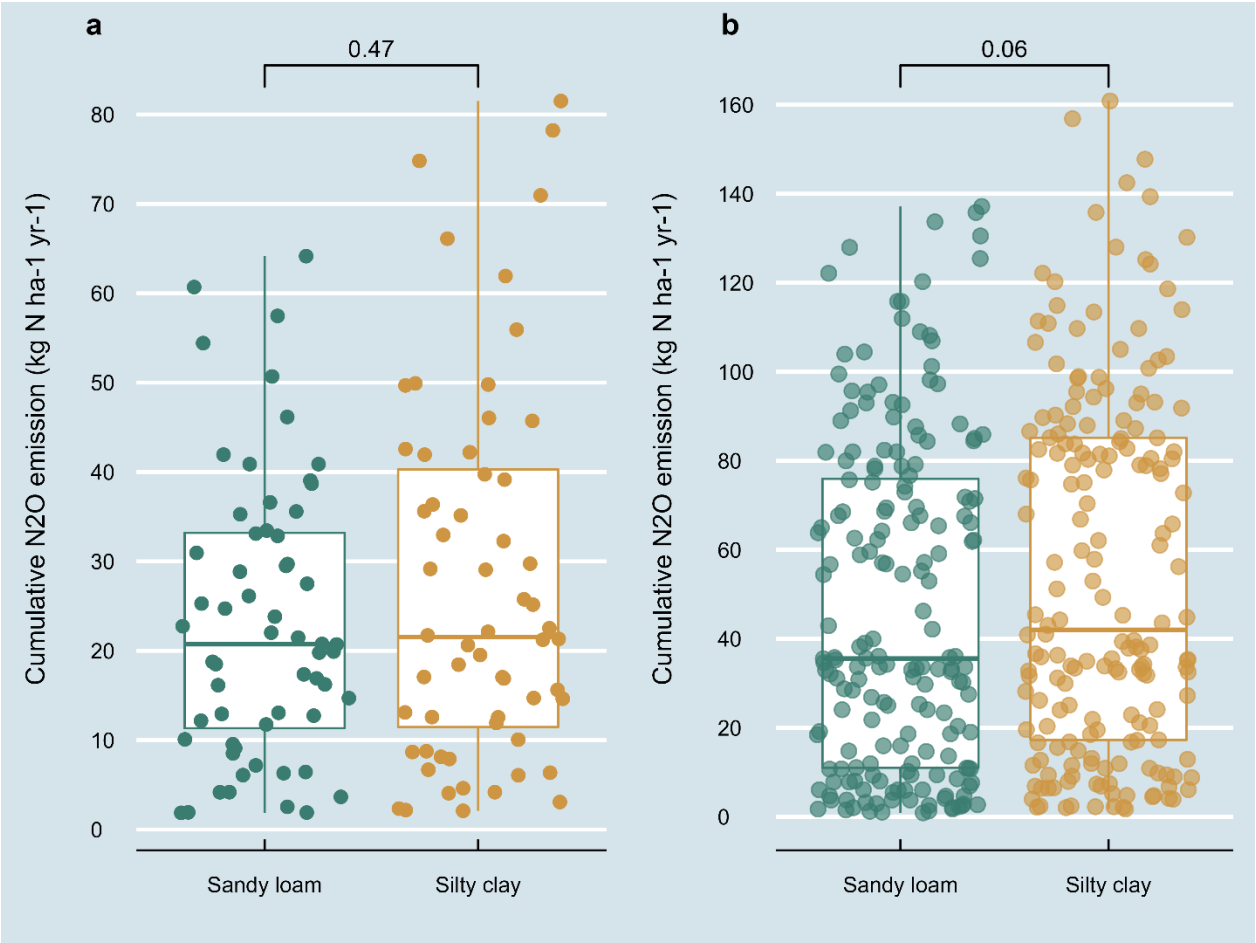

Figure 39: Effect of soil type on cumulative emission of N_2O a) Bare soil (without crop cover) b) planted soil (wheat crop)

5. DISCUSSION

5.1. Characterization

The crystal size of ZnO NPs ranged from 21 to 41 nm, with an average crystal size of 31 nm, according to X-ray diffraction data (Figure 14). The presence of ZnO in the form of nanoparticles was confirmed by peaks at planes (100), (002), (101), (102), (110), (103), (112), and (201). Our results are in accordance with the results presented by other researchers (Jayachandran et al., 2021; Umar et al., 2021). Nano-bentonite crystal sizes ranged from 6 to 50 nm, with an average crystal size of 32 nm (Figure 15). The results confirmed that the samples included montmorillonite and quartz. The montmorillonite is represented by the peaks at planes (001), (004), and (005). A similar set of findings was also published by (Burham and Sayed, 2016; Mohammed-Azizi et al., 2013).

SEM was used to do morphological analyses. The ZnO NPs looked to be clumped together and rectangular. (Figure 14). The aggregation may be due to the small size of the NPs (Tso et al., 2010). Because the Brownian motion of nanoscale particles is higher than that of bulk particles because of higher collision due to the presence of particles of the same mass, that is why the smaller size particles aggregate more quickly (Handy et al., 2008; Milani et al., 2012). Nano-bentonite emerged morphologically as a sheet-like layered structure (Figure 2). This sheet-like structure could reflect the montmorillonite in the sample, according to Chen et al. (2015).

The morphology of coated fertilizer granules was also examined (Figure 16), and it was discovered that all urea granules were entirely covered with the coating material, with no void spaces apparent, except for ZU2 granules, which had some surface cracking. The coating on the ZU1 and ZU2 granules appeared to be irregular as well. Using commercial vegetable oil as a binder, the ZU1 and ZU2 granules were coated with Zn-fortified nano-bentonite and ZnO NPs, respectively. The increased stickiness of vegetable oil may explain the uneven coating on ZU1 and ZU2 granules. Dimkpa, et al. (2020) also found that using vegetable oil as a binding agent reduced the efficacy of coating ZnO NPs and bulk ZnO onto urea granules. The coatings on ZU3 and ZU4 appeared to be consistent. Using stearic acid, paraffin oil, and paraffin wax as binding materials, the granules in ZU3 and ZU4 were coated with Zn-fortified nano-bentonite and ZnO NPs, respectively. The smoothness of the coating on ZU3 and ZU4 granules could be owing to the use of different binders, which result in less lump formation. Using paraffin oil as a binder during the coating process reduced the production of lumps and aggregates on the surface of granules, according to Irfan et al., (2018). When we employed paraffin oil as one of the binding materials in our experiment, the coating was smooth as well.

The elemental composition of coated urea granules was analyzed by XRF (Irfan et al., 2018). Results showed that the coating of Zn-fortified nano-bentonite contains Zn 1.03% while the Zn concentration in ZnO NPs coated urea was 2.01%.

5.2. Zn adsorption on nano-bentonite

According to the Langmuir model, nano-bentonite has an adsorption capacity of 13.96 mg g-1, whereas the Freundlich model has an adsorption constant of 1.0. (Table 5). According to the new model, nano-bentonite had an adsorption capacity of 16.272 mg g^{-1}. If we compare these models based on the R^2 value, the new model was the best-fit model $(R^2 = 0.992)$ followed by the Freundlich model $(R^2 = 0.94)$ and Langmuir model $(R^2 = 0.859)$. This is because the new model and the Freundlich model were created to measure multilayer adsorption, whereas the Langmuir model only measures cation monolayer adsorption (Czinkota et al., 2021; Khodabakhshloo et al., 2021).

The multilayer adsorption of Zn onto nano-bentonite was confirmed by the results of the adsorption model. Similarly, multilayer adsorption of various metal cations on bentonite clay has been reported by others (Burham and Sayed, 2016; Eren et al., 2010; Glatstein and Francisca, 2015). The new model isotherm yielded an adsorption capacity of 9.812 mg g^{-1} in the first cycle and 6.460 mg g^{-1} in the second cycle. The clay's adsorption capacity decreases with each cycle, possibly due to a decreased affinity of Zn^{+2} for adsorption sights (Perić et al., 2004; Yuvaraj and Subramanian, 2018). Figures 17 & 18 showed the behavior of adsorption isotherms.

5.3. Zn release from coated urea granules

In comparison to ZnO NPs coated urea (ZU2 and ZU4), the nano-bentonite-coated urea (ZU1 and ZU3) released much less Zn (Figure 19). The low amount of coated Zn (1%) in the form of Zn-fortified nano-bentonite, as compared to ZnO NPs (2%), is most likely the cause of the difference in Zn release. In terms of the amount of Zn released, however, there is no substantial variation between ZU1 and ZU3. Similarly, there is no substantial difference between ZU2 and ZU4. After 15 days, the greatest release of Zn from ZU1 and ZU2 was seen, but Zn release from ZU3 and ZU4 continued until the 30th day. This could be owing to the higher resistivity of the paraffin oil and paraffin wax employed in the ZU3 and ZU4 coatings. Various coating materials have different strengths and resistance, according to (Xiaoyu et al., 2013). Higher efficiency in the loading of Zn in ZU3 and ZU4 during the coating process could be another reason for the minor increase in Zn content. The findings of fitted kinetic models revealed that nano-bentonite-coated urea released Zn more slowly than ZnO NPs-

coated urea (Figures 40 & 41). When comparing bentonite-coated urea to ZnO NPs-coated urea, the dissolution rate constants reported from the Korsmeyer Peppas and Higuchi model were lower for bentonite-coated urea. The Korsmeyer-Peppas model was shown to be the most accurate kinetic model. The delayed release of Zn from nano-bentonite could be due to the intercalation of adsorbed Zn into the layers of nano-bentonite. An extended period is required to liberate the intercalated and adsorbed Zn. The slow release of intercalated urea by kaolinite clay mineral was also reported by Sempeho et al., (2015).

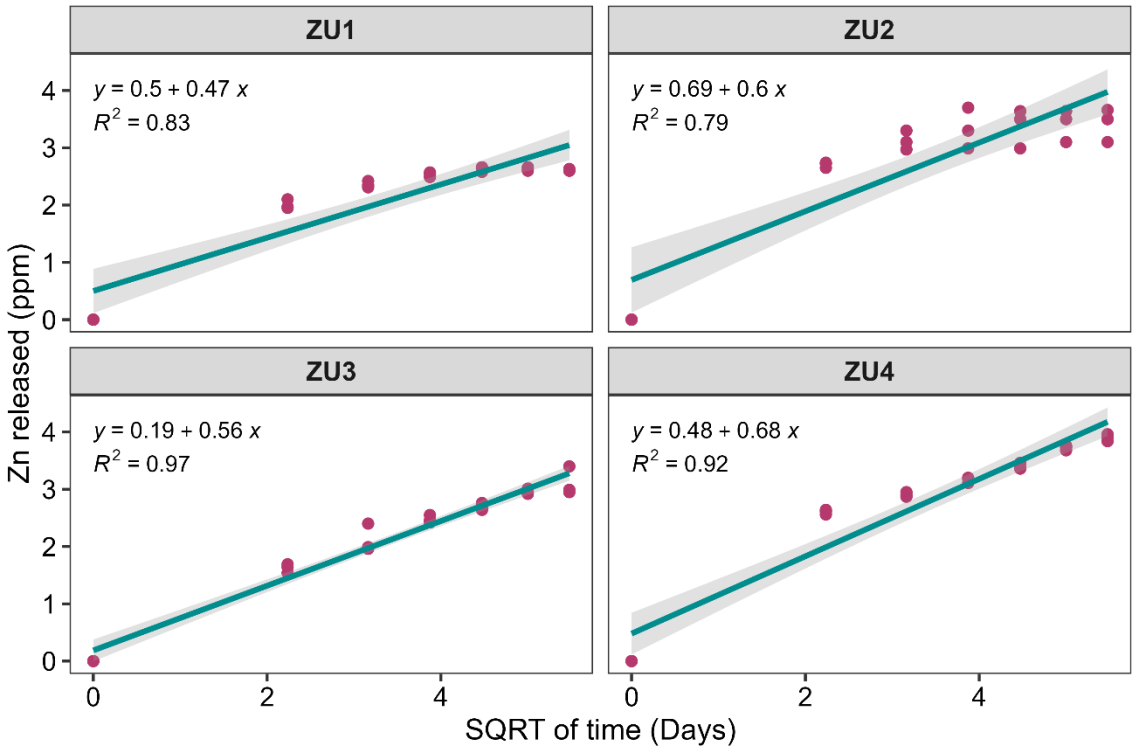

Figure 40: Zn release kinetics from Zn fortified nano-bentonite and ZnO NPs coated urea by using the Higuchi model

According to their findings, the total release of intercalated urea took roughly 150 hours. Nano-bentonite, on the other hand, possesses outstanding cation exchange capabilities, which could be one of the causes of the delayed cation release. Bennour, (2012) and Iskander et al. (2011) backed this up by reporting stronger sorption and slower release of Zn, Cu, and Mn by bentonite and zeolite, respectively. The rapid release of Zn in the case of ZnO NPs could be owing to direct exposure of ZnO NPs to the soil environment. Coated ZnO NPs had crystal sizes ranging from 21 to 41 nm. ZnO NPs are known for their slow-release qualities in addition to their coating material (Saleem et al., 2021). The release rate of Zn is dependent on the size of ZnO NPs (Milani et al., 2012). ZnO NPs have a bigger surface area, a higher surface charge density, and a higher reactivity; all of these features,

as well as other parameters such as pH, organic matter, and solution chemistry, have a major influence on the dissolution of ZnO NPs (Han et al., 2016; Umar et al., 2020). Mudunkotuwa et al. (2012) also investigated the size-dependent release of ZnO NPs and discovered that smaller particles released Zn more quickly than bigger ones.

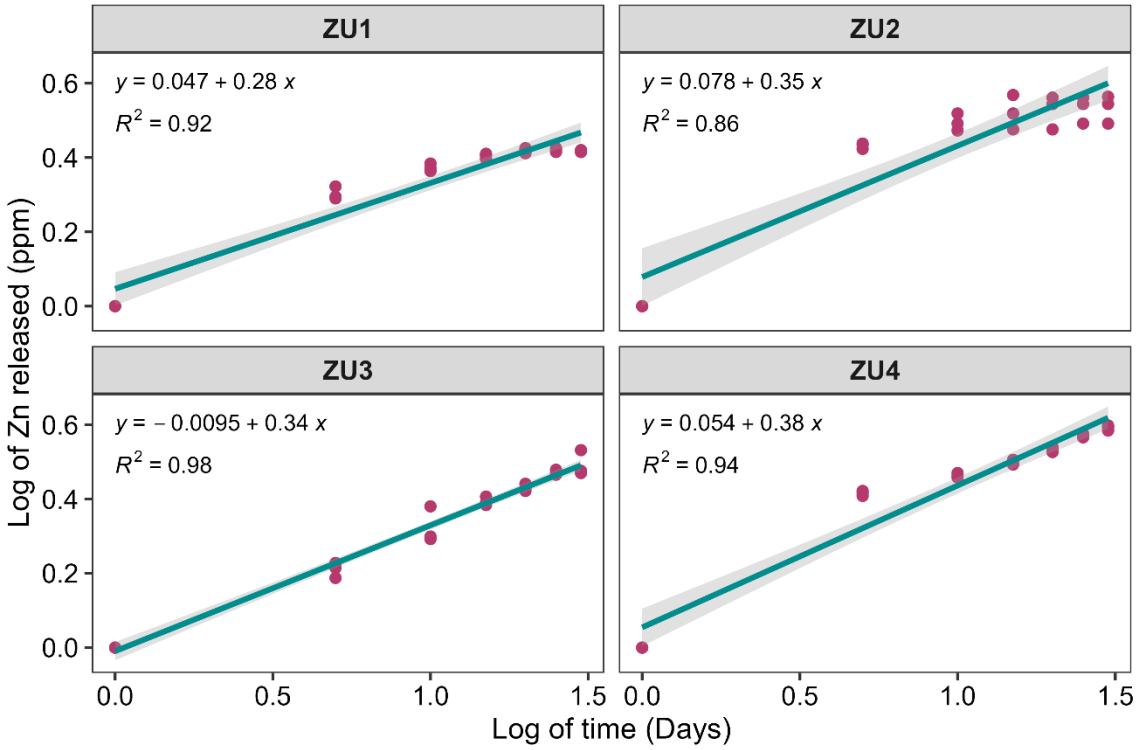

Figure 41: Zn release kinetics from Zn fortified nano-bentonite and ZnO NPs coated urea by using the Korsmeyer-Peppas model

5.4. N release from coated urea granules

The slow release of nitrogen from coated urea granules was validated by nitrogen release studies as compared to uncoated urea granules (Figure 20). When urea granules were coated in ZU3 and ZU4, the release of nitrogen was dramatically reduced when compared to ZU1, ZU2, and control. The gradual release of N by ZU3 and ZU4 was confirmed by the fitting of kinetic models (Korsmeyer Peppas and Higuchi). When compared to ZU1 and ZU2, the dissolution rate constants of ZU3 and ZU4 were lower (Figures 42 & 43). Both models were found to be the greatest match in our analysis based on R^2 values. Only 35% and 28% of N were released from ZU3 and ZU4 during the first 5 days, respectively, and it took roughly 15 days for the remaining N to be released from ZU3 and ZU4. Due to direct exposure of urea to the soil environment and urease enzyme, the total release of N from ZU1, ZU2, and control occurred in the first 5 days of the experiment. Affendi et al. (2020) noticed a similar pattern, reporting the full dissolving of uncoated urea granules within 18 hours of the experiment.

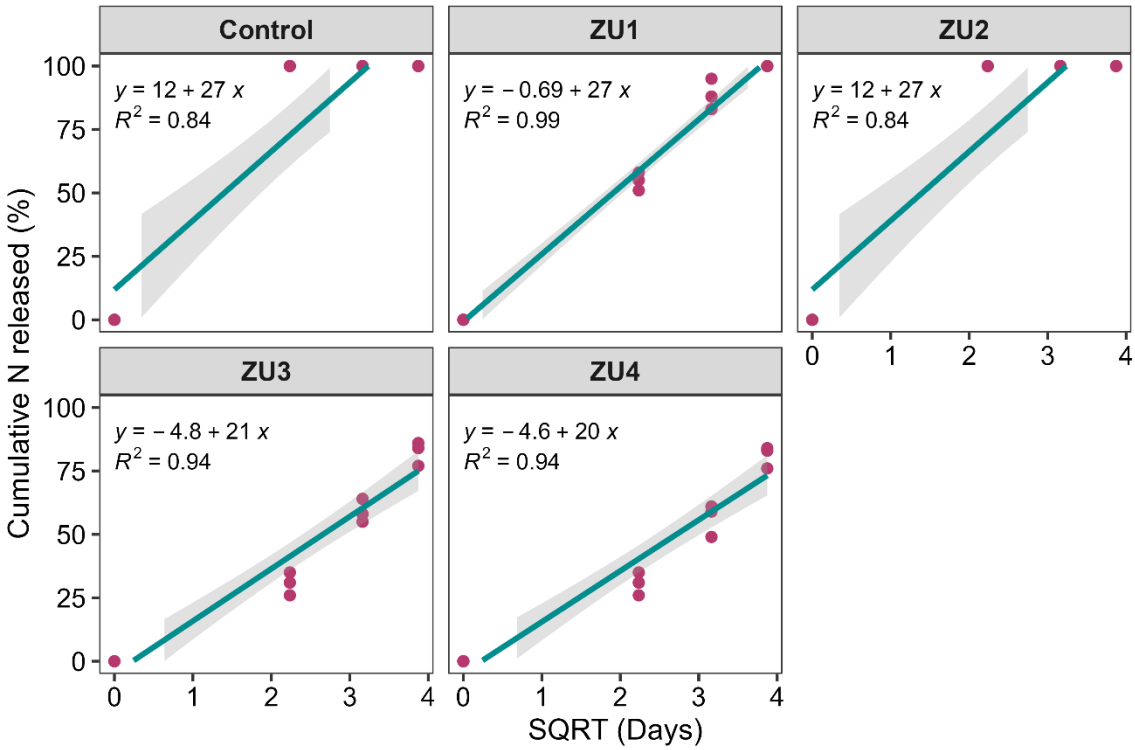

Figure 42: Evaluation of N release kinetics from coated urea by using the Higuchi model

The resistance offered by stearic acid and paraffin wax, which are hydrophobic may have slowed the release of coated granules due to limited water penetration (Chhowalla, 2017; Khalifeh and Burleigh, 2018). The slower disintegration and release of N from the granule are due to the diminished water absorption. Stearic acid is a non-toxic, biodegradable, and environmentally beneficial material (Hornberger et al., 2012); however, microorganisms break down it slowly, which may delay urea exposure to the urease enzyme. Stearic acid combines with calcium hydroxide to generate calcium stearate, which boosts the coating's strength (Affendi et al., 2020). Similarly, nanoparticles help to reduce the amount of NH^{4+} released by nitrogen fertilizers (Giroto et al., 2017). The nano-encapsulated fertilizers supplied nutrients slowly to the plants, according to Ditta (2012). Coating urea fertilizer with bentonite, similar to NPs, reduces urea fertilizer solubility. The network structure of bentonite, according to (Xiaoyu et al., 2013), increases the channel length for water penetration and reduces fertilizer dissolution. Conversely, bentonite's interaction with other binding materials lowered its porosity, resulting in less water penetration (Hermida and Agustian, 2019; Kamalakar et al., 2011). Coating thickness, on the other hand, has a significant impact on nutrient release (Ahmad et al., 2015; Tomaszewska and Jarosiewicz, 2006).

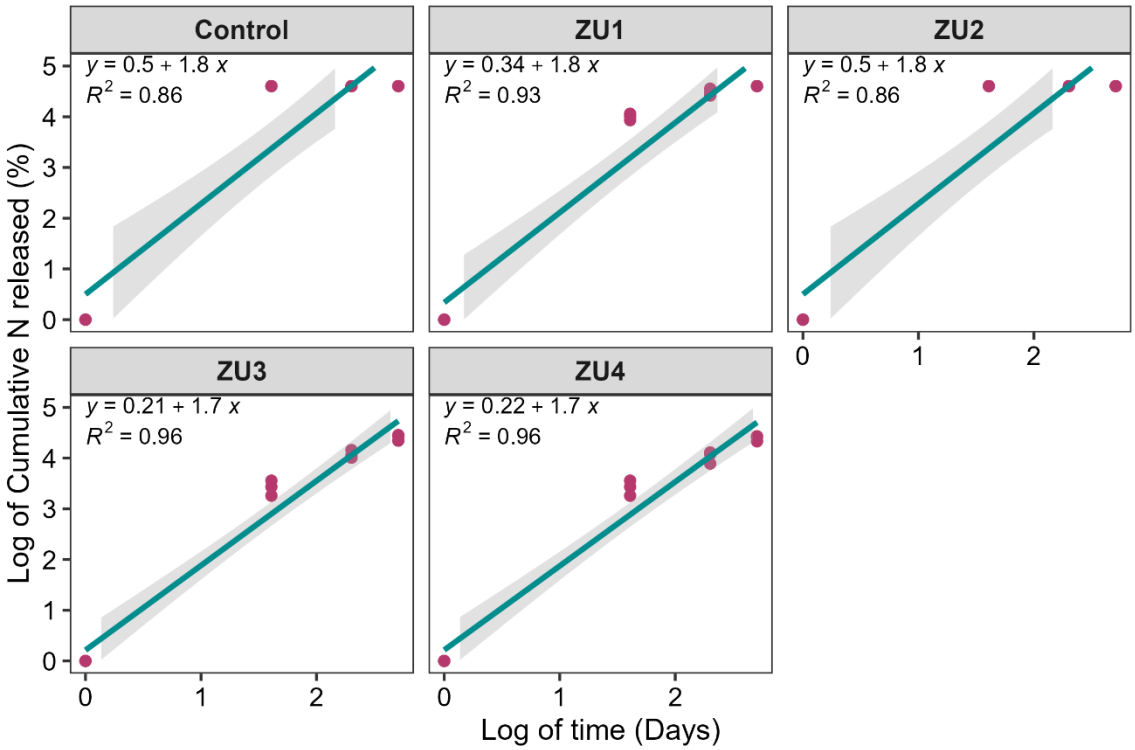

Figure 43: Evaluation of N release kinetics from coated urea by using the Korsmeyer-Peppas model

The coating's slow dissolving restricted fertilizer exposure to the soil environment and can also act as a urease inhibitor, resulting in a gradual release of NH^{4+} (Ransom et al., 2020). In our research, it was also discovered that granules with a thicker coating layer (ZU3 and ZU4) released N more slowly than granules with a thin coating layer (ZU1 and ZU2). Beig et al. (2020) also found that the rate of the coating had a positive impact on the gradual release of nitrogen. Similarly, the inverse relationship between coating percentage and nutrient release from coated fertilizers has been found by da Cruz et al. (2017) and Sofyane et al. (2020). They reported an 80 percent phosphorous release from DAP in 50 hours with a 3 percent coating, and 75 hours with a 4 percent coating. The loss of nutrients such as nitrogen from applied conventional fertilizers not only endangers the environment but also results in significant economic losses (Saleem et al., 2021; Wu and Liu, 2008). Coating fertilizers with essential plant nutrients is a good strategy for reducing fertilizer dissolution while also adding essential nutrients to the soil-plant system (Saleem et al., 2021; Wu and Liu, 2008; Dimkpa et al., 2020c).

5.5. Effect of NPs size, soil types, and incubation time on the solubility of ZnO NPs

5.5.1. Zn concentration in ZnO NPs spiked soil leachates

It has been observed that the size of NPs significantly ($p<0.05$) affects the pore water Zn concentration (Figure 21). The pore water Zn concentration was significantly higher in both soil types when spiked

with small size ZnO NPs. Results showed that cumulatively 10-13% higher concentration of soluble Zn was observed in the pore water of SC soil when spiked with small size NPs followed by 21-23% in SL soil as compared to large size NPs. The higher concentration of Zn by small size NPs might be due to their larger specific surface area (Legg et al., 2014). This fact was also supported by Mudunkotuwa et al. (Mudunkotuwa et al. 2012), who claimed the higher dissolution rate of 4 nm size ZnO NPs as compared to higher size ZnO NPs. According to Bian et al. (Bian et al. 2011), the fractions of atoms at the corners and edges of small size ZnO NPs have been much higher as compared to larger size ZnO NPs, which make it easy to break away the clusters and ions from the Lettice structure and enhance the solubility of ZnO NPs. The size of NPs also affects the aggregate size of NPs. It was reported that larger size NPs lead to higher size aggregate formation as compared to smaller size NPs (Lopes et al. 2014). They also reported that ZnO NPs with 30 nm size formed aggregates of 199 nm, smaller than the 769.2 nm formed by the NPs of >200 nm size.

Results of our experiment also showed that the soil type significantly affects the pore water Zn concentration. It was noted that pore water Zn concentration was significantly higher in SL soil as compared to SC soil. This might be due to the difference in soil properties like cation exchange capacity, organic matter, exchangeable calcium, and $CaCO_3$, EC, etc. between SL and SC soils. Soil pH is one of the main factors which affect the dissolution of ZnO NPs (Elhaj Baddar et al. 2019). In our study, the pH of SL soil is lower (7.10) as compared to SC soil (8.80). Under alkaline soil conditions complexation with organic ligands, chemisorption, and precipitation to the elements like Ca and P are the main mechanisms that reduced the solubility and availability of Zn and other cations (Nemček et al. 2020). This fact was also supported by Han et al. (Han et al. 2010) and Bian et al. (2011), who reported that Zn ions precipitate in the form of $Zn(OH)_2$ under alkaline conditions. Similarly, higher ionic strength also leads to the aggregation of NPs (Legg et al. 2014). Stewart et al. (2015) also reported a higher aggregation of ZnO NPs at 50 mM $CaCl_2$ as compared to 5 mM $CaCl_2$. These results support our findings as the SC soil possesses higher EC as compared to SL soil. The higher organic matter content and higher CEC could also be responsible for the reduced dissolution of ZnO NPs in SC soil. It was reported that organic matter fractions like humic acid and oxalic acid increased the aggregation of NPs which ultimately reduced their solubility (Pettibone et al. 2008; Dimkpa 2018). Similarly, Josko and Oleszczuk, (2013) and Moghaddasi et al. (2017) reported that higher organic matter content in the soil reduced the dissolution and bioavailability of ZnO NPs. In this study, SC soil consists of a higher amount of clay (51.95%) and higher CEC (40.1 $cmol^+ kg^{-1}$) as compared to SL soil and that could be one of the reasons for low solubility of ZnO NPs or higher

fixation of Zn^{+2} on the exchange sites of clay. It was reported in the literature that higher clay content reduced the availability of Zn (Sheoran et al. 2016; Romero-Freire et al. 2017), because of higher exchange sites and higher surface charge. According to Josko and Oleszczuk, (2013), Soils with higher CEC possess higher sorption affinity for NPs which leads to their immobilization.

5.5.2. The potential availability of Zn retained on soil matrix

To evaluate the potential availability of Zn retained on soil matrix extractant (EDTA 0.05M) was used. EDTA is a strong chelating agent which can extract a significant amount of metals from soil. EDTA can bind several heavy metals to make stable complexes (Cheng et al. 2020). According to Cheng et al. (2020), 0.05M EDTA extracted about 67% of Zn from the soil at pH 3 and the further increase in the concentration of EDTA did not increase the extraction efficiency significantly**.**

A significant amount of bioavailable Zn was extracted by 0.05 M EDTA from both SL and SC soils (Figure 22). On the other hand, soil type, size of NPs, and incubation period did not affect the extracted concentration of Zn significantly. The extraction efficiency of 0.05 M EDTA ranged from 48-53.4% in SL soil while it ranged from 54.2-56.5% in SC soil. The extraction efficiency of EDTA varied from low to very high depending on the conditions like soil type, type of metal, the concentration of metal, concentration of EDTA, and other soil properties (Alaboudi et al. 2020).

5.6. Nitrous oxide emission from planted and un-planted soils

Nitrous oxide emission was measured from silty clay and sandy loam soil fertilized with conventional and Zn-coated slow-release urea under planted and bare soil conditions. Results showed that during the first 15 days of fertilizer application the emission of N_2O from bare soil and planted soil was the same. This similarity in the N_2O emission might be because during the first 15 days the plants were not established properly. The root system of the plants was not established to uptake the higher amount of released N from the fertilizer. In addition, at the early stage of growth, the plant requirement of N is very low, so the excessively applied amount of N is lost to the environment. Similar findings were also reported by Senbayram et al. (2020), who stated that a significant increase in N_2O emission was measured from bare and planted soil after fertilizer application. The proliferation of specific microbial communities or the increase in microbial activity could also be a reason behind increased N_2O emission from planted soils (Guyonnet et al., 2017; Langarica Fuentes et al., 2018). It is reported that labile carbon in the form of root exudates can change the microbial community structure and increase the abundance of genes of bacteria and fungus and ultimately leading to increased N_2O emission through fungal denitrification (Zhong et al., 2018; Senbayram et al., 2018). In planted soils, the second

dose of fertilizer was applied on the 20th day of the experiment, and it was observed that the N_2O flux intensity was increased in the proceeding days, but the intensity of emission was not as much higher as it was after the 1st dose of fertilizer. This reduced emission of N_2O after 2nd dose of fertilizer application is because of the higher growth of the plants. The plants could have consumed a significant proportion of the available N. This fact is supported by Wei et al. (2010), who stated that in winter wheat crop the maximum N_2O emission was noted during the first 30 days of fertilization and after that, the emission was reduced significantly due to higher crop growth and root system establishment. Similar results were also reported in rice crops (Kim et al., 2021). The visualization of flux data (Figures 23, 34 & 35) showed that the flux points fluctuated on daily basis. This fluctuation is the characteristic of this process and mainly it occurs due to the process of wetting and drying (in semi-arid, arid regions, etc.) and freezing and thawing (in arctic regions) (Machado et al., 2021). During the wetting phase, the N_2O emission is reduced due to the entrapment of produced N_2O in soil pores while the N_2O emission increases during the drying phase because the entrapped N_2O released from the pores (King et al., 2021; Baral et al., 2022).

Cumulative N_2O emission was significantly higher from the conventional urea as compared to coated urea. It is because of the higher solubility of urea which resulted in the readily available N, which is lost to the environment in the form of gases and leached to the ground water. While in the case of coated urea the solubility of urea was slow which slowly released the available N to plants and ultimately reduced the N_2O emission. The results of this study are in accordance with the results presented by Ji et al. (2013) and Bordoloi et al. (2020) they reported that the cumulative emission of N_2O was significantly reduced with the application of starch-coated/neem-coated urea and resin-coated urea respectively. In silty clay soil under planted conditions, the placement of fertilizer deep in the soil significantly reduced the N_2O emission but the method of application have no significant effect on N_2O emission in sandy loam soil. The results of this study are in accordance with the results reported by Sosulski et al. (2020), who stated that the deep placement of fertilizer in sandy loam soil has no significant effect on N_2O and CO_2 emissions. The emission factors of N_2O were calculated and it was noted that the EFs in sandy loam and silty clay soils under planted and bare soil conditions were well below the defined EF of 1% for mineral fertilizers by IPCC (IPCC, 2006). In our study, the maximum EF was noted for conventional urea. For coated urea, the EFs ranged from 3.65-2.95% in planted soil. The EFs in bare soil ranged from 0.7-1.0% (uncoated urea) and 0.3-0.4% (coated urea). It was noted that under planted and bare soil conditions the EFs were higher in silty clay soil as compared to sandy loam soil. These higher EFs in silty clay are because of higher clay contents

because the chances of anaerobic conditions (denitrification) increased due to higher clay contents. Similar results were also reported by Hu et al. (2019), they reported higher N_2O emission from clay loam soil as compared to sandy loam soil. In addition to that, the higher organic matter in silty clay soil could also be the reason behind that higher emission. It was reported by Lesschen et al. (2011) that higher organic matter contents could increase the denitrification potential of the soil and ultimately increase the N_2O emissions.

5.7. Effect of coated urea on plant growth and chlorophyll contents

In this study, it was observed that the application of Zn-coated slow-release urea significantly increased the fresh and dry mass of wheat plants (Figure 26). This higher biomass production could be due to the higher uptake of N from the coated urea because the N is released slowly according to the plant's needs from the coated urea which reduced the losses and increase the plant growth. Similarly, Adhikari et al. (2016) and Gautam et al. (2022) also stated that the adequate supply of N at right time significantly increased plant growth and biomass production. The increase in biomass due to higher N uptake is because most of the proportion of the assimilated N by plants is allocated to the photosynthetic apparatus which results in increased photosynthetic activity and ultimately higher biomass production (Ghimire et al., 2017; Yan et al., 2019). Furthermore, the activity of enzymes involved in the N metabolism in plants such as nitrate reductase and GS also depends on the adequate supply of the N (Li et al., 2017; Li et al., 2021). It was also reported that the application of slow-release N fertilizer significantly increased the activity of the enzymes involved in carbon-nitrogen metabolism (Li et al., 2021). On the other hand, Zn also plays a significant role in plant growth and biomass production. The applied Zn-coated urea contains 1-2% of Zn along with N. Zinc is an important component of carbonic anhydrase which is involved in CO_2 fixation in C_3 plants. The adequate supply of Zn increased the activity of carbonic anhydrase which increased the photosynthetic efficiency and ultimately higher crop growth (Umar et al., 2020; Hacisalihoglu, 2020).

Results of Chlorophyll analysis showed that the chlorophyll *a* content was significantly ($p \leq 0.05$) higher in plants where N was applied (Figure 28). The increase in chlorophyll *a* content in plants under N fertilization is because N contents positively correlate with chlorophyll contents. The results of our study are in accordance with the results of Simko and Veres (2019), Wang et al. (2006), Wu et al. (2021), and Liu et al. (2019). They also reported the positive correlation of N fertilization with chlorophyll contents in different crops such as cotton, cabbage, and rice. It was also observed that chlorophyll *a* was significantly higher in coated urea treatments as compared to conventional urea in sandy loam soil, while there was no significant difference in chlorophyll *a* content between the

treatments in silty clay soil. This difference in chlorophyll *a* content in both soils is because of lower N contents in sandy loam soil due to low soil fertility. Another reason could be the leaching of N below the root zone in sandy loam soil when conventional urea was applied which is readily soluble and leads to the lower uptake of N and ultimately lower chlorophyll *a* (Qi et al., 2021). On the other hand, there was no significant difference in chlorophyll *b* contents between the treatments. While the total chlorophyll contents were significantly higher in N-fertilized plants as compared to the control. Furthermore, the Zn concentration in coated urea could also have a significant effect on plant chlorophyll content because Zn is involved in enzyme activation, it also acts as a structural component of proteins and is thus involved in the normal biosynthesis of the pigments (Samreen et al., 2017). It was reported that the application of ZnO NPs significantly increased the chlorophyll contents in maize crop (Umar et al., 2020; Adil et al., 2022).

5.8. Effect of coated urea on plant and soil N contents

After harvesting the plants were analyzed for N contents and the results showed that a significantly higher ($p \leq 0.001$) concentration of N was found in plants that were fertilized with Zn-coated slow-release urea as compared to conventional urea and control treatment (Figure 32). This increase in N contents in wheat plants is due to the slow release of N from the coated urea granules which increased the N uptake and accumulation by plants. Similar results were also presented by Yaseen et al. (2021) and Ghafoor et al. (2022), they stated that the application of coated N fertilizers in the wheat crop grown in semi-arid regions significantly increased the NPK concentration in wheat plants. In addition, Ali et al. (2020) stated that the application of neem-coated urea significantly increased the N contents in maize shoots due to the higher availability of N. On the other side, the application of Zn along with N could also increase the N acquisition by plants because Zn upregulates the expression of nitrate and ammonium transporter genes. This fact is supported by Ji et al. (2022), who reported that the Zn in the presence of N increased the expression level of both ammonium (OsAMT3;2, OsAMT1;3, OsAMT1;1, OsAMT2;3, OsAMT1;2) and nitrate (OSNRT2.2, OsNRT1.1B, OsNRT1.1A, OsNRT2.1) transporter genes in rice. The N contents in plants grown in silty clay soi were higher than the N contents in the plants grown in sandy loam soil. This difference could be due to the higher CEC of silty clay soil which also contain higher organic matter as compared to sandy loam soil. Similarly, Gong et al. (2020) reported that the soil C:N ratio significantly affected the plant N contents.

Analysis of soil samples (pre-sowing and post-harvest) showed that the N contents were significantly higher in the samples where N was applied as compared to control and pre-sowing soil samples in silty clay soil (Figure 33). In the case of sandy loam soil, the coated urea application showed higher

N contents in the soil as compared to the control but there was no difference between the conventional urea treatment and the control. There are a couple of reasons behind this difference between both soils. Firstly, the silty clay soil naturally has higher organic matter, higher N contents, and higher CEC as compared to sandy loam. Secondly, the immobilization rate of the mineralized N from the fertilizer could be higher in silty clay soil due to higher microbial biomass and higher microbial activity. The affinity of NH_4^+ to move on to the exchange sites could be higher in silty clay soil due to higher negative sites. These facts were supported by Li et al. (2022a), who recently found that soil types significantly affect the soil's total N contents. It was stated that the soils with higher clay contents and higher soil organic carbon possess higher total nitrogen as compared to the coarse texture soils. Similar results were also presented by Wang et al. (2009) and Liu et al. (2006).

5.9. Effect of coated urea on plant and soil Zn contents

Plant Zn analysis showed that the application of Zn-coated urea significantly ($p \leq 0.05$) increased the plant Zn contents (Figure 30). The Zn contents by the application of ZnO NPs coated urea was higher as compared to Zn fortified nano-bentonite but the difference is statistically non-significant ($p \geq 0.05$). It is widely reported in the literature that the application of Zn fertilizer significantly increased the Zn concentration in plants. Our results are in accordance with the results of different researchers who reported the increase of Zn in different crops by the application of Zn fertilizer such as winter wheat (Liu et al., 2019a; Wang et al., 2017a), Maize (Ali Raza et al., 2021), Rice (Ghoneim, 2016), and canola (Afsahi et al., 2020). The comparison of soil types showed that the plants grown in silty clay soil have higher ($p \leq 0.015$) Zn contents as compared to the plants grown in sandy loam soil. This higher Zn concentration in plants grown in silty clay soil could be due to higher bioavailable Zn contents in the soil before the start of the experiment. The silty clay soil consists of approximately 12% higher bioavailable Zn concentration as compared to sandy loam soil, which could be the reason behind the higher Zn concentration in plants.

Soil Zn analysis showed that the application of ZnO NPs coated urea significantly ($p \leq 0.001$) increased the post-harvest soil Zn levels as compared to Zn-fortified nano-bentonite application (Figure 31). This higher Zn content in soil by ZnO NPs coated urea could be due to higher Zn concentration in the coating (2% Zn) as compared to Zn-fortified nano-bentonite which contains a lower amount of Zn in the coating (1% Zn). Post-harvest soil Zn by the application of ZnO NPs coated urea was slightly higher than the Zn concentration before the start of the experiment which showed that ZnO NPs can increase or maintain the soil fertility status. This fact is supported by Sheteiwy et al. (2021) and Umar et al. (2021), who reported an increase in soil fertility with the application of ZnO NPs.

6. CONCLUSION AND RECOMMENDATIONS

6.1. Conclusion

For the fulfillment of the aims of this study the following objectives were undertaken 1) Synthesis and characterization of ZnO NPs and Zn fortified nano-bentonite. 2) Development and characterization of Zn-fortified nano-bentonite and ZnO NPs coated slow-release urea fertilizer using different binding materials (stearic acid and paraffin wax). 3) Evaluation of Zn and N release characteristics from slow-release macro-micronutrient fertilizer. 4) Evaluation of the dissolution of ZnO NPs, and $ZnSO_4$ in two different soils. 5) Evaluation of N_2O emission from coated and uncoated urea fertilizer under bare and planted soil conditions. 6) Evaluating the comparative effect of coated and uncoated urea on plant growth and development.

The first specific objective was to evaluate the synthesis and characterization of ZnO NPs and Zn-fortified nano-bentonite. The precipitation method for the synthesis of ZnO NPs proved an effective method to synthesize ZnO NPs with a size range of less than 100 nm. The shape of the NPs was round to rectangular. Nano-bentonite was proved an effective adsorbent for the cations based on the previous studies conducted for the removal of heavy metals from the liquid media. We used nano-bentonite to evaluate its adsorption potential specifically for Zn. It was proved that a significant amount of Zn was adsorbed on nano-bentonite based on the multilayer adsorption phenomenon.

The second specific objective was to prepare slow-release Zn-coated urea. To reduce the dissolution of urea hydrophobic materials were used such as stearic acid, paraffin wax and paraffin oil, vegetable oil, and the final coating of Zn-containing materials such as ZnO NPs and Zn-fortified nano-bentonite was used. Based on the characterization it was concluded that the coating was even and fine when paraffin oil was used as a final binder as compared to vegetable oil.

The third objective was to evaluate the release of N and Zn from the coated slow-release urea. It was concluded that the coating of urea with stearic acid, paraffin wax, and paraffin oil significantly delayed the solubility of urea as compared to uncoated urea. It was also concluded that both ZnO NPs and Zn-fortified nano-bentonite can act as an effective Zn carrier and could be used as a coating material on macronutrient fertilizers.

The fourth objective was to evaluate the dissolution of ZnO NPs in different soils. Based on the results it was concluded that the ZnO NPs significantly reduced the release of Zn as compared to conventional $ZnSO_4$ because the pore water Zn concentration was higher in the case of $ZnSO_4$. It was also

hypothesized that the fixation of ZnO NPs was less in both soils because the extraction of Zn using 0.05M EDTA was significantly higher in the case of ZnO NPs.

The fifth objective was to evaluate the N_2O emission from coated and uncoated urea under bare and planted soil conditions. It was concluded that the coated urea delayed the N_2O emissions and reduced the daily flux intensity in both soils under planted and bare soil conditions. It was also proved that after the establishment of the crop cover the emission of N_2O was significantly reduced. In general, it was concluded that the use of coated slow-release urea can reduce the environmental impact of applied nitrogen in agroecosystems.

The sixth specific objective was to evaluate the effect of coated fertilizer on plant growth. It was concluded that slow-release coated urea significantly increased the biomass production of wheat. The chlorophyll contents of the wheat plants were also increased with the application of slow-release urea.

6.2. Future Research Recommendations

Based on the findings this study proposes the following recommendations for future research:

- This study proved the general effectiveness of stearic acid and paraffin wax in reducing the solubility of urea. It is suggested for future research that the different concentrations of the coating materials such as stearic acid and paraffin wax should be tried to further improve the effectiveness of the coating in reducing the solubility of urea.
- The dissolution of ZnO NPs should be tested on a long-term basis and different factors such as pH, ionic strength, and the speciation of ZnO NPs in soil solution should be evaluated in future research.
- In this study, the N_2O emission from coated and uncoated urea was evaluated under laboratory conditions. In future research, it is recommended to evaluate the efficiency of coated urea under field conditions.
- It is also recommended that the variable rates of coated fertilizer application should be used to evaluate the effective amount of coated fertilizer for a specific crop.

7. SUMMARY

To meet the growing population's global food demand, a significantly higher amount of N is applied as chemical fertilizers in the agroecosystems. Currently, the nitrogen use efficiency (NUE) is very low (30-50%) in agroecosystems. In the modern agricultural system, about 50-70% of the applied N in the form of synthetic fertilizers is lost in the environment. It was reported that the use of slow-release N fertilizers can reduce the N losses and their environmental impact. The use of hydrophobic materials for coating the fertilizer granules is one of the strategies which is used to reduce the solubility of fertilizers. In this study, we evaluated the effectiveness of stearic acid and paraffin wax as hydrophobic materials to reduce the solubility of urea. We also coated micronutrient Zn on to the urea granules. To evaluate the environmental impact of coated urea nitrous oxide emission was measured. For this purpose, objectives were devised 1) Synthesis and characterization of ZnO NPs and Zn fortified nano-bentonite. For the synthesis of ZnO NPs precipitation method was followed and during this method, $ZnSO_4.H_2O$ and KOH were used as Zn salt and precipitating agent respectively. The Zn adsorption potential of nano-bentonite was evaluated by batch adsorption method. The fortification of nano-bentonite with Zn was carried out by the sonication method. 2) Development and characterization of Zn-fortified nano-bentonite and ZnO NPs coated slow-release urea fertilizer using different binding materials (stearic acid and paraffin wax). We coated stearic acid and paraffin wax on urea granules by heating them till their melting point followed by the addition of urea granules and mixing with a spatula. We used calcium hydroxide as an inert material to get the free-flowing granules. In the next step, we coated Zn materials (ZnO NPs or Zn-fortified nano-bentonite) as the last coating using paraffin oil as a binder. Characterization of ZnO NPS, nano-bentonite, and coated urea granules was carried out by using XRD and SEM. 3) Evaluation of Zn and N release characteristics from slow-release macro-micronutrient fertilizer. For this purpose, we conducted an incubation experiment using sandy loam soil. The coated granules were incubated, and moisture contents were maintained at 60% of field capacity for 30 days. The samples were taken and analyzed for N and Zn at a 5-day interval. 4) Evaluation of the dissolution of ZnO NPs, and $ZnSO_4$ in two different soils. Incubation of ZnO NPs (small size and large size) in sandy loam and silty clay soil for 7 and 14 days was done. Leaching of soil was performed using an Isocratic pump attached to stainless steel column using distilled water. The leachate was analyzed for Zn concentration. 5) Evaluation of N_2O emission from coated and uncoated urea fertilizer under bare and planted soil conditions. In the first experiment, the fertilizer was mixed with soil and water contents were maintained at 80% of the filed capacity. The N_2O measurement was carried out for 15 days on daily basis using the N_2O analyzer. In the second

experiment, the wheat crop was planted in both soils, and fertilizer was applied in two split doses using two application methods (surface placement and deep placement). The N_2O was measured for 48 days with regular intervals using the static chamber method. 6) Evaluating the comparative effect of coated and uncoated urea on plant growth and development. Plant fresh and dry biomass and chlorophyll contents were measured for plant growth evaluation.

Characterization results showed that the crystal size of the ZnO NPs and nano-bentonite ranged well below 100 nm. The SEM images confirmed the even coating of stearic acid and paraffin wax on urea granules. The Langmuir and Freundlich model showed significant adsorption of Zn on nano-bentonite following a multilayer adsorption phenomenon. Results of the experiment conducted to evaluate the N and Zn release characteristics from coated urea showed that the coating of hydrophobic materials significantly delayed the complete dissolution of urea. It took about 15 days for the complete dissolution of coated urea, while the uncoated urea completely released all the N within the first 5 days. In addition to that, coating ZnO NPs and Zn-fortified nano-bentonite proved an effective way to supply Zn along with N to plants. Both ZnO NPs and Zn-fortified nano-bentonite released the Zn slowly and for a longer period. Results of the experiment conducted to evaluate the dissolution of ZnO NPs showed that the release of Zn from ZnO NPs was very slow as compared to $ZnSO_4$. After extracting the soil with 0.05 M EDTA it was observed that the most of Zn from ZnO NPs was in bioavailable form. Nitrous oxide emissions results showed that during the first 15 days the emission of N_2O was almost the same in both planted and bare soil, while the emission decreased significantly after the establishment of the crop cover. Deep placement of fertilizer proved an effective method in silty clay soil where it reduced the N_2O emission as compared to surface application. In general, silty clay soil showed higher N_2O emission as compared to sandy loam but the difference was not statistically significant. In the end, it was concluded that the use of hydrophobic material coting on fertilizer granules can reduce nutrient losses to the environment and increase nutrient use efficiency and crop production. The use of nano-bentonite as a Zn carrier proved an effective and environmentally friendly method. It was also concluded that the use of Zn-containing materials as a coating on macronutrient fertilizer is sustainable and environmentally friendly technology to supply macro and micronutrients together to the plants.

8. NEW SCIENTIFIC RESULTS

1. In this study, nano-bentonite was tested as a Zn carrier and from the results, it was proved that nano-bentonite can adsorb a significant amount of Zn and can release it slowly courtesy of the cation exchange phenomenon. Previous studies only reported the use of bentonite and nano-bentonite as an adsorbent for the removal of pollutants from liquids. Our study is the first of its kind which is evaluating its role as an environmentally friendly nutrient carrier for crop production.
2. Coating of urea with hydrophobic materials and Zn carriers proved an effective strategy to supply both macro and micronutrients together to the crops. Even though ZnO NPs used widely as a coating material, this study is the first of its kind where Zn-fortified nano-bentonite was used as a Zn carrier on urea granules. So, this study provides insight into the further utilization of nano-bentonite as an environmentally friendly nutrient carrier.
3. The complete release of N from coated urea was delayed up to 15 days as compared to uncoated urea which completely released the N within the first 5 days. The release of Zn from coated urea was reduced and the upward trend in Zn release was noted even on the 30th day of the experiment.
4. The coating of urea proved an effective strategy in reducing the N_2O emission as compared to conventional urea. Results showed a significantly higher cumulative N_2O emission from conventional urea as compared to coated urea. The emission factor of coated urea was lower than the of conventional urea.

Figure 44: Working photos during the experiments

9. ACKNOWLEDGMENT

I wish to humbly extend my heartiest and most sincere gratitude to all the personages who have supported me in this endeavor and influenced my work in one way or the other. Clearly, without their active guidance, support, cooperation, and encouragement, the completion of this project would have remained a mirage.

I am deeply indebted to my two respected supervisors: Dr. Imre Czinkota and Dr. Miklós Gulyás for their scientific and moral support during my research and dissertation writing. Their professionalism, dynamism, commitment, sincerity, motivation, friendship, and empathy deeply inspired me to accomplish this assignment. The invaluable guidance of Dr. Imre in methodology has greatly sharpened my capacity to think logically and to present the research work as clearly as possible. I am extremely grateful to Dr. Miklós for the enormous support in developing the sampling design, and the execution of the experiments and analysis. My heartfelt gratitude to Prof Erika Micheli, the head Doctoral School of Environmental Sciences for creating a very hospitable and welcoming atmosphere at the doctoral school. I sincerely appreciate Kárász Ildikó, the institute administrator for being joyfully helpful as far as administrative matters are concerned. I am grateful to the lecturers and all the staff at the institute of Environmental Sciences for their invaluable help in my PhD training. Quite an amazing team of friendly, approachable, and welcoming souls, fun to work with!

A special mention and appreciation to Dr. Janos Balogh for his insights and provision of resources and instrumentation during the experimentation. Without the help of Dr. Janos, it would be hard to fulfill the objectives of my research. My colleague, András Sebők, your help and guidance during my laboratory work is highly appreciated. Dr. Miklós, my supervisor and team leader, your determination during experiments was astounding. I highly appreciate the help and guidance of Anita Takács, the laboratory assistance during the lab work, and sample analysis.

Many thanks to the entire management of the Hungarian University of Agriculture and Life Sciences for creating a conducive environment for the international student community. Special appreciation to Ms. Tassy Zsuzsanna, the coordinator of international students (then) for the overwhelming support and motherly love and care to the international student community. I am thankful to the Doctoral, Habilitation, and Science Organization Office for their invaluable services and support to PhD students. I extend my gratitude to the Head of the Doctoral office, Törökné Hajdu Mónika for her indefatigable dedication.

I am extremely grateful to all my friends and family who (directly or indirectly) helped me to survive all the stress and to accomplish this project. I acknowledge with a deep sense of reverence, my gratitude towards my family for their moral support. A special mention to Dr. Farheen Naz, I must say there are certain people who make the world a better place just by being in it, and you are one of those people. Thank you very much for all your support and guidance and for being with me throughout that period.

Last but most importantly, I am ineffably indebted to Allah for His sufficient grace that has sustained me to this end. *"….if anyone desires a reward in this life, We shall give it to him; and if anyone desires a reward in the Hereafter, We shall give it to him. And swiftly shall We reward those that (serve us with) gratitude" (3:145).*

10.APPENDICES

A1: Bibliography

Abd El-Hady, M., & Eldardiry, E. I. (2016). Effect of different soil conditioners application on some soil characteristics and plant growth III-Effect on saturated and unsaturated water flow. *International J. of Chem Tech Res*, *9*, 135-143.

Abdel Latef, A. A. H., Abu Alhmad, M. F., & Abdelfattah, K. E. (2017). The possible roles of priming with ZnO nanoparticles in mitigation of salinity stress in lupine (Lupinus termis) plants. Journal of plant growth regulation, 36(1), 60-70.

Adhikari, P., Baral, B. R., & Shrestha, J. (2016). Maize response to time of nitrogen application and planting seasons. Journal of Maize Research and Development, 2(1), 83-93.

Adhikari, S., Spaeth, P., Kar, A., Baaske, M. D., Khatua, S., & Orrit, M. (2020). Photothermal microscopy: imaging the optical absorption of single nanoparticles and single molecules. ACS nano, 14(12), 16414-16445.

Adil, M., Bashir, S., Bashir, S., Aslam, Z., Ahmad, N., Younas, T., ... & Elshikh, M. S. (2022). Zinc oxide nanoparticles improved chlorophyll contents, physical parameters, and wheat yield under salt stress. *Frontiers in Plant Science*, *13*.

Affendi, N. M. N., Mansor, N., & Mathialagan, R. (2020). Development and characterization of allicin using palm stearin as a binder on urea granules. Journal of Plant Nutrition, 43(5), 621-628.

Afsahi, K., Nazari, M., Omidi, H., Shekari, F., & Bostani, A. A. (2020). The effects of different methods of zinc application on canola seed yield and oil content. Journal of Plant Nutrition, 43(8), 1070-1079.

Ahmad, N. N. R., Fernando, W. J. N., & Uzir, M. H. (2015). Parametric evaluation using mechanistic model for release rate of phosphate ions from chitosan-coated phosphorus fertiliser pellets. Biosystems Engineering, 129, 78-86.

Akther, M. S., Das, U., Tahura, S., Prity, S. A., Islam, M., & Kabir, A. H. (2020). Regulation of Zn uptake and redox status confers Zn deficiency tolerance in tomato. Scientia Horticulturae, 273, 109624.

Alaboudi, K. A., Ahmed, B., & Brodie, G. (2020). Soil Washing Technology for Removing Heavy Metals from a Contaminated Soil: A Case Study. Polish Journal of Environmental Studies, 29(2).

Ali Raza, H. M., Bashir, M. A., Rehim, A., Raza, Q. U. A., Khan, K. A., Aon, M., ... & Geng, Y. (2021). Effect of K and Zn Application on Biometric and Physiological Parameters of Different Maize Genotypes. Sustainability, 13(23), 13440.

Ali, M. A., Naveed, M., Mustafa, A., & Abbas, A. (2017). The good, the bad, and the ugly of rhizosphere microbiome. In Probiotics and plant health (pp. 253-290). Springer, Singapore.

Ali, M., Maqsood, M. A., Azizl, T., & Awan, M. I. (2020). Neem (Azadirachta indica) oil coated urea improves nitrogen use efficiency and maize growth in an alkaline calcareous soil. Pakistan Journal of Agricultural Sciences, 57(3).

Alloway, B. J. (2008). Zinc in soils and crop nutrition.

Alloway, B. J. (2009). Soil factors associated with zinc deficiency in crops and humans. Environmental geochemistry and health, 31(5), 537-548.

Almahri, A. (2022). The solid-state synthetic performance of bentonite stacked manganese ferrite nanoparticles: adsorption and photo-fenton degradation of MB dye and antibacterial applications. Journal of Materials Research and Technology, 17, 2935-2949.

Almendros, P., González, D., Fernández, M. D., García-Gomez, C., & Obrador, A. (2022). Both Zn biofortification and nutrient distribution pattern in cherry tomato plants are influenced by the application of ZnO nanofertilizer. Heliyon, 8(3), e09130.

An, T., Wu, Y., Xu, B., Zhang, S., Deng, X., Zhang, Y., ... & Chen, Y. (2022). Nitrogen supply improved plant growth and Cd translocation in maize at the silking and physiological maturity under moderate Cd stress. Ecotoxicology and Environmental Safety, 230, 113137.

Andelkovic, I. B., Kabiri, S., Tavakkoli, E., Kirby, J. K., McLaughlin, M. J., & Losic, D. (2018). Graphene oxide-Fe (III) composite containing phosphate–A novel slow release fertilizer for improved agriculture management. Journal of cleaner production, 185, 97-104.

Ansari, M. S., Ahmad, G., Khan, A. A., Mohamed, H. I., & Elhakem, A. (2022). Coal Fly Ash and Nitrogen Application as Eco-friendly Approaches for Modulating the Growth, Yield, and Biochemical Constituents of Radish Plants. Saudi Journal of Biological Sciences, 103306.

Arafa, E. G., Sabaa, M. W., Mohamed, R. R., Elzanaty, A. M., & Abdel-Gawad, O. F. (2022). Preparation of biodegradable sodium alginate/carboxymethylchitosan hydrogels for the slow-

release of urea fertilizer and their antimicrobial activity. Reactive and Functional Polymers, 174, 105243.

Atakora, W. K., Kwakye, P. K., Weymann, D., & Brüggemann, N. (2019). Stimulus of nitrogen fertilizers and soil characteristics on maize yield and nitrous oxide emission from Ferric Luvisol in the Guinea Savanna agro-ecological zone of Ghana. Scientific African, 6, e00141.

Azam, M., Bhatti, H. N., Khan, A., Zafar, L., & Iqbal, M. (2022). Zinc oxide nano-fertilizer application (foliar and soil) effect on the growth, photosynthetic pigments and antioxidant system of maize cultivar. Biocatalysis and Agricultural Biotechnology, 42, 102343.

Babajani, A., Iranbakhsh, A., Oraghi Ardebili, Z., & Eslami, B. (2019). Differential growth, nutrition, physiology, and gene expression in Melissa officinalis mediated by zinc oxide and elemental selenium nanoparticles. Environmental Science and Pollution Research, 26(24), 24430-24444.

Baddar, Z. E., Matocha, C. J., & Unrine, J. M. (2019). Surface coating effects on the sorption and dissolution of ZnO nanoparticles in soil. Environmental Science: Nano, 6(8), 2495-2507.

Bai, T., Liu, Y. Y., Muhammad, I., Yang, X., Yin, X. J., Bai, L., & Wang, Y. J. (2020). Mixed nitrogen form addition facilitates the growth adaptation of legume plant to heavy metal contamination in degraded mining areas. Global Ecology and Conservation, 24, e01387.

Bankaji, I., Pérez-Clemente, R. M., Caçador, I., & Sleimi, N. (2019). Accumulation potential of Atriplex halimus to zinc and lead combined with NaCl: effects on physiological parameters and antioxidant enzymes activities. South African Journal of Botany, 123, 51-61.

Baral, K. R., Jayasundara, S., Brown, S. E., & Wagner-Riddle, C. (2022). Long-term variability in N2O emissions and emission factors for corn and soybeans induced by weather and management at a cold climate site. Science of The Total Environment, 815, 152744.

Barth, G., Otto, R., Mira, A. B., Ferraz-Almeida, R., Vitti, A. C., Cantarella, H., & Vitti, G. C. (2020). Performance of enhanced efficiency nitrogen fertilizers in green-harvesting sugarcane. Agrosystems, Geosciences & Environment, 3(1), e20015.

Beig, B., Niazi, M. B. K., Jahan, Z., Hussain, A., Zia, M. H., & Mehran, M. T. (2020). Coating materials for slow release of nitrogen from urea fertilizer: A review. Journal of Plant Nutrition, 43(10), 1510-1533.

Bennour, H. A. (2012). Influence of pH and ionic strength on the adsorption of copper and zinc in bentonite clay. Chemical Science Transactions, 1(2), 371-381.

Bian, S. W., Mudunkotuwa, I. A., Rupasinghe, T., & Grassian, V. H. (2011). Aggregation and dissolution of 4 nm ZnO nanoparticles in aqueous environments: influence of pH, ionic strength, size, and adsorption of humic acid. Langmuir, 27(10), 6059-6068.

Bordoloi, N., Baruah, K. K., & Hazarika, B. (2020). Fertilizer management through coated urea to mitigate greenhouse gas (N2O) emission and improve soil quality in agroclimatic zone of Northeast India. Environmental Science and Pollution Research, 27(11), 11919-11931.

Bouwman, A. F., Boumans, L. J. M., & Batjes, N. H. (2002). Emissions of N2O and NO from fertilized fields: Summary of available measurement data. Global biogeochemical cycles, 16(4), 6-1.

Broadley, M. R., White, P. J., Hammond, J. P., Zelko, I., & Lux, A. (2007). Zinc in plants. New phytologist, 173(4), 677-702.

Burham, N., & Sayed, M. (2016). Adsorption behavior of Cd2+ and Zn2+ onto natural Egyptian bentonitic clay. Minerals, 6(4), 129.

Cameron, K. C., Di, H. J., & Moir, J. L. (2013). Nitrogen losses from the soil/plant system: a review. Annals of applied biology, 162(2), 145-173.

Castillo-González, J., Ojeda-Barrios, D., Hernández-Rodríguez, A., González-Franco, A. C., Robles-Hernández, L., & López-Ochoa, G. R. (2018). Zinc metalloenzymes in plants. Interciencia, 43(4), 242-248.

Chakraborty, S., & Mishra, A. K. (2020). Mitigation of zinc toxicity through differential strategies in two species of the cyanobacterium Anabaena isolated from zinc polluted paddy field. Environmental Pollution, 263, 114375.

Charles, A., Rochette, P., Whalen, J. K., Angers, D. A., Chantigny, M. H., & Bertrand, N. (2017). Global nitrous oxide emission factors from agricultural soils after addition of organic amendments: A meta-analysis. Agriculture, Ecosystems & Environment, 236, 88-98.

Chen, C., Liu, H., Chen, T., Chen, D., & Frost, R. L. (2015). An insight into the removal of Pb (II), Cu (II), Co (II), Cd (II), Zn (II), Ag (I), Hg (I), Cr (VI) by Na (I)-montmorillonite and Ca (II)-montmorillonite. Applied Clay Science, 118, 239-247.

Chen, F., Ameen, A., Tang, C. C., Du, F., Yang, X. L., & Xie, G. H. (2017). Effects of nitrogen fertilization on soil nitrogen for energy sorghum on marginal land in China. Agronomy Journal, 109(2), 636-645.

Chen, J., Lü, S., Zhang, Z., Zhao, X., Li, X., Ning, P., & Liu, M. (2018). Environmentally friendly fertilizers: A review of materials used and their effects on the environment. Science of the total environment, 613, 829-839.

Chen, S., Han, Y., Yang, M., Zhu, X., Liu, C., Liu, H., & Zou, H. (2020). Hydrophobically modified water-based polymer for slow-release urea formulation. Progress in Organic Coatings, 149, 105964.

Cheng, S., Lin, Q., Wang, Y., Luo, H., Huang, Z., Fu, H., ... & Xiao, R. (2020). The removal of Cu, Ni, and Zn in industrial soil by washing with EDTA-organic acids. Arabian Journal of Chemistry, 13(4), 5160-5170.

Cheng, Y., Elrys, A. S., Wang, J., Xu, C., Ni, K., Zhang, J., ... & Pacholski, A. (2022). Application of enhanced-efficiency nitrogen fertilizers reduces mineral nitrogen usage and emissions of both N2O and NH3 while sustaining yields in a wheat-rice rotation system. Agriculture, Ecosystems & Environment, 324, 107720.

Cheng, Y., Elrys, A. S., Wang, J., Xu, C., Ni, K., Zhang, J., ... & Pacholski, A. (2022). Application of enhanced-efficiency nitrogen fertilizers reduces mineral nitrogen usage and emissions of both N2O and NH3 while sustaining yields in a wheat-rice rotation system. Agriculture, Ecosystems & Environment, 324, 107720.

Chhowalla, M. (2017). Slow release nanofertilizers for bumper crops. ACS Central Science. 2017, 3, 3, 156–157. https://doi.org/10.1021/acscentsci.7b00091

Chu, Q., Xu, S., Xue, L., Liu, Y., Feng, Y., Yu, S., ... & Xing, B. (2020). Bentonite hydrochar composites mitigate ammonia volatilization from paddy soil and improve nitrogen use efficiency. Science of the Total Environment, 718, 137301.

Ciais, P., Sabine, C., Bala, G., Bopp, L., Brovkin, V., Canadell, J., ... & Thornton, P. (2014). Carbon and other biogeochemical cycles. In Climate change 2013: the physical science basis. Contribution of Working Group I to the Fifth Assessment Report of the Intergovernmental Panel on Climate Change (pp. 465-570). Cambridge University Press.

Coffin, M. D., & Slaton, N. A. (2020). Effect of low-use-rate zinc fertilization on rice growth and grain yield. Agrosystems, Geosciences & Environment, 3(1), e20016.

Coskun, D., Britto, D. T., Shi, W., & Kronzucker, H. J. (2017). Nitrogen transformations in modern agriculture and the role of biological nitrification inhibition. Nature Plants, 3(6), 1-10.

Cruz NC, Farto M, Mourinha C, et al (2021) Dissolution of ag nanoparticles in agricultural soils and effects on soil exoenzyme activities. Environ - MDPI 8:1–15. https://doi.org/10.3390/environments8030022

Cui, N., Cai, M., Zhang, X., Abdelhafez, A. A., Zhou, L., Sun, H., ... & Zhou, S. (2020a). Runoff loss of nitrogen and phosphorus from a rice paddy field in the east of China: Effects of long-term chemical N fertilizer and organic manure applications. Global Ecology and Conservation, 22, e01011.

Cui, Y., Xiang, Y., Xu, Y., Wei, J., Zhang, Z., Li, L., & Li, J. (2020b). Poly-acrylic acid grafted natural rubber for multi-coated slow release compound fertilizer: Preparation, properties and slow-release characteristics. International Journal of Biological Macromolecules, 146, 540-548.

Cyriac, J., Melethil, K., Thomas, B., Sreejit, M., & Varghese, T. (2020). Synthesis of biogenic ZnO nanoparticles and its impact on seed germination and root growth of Oryza sativa L. and Vigna unguiculata L. Materials Today: Proceedings, 25, 224-229.

Czaban, J., Czyz, E., Siebielec, G., & Niedzwiecki, J. (2014). Long-lasting effects of bentonite on properties of a sandy soil deprived of the humus layer. International Agrophysics, 28(3).

Czinkota, I., Filep, T., Rétháti, G., Tolner, L., Gulyás, M., Sebők, A., & Dálnoki, B. (2021). Derivation and application of a generalised exchange-adsorption isotherm for the adsorption of hydrophobic compounds on soils. Soil and Water Research, 16(2), 67-73.

da Cruz, D. F., Bortoletto-Santos, R., Guimarães, G. G. F., Polito, W. L., & Ribeiro, C. (2017). Role of polymeric coating on the phosphate availability as a fertilizer: insight from phosphate release by castor polyurethane coatings. Journal of agricultural and food chemistry, 65(29), 5890-5895.

da Silva Cardoso, A., Oliveira, S. C., Janusckiewicz, E. R., Brito, L. F., da Silva Morgado, E., Reis, R. A., & Ruggieri, A. C. (2019). Seasonal effects on ammonia, nitrous oxide, and methane emissions for beef cattle excreta and urea fertilizer applied to a tropical pasture. Soil and Tillage Research, 194, 104341.

Das, S. K., & Ghosh, G. K. (2022). Hydrogel-biochar composite for agricultural applications and controlled release fertilizer: A step towards pollution free environment. Energy, 242, 122977.

Davidson, E. A. (2009). The contribution of manure and fertilizer nitrogen to atmospheric nitrous oxide since 1860. Nature Geoscience, 2(9), 659-662.

Davis, B. W., Mirsky, S. B., Needelman, B. A., Cavigelli, M. A., & Yarwood, S. A. (2019). Nitrous oxide emissions increase exponentially with organic N rate from cover crops and applied poultry litter. Agriculture, Ecosystems & Environment, 272, 165-174.

Dawar, K., Khan, A., Sardar, K., Fahad, S., Saud, S., Datta, R., & Danish, S. (2021). Effects of the nitrification inhibitor nitrapyrin and mulch on N2O emission and fertilizer use efficiency using 15N tracing techniques. Science of The Total Environment, 757, 143739.

de Almeida, H. J., Vergara Carmona, V. M., Ferreira Inocêncio, M., Furtini Neto, A. E., Cecílio Filho, A. B., & Mauad, M. (2020). Soil type and zinc doses in agronomic biofortification of lettuce genotypes. Agronomy, 10(1), 124.

de Silva, M., Siriwardena, D. P., Sandaruwan, C., Priyadarshana, G., Karunaratne, V., & Kottegoda, N. (2020). Urea-silica nanohybrids with potential applications for slow and precise release of nitrogen. Materials Letters, 272, 127839.

de Silva, M., Siriwardena, D. P., Sandaruwan, C., Priyadarshana, G., Karunaratne, V., & Kottegoda, N. (2020). Urea-silica nanohybrids with potential applications for slow and precise release of nitrogen. Materials Letters, 272, 127839.

Diatta, A. A., Thomason, W. E., Abaye, O., Thompson, T. L., Battaglia, M. L., Vaughan, L. J., & Lo, M. (2020). Assessment of nitrogen fixation by mungbean genotypes in different soil textures using 15N natural abundance method. Journal of Soil Science and Plant Nutrition, 20(4), 2230-2240.

Dimkpa, C. O. (2018). Soil properties influence the response of terrestrial plants to metallic nanoparticles exposure. Current Opinion in Environmental Science & Health, 6, 1-8.

Dimkpa, C. O., & Bindraban, P. S. (2016). Fortification of micronutrients for efficient agronomic production: a review. Agronomy for Sustainable Development, 36(1), 1-27.

Dimkpa, C. O., Andrews, J., Fugice, J., Singh, U., Bindraban, P. S., Elmer, W. H., ... & White, J. C. (2020a). Facile coating of urea with low-dose ZnO nanoparticles promotes wheat performance and enhances Zn uptake under drought stress. Frontiers in Plant Science, 11, 168.

Dimkpa, C. O., Andrews, J., Sanabria, J., Bindraban, P. S., Singh, U., Elmer, W. H., ... & White, J. C. (2020b). Interactive effects of drought, organic fertilizer, and zinc oxide nanoscale and bulk particles on wheat performance and grain nutrient accumulation. Science of the Total Environment, 722, 137808.

Dimkpa, C. O., Fugice, J., Singh, U., & Lewis, T. D. (2020c). Development of fertilizers for enhanced nitrogen use efficiency–Trends and perspectives. Science of the Total Environment, 731, 139113.

Dimkpa, C. O., White, J. C., Elmer, W. H., & Gardea-Torresdey, J. (2017). Nanoparticle and ionic Zn promote nutrient loading of sorghum grain under low NPK fertilization. Journal of agricultural and food chemistry, 65(39), 8552-8559.

Ditta, A. (2012). How helpful is nanotechnology in agriculture?. Advances in Natural Sciences: Nanoscience and Nanotechnology, 3(3), 033002.

Eghbali Babadi, F., Yunus, R., Masoudi Soltani, S., & Shotipruk, A. (2021). Release Mechanisms and Kinetic Models of gypsum–sulfur–zeolite-coated urea sealed with microcrystalline wax for regulated dissolution. ACS omega, 6(17), 11144-11154.

Elhaj Baddar Z, Matocha CJ, Unrine JM (2019) Surface coating effects on the sorption and dissolution of ZnO nanoparticles in soil. Environ Sci Nano 6:2495–2507. https://doi.org/10.1039/c9en00348g

Elhassani, C. E., Essamlali, Y., Aqlil, M., Nzenguet, A. M., Ganetri, I., & Zahouily, M. (2019). Urea-impregnated HAP encapsulated by lignocellulosic biomass-extruded composites: A novel slow-release fertilizer. Environmental Technology & Innovation, 15, 100403.

Ellison, E., Blaylock, A., Sanchez, C., & Smith, R. (2013). Exploring controlled release nitrogen fertilizers for vegetable and melon crop production in California and Arizona. In 2013 Western Nutrient Management Conference. Reno, NV (pp. 17-22).

El-Nagar, D. A., & Sary, D. H. (2021). Synthesis and characterization of nano bentonite and its effect on some properties of sandy soils. Soil and Tillage Research, 208, 104872.

El-Saadony, M. T., Alkhatib, F. M., Alzahrani, S. O., Shafi, M. E., Abdel-Hamid, S. E., Taha, T. F., ... & Ahmed, N. H. (2021). Impact of mycogenic zinc nanoparticles on performance, behavior, immune response, and microbial load in Oreochromis niloticus. Saudi journal of biological sciences, 28(8), 4592-4604.

Eren, E., Tabak, A., & Eren, B. (2010). Performance of magnesium oxide-coated bentonite in removal process of copper ions from aqueous solution. Desalination, 257(1-3), 163-169.

Erisman, J. W., Sutton, M. A., Galloway, J., Klimont, Z., & Winiwarter, W. (2008). How a century of ammonia synthesis changed the world. Nature geoscience, 1(10), 636-639.

Faizan, M., Bhat, J. A., Chen, C., Alyemeni, M. N., Wijaya, L., Ahmad, P., & Yu, F. (2021). Zinc oxide nanoparticles (ZnO-NPs) induce salt tolerance by improving the antioxidant system and photosynthetic machinery in tomato. Plant Physiology and Biochemistry, 161, 122-130.

Feng, J., Li, F., Deng, A., Feng, X., Fang, F., & Zhang, W. (2016). Integrated assessment of the impact of enhanced-efficiency nitrogen fertilizer on N2O emission and crop yield. Agriculture, Ecosystems & Environment, 231, 218-228.

Feregrino-Perez, A. A., Magaña-López, E., Guzmán, C., & Esquivel, K. (2018). A general overview of the benefits and possible negative effects of the nanotechnology in horticulture. Scientia Horticulturae, 238, 126-137.

Fowler, D., Coyle, M., Skiba, U., Sutton, M. A., Cape, J. N., Reis, S., ... & Voss, M. (2013). The global nitrogen cycle in the twenty-first century. Philosophical Transactions of the Royal Society B: Biological Sciences, 368(1621), 20130164.

Freundlich, H. (1907). About the adsorption in solutions. Journal of Physical Chemistry , 57 (1), 385-470.

Galloway, J. N., Townsend, A. R., Erisman, J. W., Bekunda, M., Cai, Z., Freney, J. R., ... & Sutton, M. A. (2008). Transformation of the nitrogen cycle: recent trends, questions, and potential solutions. Science, 320(5878), 889-892.

García-Gómez, C., García, S., Obrador, A. F., González, D., Babín, M., & Fernández, M. D. (2018). Effects of aged ZnO NPs and soil type on Zn availability, accumulation and toxicity to pea and beet in a greenhouse experiment. Ecotoxicology and Environmental Safety, 160, 222-230.

Gautam, S., Tiwari, U., Sapkota, B., Sharma, B., Parajuli, S., Pandit, N. R., ... & Dhakal, K. (2022). Field evaluation of slow-release nitrogen fertilizers and real-time nitrogen management tools to improve grain yield and nitrogen use efficiency of spring maize in Nepal. Heliyon, e09566.

Ghafoor, I., Hasnain, M. U., Ikram, R. M., Khan, M. A., Iqbal, R., Hussain, M. I., & Sabagh, A. E. (2022). Effect of slow-release nitrogenous fertilizers on dry matter accumulation, grain nutritional quality, water productivity and wheat yield under an arid environment. Scientific Reports, 12(1), 1-10.

Ghimire, B., Riley, W. J., Koven, C. D., Kattge, J., Rogers, A., Reich, P. B., & Wright, I. J. (2017). A global trait-based approach to estimate leaf nitrogen functional allocation from observations. Ecological Applications, 27(5), 1421-1434.

Ghoneim, A. M. (2016). Effect of different methods of Zn application on rice growth, yield and nutrients dynamics in plant and soil. Journal of Agriculture and Ecology Research International, 6(2), 1-9.

Gillman, M. A. (2019). Mini-review: a brief history of nitrous oxide (N2O) use in neuropsychiatry. Current Drug Research Reviews Formerly: Current Drug Abuse Reviews, 11(1), 12-20.

Giroto, A. S., Guimarães, G. G., Foschini, M., & Ribeiro, C. (2017). Role of slow-release nanocomposite fertilizers on nitrogen and phosphate availability in soil. Scientific Reports, 7(1), 1-11.

Glatstein, D. A., & Francisca, F. M. (2015). Influence of pH and ionic strength on Cd, Cu and Pb removal from water by adsorption in Na-bentonite. Applied Clay Science, 118, 61-67.

Glenn, A. J., Moulin, A. P., Roy, A. K., & Wilson, H. F. (2021). Soil nitrous oxide emissions from no-till canola production under variable rate nitrogen fertilizer management. Geoderma, 385, 114857.

Godfray, H. C. J., Beddington, J. R., Crute, I. R., Haddad, L., Lawrence, D., Muir, J. F., ... & Toulmin, C. (2010). Food security: the challenge of feeding 9 billion people. science, 327(5967), 812-818.

Gong, H., Li, Y., Yu, T., Zhang, S., Gao, J., Zhang, S., & Sun, D. (2020). Soil and climate effects on leaf nitrogen and phosphorus stoichiometry along elevational gradients. Global Ecology and Conservation, 23, e01138.

Guha, T., Gopal, G., Mukherjee, A., & Kundu, R. (2022). Fe3O4-urea nanocomposites as a novel nitrogen fertilizer for improving nutrient utilization efficiency and reducing environmental pollution. Environmental Pollution, 292, 118301.

Guo, L., Wang, Y., Wang, M., Shaghaleh, H., Hamoud, Y. A., Xu, X., & Liu, H. (2021). Synthesis of bio-based MIL-100 (Fe)@ CNF-SA composite hydrogel and its application in slow-release N-fertilizer. Journal of Cleaner Production, 324, 129274.

Gupta, N., Ram, H., & Kumar, B. (2016). Mechanism of Zinc absorption in plants: uptake, transport, translocation and accumulation. Reviews in Environmental Science and Bio/Technology, 15(1), 89-109.

Guru, T., Veronica, N., Thatikunta, R., & Reddy, S. N. (2015). Crop nutrition management with nano fertilizers. Int. J. Environ. Sci. Technol, 1(1), 4-6.

Gurung, R. B., Ogle, S. M., Breidt, F. J., Parton, W. J., Del Grosso, S. J., Zhang, Y., ... & Venterea, R. T. (2021). Modeling nitrous oxide mitigation potential of enhanced efficiency nitrogen fertilizers from agricultural systems. Science of The Total Environment, 801, 149342.

Guyonnet, J. P., Vautrin, F., Meiffren, G., Labois, C., Cantarel, A. A., Michalet, S., ... & Haichar, F. E. Z. (2017). The effects of plant nutritional strategy on soil microbial denitrification activity through rhizosphere primary metabolites. FEMS microbiology ecology, 93(4), fix022.

Hacisalihoglu, G. (2020). Zinc (Zn): the last nutrient in the alphabet and shedding light on Zn efficiency for the future of crop production under suboptimal Zn. Plants, 9(11), 1471.

Han, J., Qiu, W., & Gao, W. (2010). Potential dissolution and photo-dissolution of ZnO thin films. Journal of hazardous materials, 178(1-3), 115-122.

Han, Y., Hwang, G., Kim, D., Bradford, S. A., Lee, B., Eom, I., ... & Kim, H. (2016). Transport, retention, and long-term release behavior of ZnO nanoparticle aggregates in saturated quartz sand: Role of solution pH and biofilm coating. Water research, 90, 247-257.

Handy, R. D., Von der Kammer, F., Lead, J. R., Hassellöv, M., Owen, R., & Crane, M. (2008). The ecotoxicology and chemistry of manufactured nanoparticles. Ecotoxicology, 17(4), 287-314.

Haque, M. A., & Haque, M. M. (2016). Growth, yield and nitrogen use efficiency of new rice variety under variable nitrogen rates. American Journal of Plant Sciences, 7(3), 612-622.

Harindintwali, J. D., Zhou, J., Muhoza, B., Wang, F., Herzberger, A., & Yu, X. (2021). Integrated eco-strategies towards sustainable carbon and nitrogen cycling in agriculture. Journal of Environmental Management, 293, 112856.

Hashim, M. M. A., Yusop, M. K., Othman, R., & Wahid, S. A. (2015). Characterization of nitrogen uptake pattern in Malaysian rice MR219 at different growth stages using 15N isotope. Rice Science, 22(5), 250-254.

He, H., Cao, J., Fei, X., & Duan, N. (2019). High-temperature annealing of ZnO nanoparticles increases the dissolution magnitude and rate in water by altering O vacancy distribution. Environment international, 130, 104930.

He, Y., Wu, Z., Tu, L., Han, Y., Zhang, G., & Li, C. (2015). Encapsulation and characterization of slow-release microbial fertilizer from the composites of bentonite and alginate. Applied Clay Science, 109, 68-75.

Hermida, L., & Agustian, J. (2019). Slow release urea fertilizer synthesized through recrystallization of urea incorporating natural bentonite using various binders. Environmental Technology & Innovation, 13, 113-121.

Higuchi, T. (1961). Rate of release of medicaments from ointment bases containing drugs in suspension. Journal of pharmaceutical sciences, 50(10), 874-875.

Hornberger, H., Virtanen, S., & Boccaccini, A. R. (2012). Biomedical coatings on magnesium alloys–a review. Acta biomaterialia, 8(7), 2442-2455.

Hou, X., Zhan, X., Zhou, F., Yan, X., Gu, B., Reis, S., ... & Tang, Y. (2018). Detection and attribution of nitrogen runoff trend in China's croplands. Environmental pollution, 234, 270-278.

Hu, N., Chen, Q., & Zhu, L. (2019). The responses of soil N2O emissions to residue returning systems: a meta-analysis. Sustainability, 11(3), 748.

Hussain, A., Ali, S., Rizwan, M., ur Rehman, M. Z., Javed, M. R., Imran, M., ... & Nazir, R. (2018). Zinc oxide nanoparticles alter the wheat physiological response and reduce the cadmium uptake by plants. Environmental Pollution, 242, 1518-1526.

IPCC (2014). Mitigation of climate change. Contribution of working group III to the fifth assessment report of the intergovernmental panel on climate change, 1454, 147.

IPCC, I. (2006). Guidelines for national greenhouse gas inventories. Prepared by the National Greenhouse Gas Inventories Programme. Eggleston HS, Buendia L, Miwa K, Ngara T, Tanabe K, editors. Published: IGES, Japan.

IPCC. (2019). 2019 refinement to the 2006 IPCC guidelines for national greenhouse gas inventories. Chapter 10. Emissions From Livestock And Manure Management. 209p.

Irfan, M., Khan Niazi, M. B., Hussain, A., Farooq, W., & Zia, M. H. (2018). Synthesis and characterization of zinc-coated urea fertilizer. Journal of Plant Nutrition, 41(13), 1625-1635.

Iskander, A. L., Khald, E. M., & Sheta, A. S. (2011). Zinc and manganese sorption behavior by natural zeolite and bentonite. Annals of Agricultural Sciences, 56(1), 43-48.

Jayachandran, A., Aswathy, T. R., & Nair, A. S. (2021). Green synthesis and characterization of zinc oxide nanoparticles using Cayratia pedata leaf extract. Biochemistry and Biophysics Reports, 26, 100995.

Ji, C., Li, J., Jiang, C., Zhang, L., Shi, L., Xu, F., & Cai, H. (2022). Zinc and nitrogen synergistic act on root-to-shoot translocation and preferential distribution in rice. Journal of advanced research, 35, 187-198.

Ji, Y., Liu, G., Ma, J., Zhang, G., Xu, H., & Yagi, K. (2013). Effect of controlled-release fertilizer on mitigation of N2O emission from paddy field in South China: a multi-year field observation. Plant and soil, 371(1), 473-486.

Jiang, Y., Deng, A., Bloszies, S., Huang, S., & Zhang, W. (2017). Nonlinear response of soil ammonia emissions to fertilizer nitrogen. Biology and Fertility of Soils, 53(3), 269-274.

Jośko, I., & Oleszczuk, P. (2013). Influence of soil type and environmental conditions on ZnO, TiO2 and Ni nanoparticles phytotoxicity. Chemosphere, 92(1), 91-99.

Kabata-Pendias, A. (2011). Trace elements in soils and plants. (C. Press, Ed.) (Fourth.). Boca Raton, FL: CRC Press Taylor & Francis Group. https://doi.org/10.1201/b10158

Kamalakar, D., Rao, N. L., Jayanthi, J. L., & Rao, M. V. (2011). Zinc sulfate controlled release fertilizer with fly ash as inert matrix. Ind. Streams Res. J. I.

Kantesaria, N., & Sharma, S. (2020). Exfoliation and extraction of nanoclay from montmorillonite mineral rich bentonite soil. In Advances in Computer Methods and Geomechanics (pp. 1-12). Springer, Singapore.

Karnakar, R. R., Shankapal, P. P., Suryawanshi, R. D., & Gite, V. V. (2022). Coating of urea granules with epoxidised vegetable oil cured by triethylenetetramine for control release: A green approach. Materials Today: Proceedings.

Kenawy, E. R., Seggiani, M., Cinelli, P., Elnaby, H. M. H., & Azaam, M. M. (2020). Swelling capacity of sugarcane bagasse-g-poly (acrylamide)/attapulgite superabsorbent composites and their application as slow release fertilizer. European Polymer Journal, 133, 109769.

Khalid, U., Sher, F., Noreen, S., Lima, E. C., Rasheed, T., Sehar, S., & Amami, R. (2022). Comparative effects of conventional and nano-enabled fertilizers on morphological and physiological attributes of Caesalpinia bonducella plants. Journal of the Saudi Society of Agricultural Sciences, 21(1), 61-72.

Khalifeh, S., & Burleigh, T. D. (2018). Super-hydrophobic stearic acid layer formed on anodized high purified magnesium for improving corrosion resistance of bioabsorbable implants. Journal of Magnesium and Alloys, 6(4), 327-336.

Khan, F., & Ajlouni, A. F. A. (2020). 4 Characterization of eco-friendly bentonite materials and their applications. Nanomaterials for Water Remediation, 93.

Khan, M. Z. H., Islam, M. R., Nahar, N., Al-Mamun, M. R., Khan, M. A. S., & Matin, M. A. (2021). Synthesis and characterization of nanozeolite based composite fertilizer for sustainable release and use efficiency of nutrients. Heliyon, 7(1), e06091.

Khatun, M. A., Hossain, M. M., Bari, M. A., Abdullahil, K. M., Parvez, M. S., Alam, M. F., & Kabir, A. H. (2018). Zinc deficiency tolerance in maize is associated with the up-regulation of Zn transporter genes and antioxidant activities. Plant Biology, 20(4), 765-770.

Khodabakhshloo, N., Biswas, B., Moore, F., Du, J., & Naidu, R. (2021). Organically functionalized bentonite for the removal of perfluorooctane sulfonate, phenanthrene and copper mixtures from wastewater. Applied Clay Science, 200, 105883.

Kim, D. G., Hernandez-Ramirez, G., & Giltrap, D. (2013). Linear and nonlinear dependency of direct nitrous oxide emissions on fertilizer nitrogen input: A meta-analysis. Agriculture, Ecosystems & Environment, 168, 53-65.

Kim, G. W., Kim, P. J., Khan, M. I., & Lee, S. J. (2021). Effect of Rice planting on nitrous oxide (N2O) emission under different levels of nitrogen fertilization. Agronomy, 11(2), 217.

Kim, H. Y. (2014). Analysis of variance (ANOVA) comparing means of more than two groups. Restorative dentistry & endodontics, 39(1), 74-77.

Kim, T. K., & Park, J. H. (2019). More about the basic assumptions of t-test: normality and sample size. Korean journal of anesthesiology, 72(4), 331-335.

King, A. E., Rezanezhad, F., & Wagner-Riddle, C. (2021). Evidence for microbial rather than aggregate origin of substrates fueling freeze-thaw induced N2O emissions. Soil Biology and Biochemistry, 160, 108352.

Klimczyk, M., Siczek, A., & Schimmelpfennig, L. (2021). Improving the efficiency of urea-based fertilization leading to reduction in ammonia emission. Science of the Total Environment, 771, 145483.

Kolenčík, M., Ernst, D., Komár, M., Urík, M., Šebesta, M., Dobročka, E., ... & Kratošová, G. (2019). Effect of foliar spray application of zinc oxide nanoparticles on quantitative, nutritional, and physiological parameters of foxtail millet (Setaria italica l.) under field conditions. Nanomaterials, 9(11), 1559.

Kolenčík, M., Ernst, D., Komár, M., Urík, M., Šebesta, M., Ďurišová, Ľ., ... & Aydın, E. (2022). Effects of Foliar Application of ZnO Nanoparticles on Lentil Production, Stress Level and Nutritional Seed Quality under Field Conditions. Nanomaterials, 12(3), 310.

Korsmeyer, R. W., Gurny, R., Doelker, E., Buri, P., & Peppas, N. A. (1983). Mechanisms of solute release from porous hydrophilic polymers. International journal of pharmaceutics, 15(1), 25-35.

Kudeyarov, V. N. (2020). Nitrous oxide emission from fertilized soils: an analytical review. Eurasian Soil Science, 53(10), 1396-1407.

Ladha, J. K., Pathak, H., Krupnik, T. J., Six, J., & van Kessel, C. (2005). Efficiency of fertilizer nitrogen in cereal production: retrospects and prospects. Advances in agronomy, 87, 85-156.

Lam, S. K., Suter, H., Bai, M., Walker, C., Mosier, A. R., van Grinsven, H., & Chen, D. (2019). Decreasing ammonia loss from an Australian pasture with the use of enhanced efficiency fertilizers. Agriculture, Ecosystems & Environment, 283, 106553.

Langarica-Fuentes, A., Manrubia, M., Giles, M. E., Mitchell, S., & Daniell, T. J. (2018). Effect of model root exudate on denitrifier community dynamics and activity at different water-filled pore space levels in a fertilised soil. Soil Biology and Biochemistry, 120, 70-79.

Langmuir, I. (1916). The constitution and fundamental properties of solids and liquids. Part I. Solids. Journal of the American chemical society, 38(11), 2221-2295.

Legg, B. A., Zhu, M., Comolli, L. R., Gilbert, B., & Banfield, J. F. (2014). Impacts of ionic strength on three-dimensional nanoparticle aggregate structure and consequences for environmental transport and deposition. Environmental science & technology, 48(23), 13703-13710.

Lesschen, J. P., Velthof, G. L., de Vries, W., & Kros, J. (2011). Differentiation of nitrous oxide emission factors for agricultural soils. Environmental pollution, 159(11), 3215-3222.

LI, G. H., CHENG, G. G., LU, W. P., & LU, D. L. (2021). Differences of yield and nitrogen use efficiency under different applications of slow release fertilizer in spring maize. Journal of Integrative Agriculture, 20(2), 554-564.

Li, G., Zhao, B., Dong, S., Zhang, J., Liu, P., & Vyn, T. J. (2017). Interactive effects of water and controlled release urea on nitrogen metabolism, accumulation, translocation, and yield in summer maize. The Science of Nature, 104(9), 1-12.

Li, M., Han, X., & Li, L. J. (2022a). Total Nitrogen Stock in Soil Profile Affected by Land Use and Soil Type in Three Counties of Mollisols. Frontiers in Environmental Science, 1001.

Li, Y., Jia, C., Zhang, X., Jiang, Y., Zhang, M., Lu, P., & Chen, H. (2018). Synthesis and performance of bio-based epoxy coated urea as controlled release fertilizer. Progress in Organic Coatings, 119, 50-56.

Li, Y., Ming, B., Fan, P., Liu, Y., Wang, K., Hou, P., ... & Xie, R. (2022b). Quantifying contributions of leaf area and longevity to leaf area duration under increased planting density and nitrogen input regimens during maize yield improvement. Field Crops Research, 283, 108551.

Li, Z., Zeng, Z., Song, Z., Tian, D., Huang, X., Nie, S., ... & Niu, S. (2022c). Variance and main drivers of field nitrous oxide emissions: A global synthesis. Journal of Cleaner Production, 131686.

Liao, X., Liu, D., Niu, Y., Chen, Z., He, T., & Ding, W. (2021). Effect of field-aged biochar on fertilizer N retention and N2O emissions: A field microplot experiment with 15N-labeled urea. Science of The Total Environment, 773, 145645.

Liao, Z., Zeng, H., Fan, J., Lai, Z., Zhang, C., Zhang, F., ... & Wu, P. (2022). Effects of plant density, nitrogen rate and supplemental irrigation on photosynthesis, root growth, seed yield and water-nitrogen use efficiency of soybean under ridge-furrow plastic mulching. Agricultural Water Management, 107688.

Lilay, G. H., Castro, P. H., Guedes, J. G., Almeida, D. M., Campilho, A., Azevedo, H., ... & Assunção, A. G. (2020). Rice F-bZIP transcription factors regulate the zinc deficiency response. Journal of Experimental Botany, 71(12), 3664-3677.

Liu, D. Y., Liu, Y. M., Zhang, W., Chen, X. P., & Zou, C. Q. (2019). Zinc uptake, translocation, and remobilization in winter wheat as affected by soil application of Zn fertilizer. Frontiers in Plant Science, 10, 426.

Liu, Q. H., Shi, X. Z., Weindorf, D. C., Yu, D. S., Zhao, Y. C., Sun, W. X., & Wang, H. J. (2006). Soil organic carbon storage of paddy soils in China using the 1: 1,000,000 soil database and their implications for C sequestration. Global Biogeochemical Cycles, 20(3).

Liu, Q., Qin, Y., Zou, J., Guo, Y., & Gao, Z. (2013). Annual nitrous oxide emissions from open-air and greenhouse vegetable cropping systems in China. Plant and soil, 370(1), 223-233.

Liu, R., & Lal, R. (2015). Potentials of engineered nanoparticles as fertilizers for increasing agronomic productions. Science of the total environment, 514, 131-139.

Liu, R., Fu, K., Zhang, B., Mei, D., Zhang, H., & Liu, J. (2012). Removal of methyl orange by modified halloysite nanotubes. Journal of dispersion science and technology, 33(5), 711-718.

Liu, R., Hu, H., Suter, H., Hayden, H. L., He, J., Mele, P., & Chen, D. (2016). Nitrification is a primary driver of nitrous oxide production in laboratory microcosms from different land-use soils. Frontiers in microbiology, 7, 1373.

Liu, S., Lin, F., Wu, S., Ji, C., Sun, Y., Jin, Y., ... & Zou, J. (2017). A meta-analysis of fertilizer-induced soil NO and combined NO+ N2O emissions. Global Change Biology, 23(6), 2520-2532.

Liu, T., Huang, J., Chai, K., Cao, C., & Li, C. (2018). Effects of N fertilizer sources and tillage practices on NH3 volatilization, grain yield, and N use efficiency of rice fields in Central China. Frontiers in Plant Science, 9, 385.

Liu, X., Li, M., Guo, P., & Zhang, Z. (2019). Optimization of water and fertilizer coupling system based on rice grain quality. Agricultural Water Management, 221, 34-46.

Liu, Y. M., Liu, D. Y., Zhao, Q. Y., Zhang, W., Chen, X. X., Xu, S. J., & Zou, C. Q. (2020). Zinc fractions in soils and uptake in winter wheat as affected by repeated applications of zinc fertilizer. Soil and Tillage Research, 200, 104612.

Liu, Y., Zou, Y., Kong, L., Bai, G., Luo, F., Liu, Z., ... & Zhang, Y. (2021). Effects of bentonite on the growth process of submerged macrophytes and sediment microenvironment. Journal of Environmental Management, 287, 112308.

Lopes, S., Ribeiro, F., Wojnarowicz, J., Łojkowski, W., Jurkschat, K., Crossley, A., ... & Loureiro, S. (2014). Zinc oxide nanoparticles toxicity to Daphnia magna: size-dependent effects and dissolution. Environmental toxicology and chemistry, 33(1), 190-198.

Louha, H., Balassone, G., Boutaleb, A., Boni, M., Joachimski, M. M., & Mondillo, N. (2021). The Pb-Zn (Ba) Nonsulfide Mineralizations at Bou Caïd (Ouarsenis, Algeria): Mineralogy, Isotope Geochemistry, and Genetic Inferences. Minerals, 11(7), 687.

Luo, L., Pan, S., Liu, X., Wang, H., & Xu, G. (2017). Nitrogen deficiency inhibits cell division-determined elongation, but not initiation, of rice tiller buds. Israel Journal of Plant Sciences, 64(3-4), 32-40.

Lv, Z., Sun, H., Du, W., Li, R., Mao, H., & Kopittke, P. M. (2021). Interaction of different-sized ZnO nanoparticles with maize (Zea mays): Accumulation, biotransformation and phytotoxicity. Science of The Total Environment, 796, 148927.

Lyu, X., Wang, T., Song, X., Zhao, C., Rees, R. M., Liu, Z., ... & Siddique, K. H. (2021). Reducing N2O emissions with enhanced efficiency nitrogen fertilizers (EENFs) in a high-yielding spring maize system. Environmental Pollution, 273, 116422.

Machado, P. V. F., Farrell, R. E., & Wagner-Riddle, C. (2021). Spatial variation of nitrous oxide fluxes during growing and non-growing seasons at a location subjected to seasonally frozen soils. Canadian Journal of Soil Science, 101(3), 555-564.

Machado, P. V. F., Neufeld, K., Brown, S. E., Voroney, P. R., Bruulsema, T. W., & Wagner-Riddle, C. (2020). High temporal resolution nitrous oxide fluxes from corn (Zea mays L.) in response to the combined use of nitrification and urease inhibitors. Agriculture, Ecosystems & Environment, 300, 106996.

Małecki, J. J., Kadzikiewicz-Schoeneich, M., & Szostakiewicz-Hołownia, M. (2016). Concentration and mobility of copper and zinc in the hypergenic zone of a highly urbanized area. Environmental Earth Sciences, 75(1), 1-13.

Mariano, E., de Sant Ana Filho, C. R., Bortoletto-Santos, R., Bendassolli, J. A., & Trivelin, P. C. (2019). Ammonia losses following surface application of enhanced-efficiency nitrogen fertilizers and urea. Atmospheric Environment, 203, 242-251.

Marreiro, D. D. N., Cruz, K. J. C., Morais, J. B. S., Beserra, J. B., Severo, J. S., & De Oliveira, A. R. S. (2017). Zinc and oxidative stress: current mechanisms. Antioxidants, 6(2), 24.

Mateos-Naranjo, E., Pérez-Romero, J. A., Redondo-Gómez, S., Mesa-Marín, J., Castellanos, E. M., & Davy, A. J. (2018). Salinity alleviates zinc toxicity in the saltmarsh zinc-accumulator Juncus acutus. Ecotoxicology and environmental safety, 163, 478-485.

Mattiello, E. M., Ruiz, H. A., Neves, J. C., Ventrella, M. C., & Araújo, W. L. (2015). Zinc deficiency affects physiological and anatomical characteristics in maize leaves. Journal of plant physiology, 183, 138-143.

Mazumder, J. A., Khan, E., Perwez, M., Gupta, M., Kumar, S., Raza, K., & Sardar, M. (2020). Exposure of biosynthesized nanoscale ZnO to Brassica juncea crop plant: morphological, biochemical and molecular aspects. Scientific Reports, 10(1), 1-13.

McCall, K. A., Huang, C. C., & Fierke, C. A. (2000). Function and mechanism of zinc metalloenzymes. The Journal of nutrition, 130(5), 1437S-1446S.

Milani, N., McLaughlin, M. J., Stacey, S. P., Kirby, J. K., Hettiarachchi, G. M., Beak, D. G., & Cornelis, G. (2012). Dissolution kinetics of macronutrient fertilizers coated with manufactured zinc oxide nanoparticles. Journal of agricultural and food chemistry, 60(16), 3991-3998.

Ministry of Agriculture and Rural Development. Advisory Code of Good Agricultural Practice on Limitation of Ammonia Emissions. Institute of Technology and Life Sciences: Falenty, Poland, 2019; 13-16, 66-70.009, 93, 9-11.

Moghaddasi, S., Fotovat, A., Khoshgoftarmanesh, A. H., Karimzadeh, F., Khazaei, H. R., & Khorassani, R. (2017). Bioavailability of coated and uncoated ZnO nanoparticles to cucumber in soil with or without organic matter. Ecotoxicology and environmental safety, 144, 543-551.

Mohammed-Azizi, F., Dib, S., & Boufatit, M. (2013). Removal of heavy metals from aqueous solutions by Algerian bentonite. Desalination and Water Treatment, 51(22-24), 4447-4458.

Montzka, S. A., Reimann, S. C. L. A., O'Doherty, S., Engel, A., Krüger, K., & Sturges, W. T. (2011). Ozone-depleting substances (ODSs) and related chemicals. World Meteorological Organization.

Moreno-Lora, A., & Delgado, A. (2020). Factors determining Zn availability and uptake by plants in soils developed under Mediterranean climate. Geoderma, 376, 114509.

Mossa, A. W., Young, S. D., & Crout, N. M. (2020). Zinc uptake and phyto-toxicity: Comparing intensity-and capacity-based drivers. Science of the Total Environment, 699, 134314.

Mudunkotuwa, I. A., Rupasinghe, T., Wu, C. M., & Grassian, V. H. (2012). Dissolution of ZnO nanoparticles at circumneutral pH: a study of size effects in the presence and absence of citric acid. Langmuir, 28(1), 396-403.

Nakayama, S., Sugano, S. S., Hirokawa, H., Mori, I. C., Daimon, H., Kimura, S., & Fukao, Y. (2020). Manganese treatment alleviates zinc deficiency symptoms in arabidopsis seedlings. Plant and Cell Physiology, 61(10), 1711-1723.

Nardi, P., Ulderico, N. E. R. I., Di Matteo, G., Trinchera, A., Napoli, R., Farina, R., ... & Benedetti, A. (2018). Nitrogen release from slow-release fertilizers in soils with different microbial activities. Pedosphere, 28(2), 332-340.

Natasha, N., Shahid, M., Bibi, I., Iqbal, J., Khalid, S., Murtaza, B., ... & Arshad, M. (2022). Zinc in soil-plant-human system: A data-analysis review. Science of The Total Environment, 808, 152024.

NDABA, B., ROOPNARAIN, A., Haripriya, R. A. M. A., & MAAZA, M. (2022). Biosynthesized metallic nanoparticles as fertilizers: An emerging precision agriculture strategy. Journal of Integrative Agriculture, 21(5), 1225-1242.

Nehe, A. S., Misra, S., Murchie, E. H., Chinnathambi, K., & Foulkes, M. J. (2018). Genetic variation in N-use efficiency and associated traits in Indian wheat cultivars. Field Crops Research, 225, 152-162.

Nemček, L., Šebesta, M., Urík, M., Bujdoš, M., Dobročka, E., & Vávra, I. (2020). Impact of bulk ZnO, ZnO nanoparticles and dissolved Zn on early growth stages of barley—a pot experiment. Plants, 9(10), 1365.

Nie, W., Pan, X., Cui, H., & Jiang, M. (2016). The influence of soil carbon and nitrogen on soil N2O emission. Inter J Environ Res, 5, 15-20.

Noman, A., Aqeel, M., Khalid, N., Islam, W., Sanaullah, T., Anwar, M., ... & Lou, Y. (2019). Zinc finger protein transcription factors: Integrated line of action for plant antimicrobial activity. Microbial pathogenesis, 132, 141-149.

Norton, J., & Ouyang, Y. (2019). Controls and adaptive management of nitrification in agricultural soils. Frontiers in microbiology, 1931.

Nriagu, J. (2007). Zinc toxicity in humans. School of Public Health, University of Michigan, 1-7.

Nriagu, J. Zinc toxicity in humans. Nriagu J (Ed.), Encyclopedia of Environmental Health (Second edition), Elsevier, Oxford (2019), pp. 500-508.

Peng, Q., Kong, D., Shi, L., Wang, X., Meng, X., & Liu, N. (2020). Preparation of a novel bentonite intercalation composite by changing the chemical state of aluminum. Journal of the Chinese Chemical Society, 67(6), 1009-1015.

Perić, J., Trgo, M., & Medvidović, N. V. (2004). Removal of zinc, copper and lead by natural zeolite—a comparison of adsorption isotherms. Water research, 38(7), 1893-1899.

Pettibone, J. M., Cwiertny, D. M., Scherer, M., & Grassian, V. H. (2008). Adsorption of organic acids on TiO2 nanoparticles: effects of pH, nanoparticle size, and nanoparticle aggregation. Langmuir, 24(13), 6659-6667.

Prakash, V., Rai, P., Sharma, N. C., Singh, V. P., Tripathi, D. K., Sharma, S., & Sahi, S. (2022). Application of zinc oxide nanoparticles as fertilizer boosts growth in rice plant and alleviates chromium stress by regulating genes involved in regulating oxidative stress. Chemosphere, 134554.

Qi, Z., Dong, Y., He, M., Wang, M., Li, Y., & Dai, X. (2021). Coated, Stabilized Enhanced-Efficiency Nitrogen Fertilizers: Preparation and Effects on Maize Growth and Nitrogen Utilization. Frontiers in Plant Science, 12, 792262-792262.

Rahman, M. H., Haque, K. S., & Khan, M. Z. H. (2021). A review on application of controlled released fertilizers influencing the sustainable agricultural production: A Cleaner production process. Environmental Technology & Innovation, 23, 101697.

Rai-Kalal, P., Tomar, R. S., & Jajoo, A. (2021). H2O2 signaling regulates seed germination in ZnO nanoprimed wheat (Triticum aestivum L.) seeds for improving plant performance under drought stress. Environmental and Experimental Botany, 189, 104561.

Rajan, M., Shahena, S., Chandran, V., & Mathew, L. (2021). Controlled release of fertilizers—concept, reality, and mechanism. In Controlled Release Fertilizers for Sustainable Agriculture (pp. 41-56). Academic Press.

Raliya, R., Biswas, P., & Tarafdar, J. C. (2015). TiO2 nanoparticle biosynthesis and its physiological effect on mung bean (Vigna radiata L.). Biotechnology Reports, 5, 22-26.

Raliya, R., Tarafdar, J. C., & Biswas, P. (2016). Enhancing the mobilization of native phosphorus in the mung bean rhizosphere using ZnO nanoparticles synthesized by soil fungi. Journal of agricultural and food chemistry, 64(16), 3111-3118.

Ransom, C. J., Jolley, V. D., Blair, T. A., Sutton, L. E., & Hopkins, B. G. (2020). Nitrogen release rates from slow-and controlled-release fertilizers influenced by placement and temperature. Plos one, 15(6), e0234544.

Reay, D. S., Davidson, E. A., Smith, K. A., Smith, P., Melillo, J. M., Dentener, F., & Crutzen, P. J. (2012). Global agriculture and nitrous oxide emissions. Nature climate change, 2(6), 410-416.

Recio, J., Montoya, M., Álvarez, J. M., & Vallejo, A. (2020). Inhibitor-coated enhanced-efficiency N fertilizers for mitigating NOx and N2O emissions in a high-temperature irrigated agroecosystem. Agricultural and Forest Meteorology, 292, 108110.

Reda, F. M., El-Saadony, M. T., El-Rayes, T. K., Attia, A. I., El-Sayed, S. A., Ahmed, S. Y., ... & Alagawany, M. (2021). Use of biological nano zinc as a feed additive in quail nutrition: biosynthesis, antimicrobial activity and its effect on growth, feed utilisation, blood metabolites and intestinal microbiota. Italian Journal of Animal Science, 20(1), 324-335.

Rehman, S., Abbas, G., Shahid, M., Saqib, M., Farooq, A. B. U., Hussain, M., ... & Farooq, A. (2019). Effect of salinity on cadmium tolerance, ionic homeostasis and oxidative stress responses in conocarpus exposed to cadmium stress: Implications for phytoremediation. Ecotoxicology and Environmental Safety, 171, 146-153.

Ritger, P. L., & Peppas, N. A. (1987). A simple equation for description of solute release II. Fickian and anomalous release from swellable devices. Journal of controlled release, 5(1), 37-42.

Romero-Freire, A., Lofts, S., Martín Peinado, F. J., & van Gestel, C. A. (2017). Effects of aging and soil properties on zinc oxide nanoparticle availability and its ecotoxicological effects to the earthworm Eisenia andrei. Environmental Toxicology and Chemistry, 36(1), 137-146.

Ros, G. H., Temminghoff, E. J. M., & Hoffland, E. (2011). Nitrogen mineralization: a review and meta-analysis of the predictive value of soil tests. European Journal of Soil Science, 62(1), 162-173.

Rostami, M., Talarposhti, R. M., Mohammadi, H., & Demyan, M. S. (2019). Morpho-physiological response of Saffron (Crocus Sativus L.) to particle size and rates of zinc fertilizer. Communications in Soil Science and Plant Analysis, 50(10), 1250-1257.

Rudmin, M., Banerjee, S., Yakich, T., Tabakaev, R., Ibraeva, K., Buyakov, A., ... & Ruban, A. (2020). Formulation of a slow-release fertilizer by mechanical activation of smectite/glauconite and urea mixtures. Applied Clay Science, 196, 105775.

Ruiz-Hitzky, E., Darder, M., Wicklein, B., Castro-Smirnov, F. A., & Aranda, P. (2019). Clay-based biohybrid materials for biomedical and pharmaceutical applications. Clays and Clay Minerals, 67(1), 44-58.

Sabir, S., Zahoor, M. A., Waseem, M., Siddique, M. H., Shafique, M., Imran, M., ... & Muzammil, S. (2020). Biosynthesis of ZnO nanoparticles using bacillus subtilis: characterization and nutritive significance for promoting plant growth in Zea mays L. Dose-Response, 18(3), 1559325820958911.

Sadeghzadeh, B. (2013). A review of zinc nutrition and plant breeding. Journal of soil science and plant nutrition, 13(4), 905-927.

Saggar, S., Jha, N., Deslippe, J., Bolan, N. S., Luo, J., Giltrap, D. L., ... & Tillman, R. W. (2013). Denitrification and N2O: N2 production in temperate grasslands: Processes, measurements, modelling and mitigating negative impacts. Science of the Total Environment, 465, 173-195.

Sahoo, S. K., Dwivedi, G. K., Dey, P., & Praharaj, S. (2021). Green synthesized ZnO nanoparticles for sustainable production and nutritional biofortification of green gram. Environmental Technology & Innovation, 24, 101957.

Salama, Z. A., El-Fouly, M. M., Lazova, G., & Popova, L. P. (2006). Carboxylating enzymes and carbonic anhydrase functions were suppressed by zinc deficiency in maize and chickpea plants. Acta Physiologiae Plantarum, 28(5), 445-451.

Saleem, I., Maqsood, M. A., ur Rehman, M. Z., Aziz, T., Bhatti, I. A., & Ali, S. (2021). Potassium ferrite nanoparticles on DAP to formulate slow release fertilizer with auxiliary nutrients. Ecotoxicology and Environmental Safety, 215, 112148.

Salimi, M., Motamedi, E., Motesharezedeh, B., Hosseini, H. M., & Alikhani, H. A. (2020). Starch-g-poly (acrylic acid-co-acrylamide) composites reinforced with natural char nanoparticles toward environmentally benign slow-release urea fertilizers. Journal of Environmental Chemical Engineering, 8(3), 103765.

Salinitro, M., van der Ent, A., Tognacchini, A., & Tassoni, A. (2020). Stress responses and nickel and zinc accumulation in different accessions of Stellaria media (L.) Vill. in response to solution pH variation in hydroponic culture. Plant Physiology and Biochemistry, 148, 133-141.

Samreen, T., Shah, H. U., Ullah, S., & Javid, M. (2017). Zinc effect on growth rate, chlorophyll, protein and mineral contents of hydroponically grown mungbeans plant (Vigna radiata). Arabian Journal of Chemistry, 10, S1802-S1807.

Schmidt, S. B., & Husted, S. (2019). The biochemical properties of manganese in plants. Plants, 8(10), 381.

Seleiman, M. F., Almutairi, K. F., Alotaibi, M., Shami, A., Alhammad, B. A., & Battaglia, M. L. (2020). Nano-fertilization as an emerging fertilization technique: why can modern agriculture benefit from its use?. Plants, 10(1), 2.

Semalulu, O., Elobu, P., Namazzi, S., Kyebogola, S., & Mubiru, D. N. (2017). Higher cereal and legume yields using Ca-bentonite on sandy soils in the dry eastern uganda: Increased productivity versus profitability. Univers. J. Agric. Res, 5(2), 140-147.

Sempeho, S. I., Kim, H. T., Mubofu, E., Pogrebnoi, A., Shao, G., & Hilonga, A. (2015). Encapsulated urea-Kaolinite Nanocomposite for controlled release fertilizer formulations. Journal of Chemistry, 2015.

Senbayram, M., Well, R., Bol, R., Chadwick, D. R., Jones, D. L., & Wu, D. (2018). Interaction of straw amendment and soil NO3− content controls fungal denitrification and denitrification product stoichiometry in a sandy soil. Soil Biology and Biochemistry, 126, 204-212.

Senbayram, M., Well, R., Shan, J., Bol, R., Burkart, S., Jones, D. L., & Wu, D. (2020). Rhizosphere processes in nitrate-rich barley soil tripled both N2O and N2 losses due to enhanced bacterial and fungal denitrification. Plant and soil, 448(1), 509-522.

Service, R. (2019). New reactor could halve carbon dioxide emissions from ammonia production Science, 80, 10.1126/science.aba1262

Shabbir, Z., Sardar, A., Shabbir, A., Abbas, G., Shamshad, S., Khalid, S., ... & Shahid, M. (2020). Copper uptake, essentiality, toxicity, detoxification and risk assessment in soil-plant environment. Chemosphere, 259, 127436.

Shah, A. N., Wu, Y., Iqbal, J., Tanveer, M., Bashir, S., Rahman, S. U., ... & Yang, G. (2021). Nitrogen and plant density effects on growth, yield performance of two different cotton cultivars from different origin. Journal of King Saud University-Science, 33(6), 101512.

Shahid, M., Pourrut, B., Dumat, C., Nadeem, M., Aslam, M., & Pinelli, E. (2014). Heavy-metal-induced reactive oxygen species: phytotoxicity and physicochemical changes in plants. Reviews of Environmental Contamination and Toxicology Volume 232, 1-44.

Shaik, A. M., David Raju, M., & Rama Sekhara Reddy, D. (2020). Green synthesis of zinc oxide nanoparticles using aqueous root extract of Sphagneticola trilobata Lin and investigate its role in toxic metal removal, sowing germination and fostering of plant growth. Inorganic and nano-metal chemistry, 50(7), 569-579.

Shakoor, A., Ashraf, F., Shakoor, S., Mustafa, A., Rehman, A., & Altaf, M. M. (2020). Biogeochemical transformation of greenhouse gas emissions from terrestrial to atmospheric environment and potential feedback to climate forcing. Environmental Science and Pollution Research, 27(31), 38513-38536.

Shakoor, A., Xu, Y., Wang, Q., Chen, N., He, F., Zuo, H., ... & Yang, S. (2018). Effects of fertilizer application schemes and soil environmental factors on nitrous oxide emission fluxes in a rice-wheat cropping system, east China. PloS one, 13(8), e0202016.

Shang, Y., Hasan, M., Ahammed, G. J., Li, M., Yin, H., & Zhou, J. (2019). Applications of nanotechnology in plant growth and crop protection: a review. Molecules, 24(14), 2558.

Sharma, A., Patni, B., Shankhdhar, D., & Shankhdhar, S. C. (2013). Zinc–an indispensable micronutrient. Physiology and Molecular Biology of Plants, 19(1), 11-20.

Shcherbak, I., Millar, N., & Robertson, G. P. (2014). Global metaanalysis of the nonlinear response of soil nitrous oxide (N2O) emissions to fertilizer nitrogen. Proceedings of the National Academy of Sciences, 111(25), 9199-9204.

Sheoran, V., Sheoran, A. S., & Poonia, P. (2016). Factors affecting phytoextraction: a review. Pedosphere, 26(2), 148-166.

Sheteiwy, M. S., Shaghaleh, H., Hamoud, Y. A., Holford, P., Shao, H., Qi, W., ... & Wu, T. (2021). Zinc oxide nanoparticles: Potential effects on soil properties, crop production, food processing, and food quality. Environmental Science and Pollution Research, 28(28), 36942-36966.

Shi, T., Hu, X., Guo, L., Su, F., Tu, W., Hu, Z., ... & Wu, G. (2021). Digital mapping of zinc in urban topsoil using multisource geospatial data and random forest. Science of The Total Environment, 792, 148455.

Shi, X., Li, X., Guo, C., Feng, P., & Hu, K. (2022). Modeling ammonia volatilization following urea and controlled-release urea application to paddy fields. Computers and Electronics in Agriculture, 196, 106888.

SHOKOUH, S. Z., FARHADIAN, O., & Ramezanian, N. (2019). Antimicrobial properties of chitosan composite with activated bentonite against Aquaculture pathogenic bacteria: Aeromonas hydrophila.

Sidhu, G. P. S., Bali, A. S., Singh, H. P., Batish, D. R., & Kohli, R. K. (2020). Insights into the tolerance and phytoremediation potential of Coronopus didymus L.(Sm) grown under zinc stress. Chemosphere, 244, 125350.

Signor, D., Cerri, C. E. P., & Conant, R. (2013). N2O emissions due to nitrogen fertilizer applications in two regions of sugarcane cultivation in Brazil. Environmental Research Letters, 8(1), 015013.

Simkó, A., & Veres, S. (2019). Evaluation of the correlation between SPAD readings and absolute chlorophyll content of maize under different nitrogen supply conditions. Acta Agraria Debreceniensis, (2), 121-126.

Singh, J., Kumar, S., Alok, A., Upadhyay, S. K., Rawat, M., Tsang, D. C., ... & Kim, K. H. (2019). The potential of green synthesized zinc oxide nanoparticles as nutrient source for plant growth. Journal of Cleaner Production, 214, 1061-1070.

Sofyane, A., Ablouh, E., Lahcini, M., Elmeziane, A., Khouloud, M., Kaddami, H., & Raihane, M. (2021). Slow-release fertilizers based on starch acetate/glycerol/polyvinyl alcohol biocomposites for sustained nutrient release. Materials Today: Proceedings, 36, 74-81.

Song, X., Liu, M., Ju, X., Gao, B., Su, F., Chen, X., & Rees, R. M. (2018). Nitrous oxide emissions increase exponentially when optimum nitrogen fertilizer rates are exceeded in the North China Plain. Environmental science & technology, 52(21), 12504-12513.

Sosulski, T., Stępień, W., Wąs, A., & Szymańska, M. (2020). N2O and CO2 emissions from bare soil: effect of fertilizer management. Agriculture, 10(12), 602.

Sousa, S. F., Lopes, A. B., Fernandes, P. A., & Ramos, M. J. (2009). The Zinc proteome: a tale of stability and functionality. Dalton Transactions, (38), 7946-7956.

Souza, S. C., Souza, L. A., Schiavinato, M. A., de Oliveira Silva, F. M., & de Andrade, S. A. (2020). Zinc toxicity in seedlings of three trees from the Fabaceae associated with arbuscular mycorrhizal fungi. Ecotoxicology and Environmental Safety, 195, 110450.

Stocker, T. F., Qin, D., Plattner, G. K., Tignor, M. M., Allen, S. K., Boschung, J., ... & Midgley, P. M. (2014). Climate Change 2013: The physical science basis. contribution of working group I to the fifth assessment report of IPCC the intergovernmental panel on climate change.

Sturikova, H., Krystofova, O., Huska, D., & Adam, V. (2018). Zinc, zinc nanoparticles and plants. Journal of hazardous materials, 349, 101-110.

Subbarao, G. V., Sahrawat, K. L., Nakahara, K., Ishikawa, T., Kishii, M., Rao, I. M., ... & Lata, J. C. (2012). Biological nitrification inhibition—a novel strategy to regulate nitrification in agricultural systems. Advances in agronomy, 114, 249-302.

SUN, B. F., Hong, Z. H. A. O., Lü, Y. Z., Fei, L. U., & WANG, X. K. (2016). The effects of nitrogen fertilizer application on methane and nitrous oxide emission/uptake in Chinese croplands. Journal of integrative agriculture, 15(2), 440-450.

Sun, H., Du, W., Peng, Q., Lv, Z., Mao, H., & Kopittke, P. M. (2020a). Development of ZnO nanoparticles as an efficient Zn fertilizer: Using synchrotron-based techniques and laser ablation to examine elemental distribution in wheat grain. Journal of Agricultural and Food Chemistry, 68(18), 5068-5075.

Sun, H., Zhou, S., Zhang, J., Zhang, X., & Wang, C. (2020b). Effects of controlled-release fertilizer on rice grain yield, nitrogen use efficiency, and greenhouse gas emissions in a paddy field with straw incorporation. Field Crops Research, 253, 107814.

Sun, Y., Mi, W., Su, L., Shan, Y., & Wu, L. (2019). Controlled-release fertilizer enhances rice grain yield and N recovery efficiency in continuous non-flooding plastic film mulching cultivation system. Field Crops Research, 231, 122-129.

Tapan, A., Biswas, A. K., & Kundu, S. (2010). Nano-fertiliser-a new dimension in agriculture. Indian Journal of Fertilisers, 6(8), 22-24.

Tayebee, R., & Mazruy, V. (2018). Acid-thermal activated nanobentonite as an economic industrial adsorbent for malachite green from aqueous solutions. Optimization, isotherm, and thermodynamic studies. Journal of Water and Environmental Nanotechnology, 3(1), 40-50.

Thangarajan, R., Bolan, N. S., Kunhikrishnan, A., Wijesekara, H., Xu, Y., Tsang, D. C., ... & Hou, D. (2018). The potential value of biochar in the mitigation of gaseous emission of nitrogen. Science of the Total Environment, 612, 257-268.

Tian, H., Xu, R., Canadell, J. G., Thompson, R. L., Winiwarter, W., Suntharalingam, P., ... & Yao, Y. (2020). A comprehensive quantification of global nitrous oxide sources and sinks. Nature, 586(7828), 248-256.

Tibbett, M., Green, I., Rate, A., De Oliveira, V. H., & Whitaker, J. (2021). The transfer of trace metals in the soil-plant-arthropod system. Science of the Total Environment, 779, 146260.

Tomaszewska, M., & Jarosiewicz, A. (2006). Encapsulation of mineral fertilizer by polysulfone using a spraying method. Desalination, 198(1-3), 346-352.

Tso, C. P., Zhung, C. M., Shih, Y. H., Tseng, Y. M., Wu, S. C., & Doong, R. A. (2010). Stability of metal oxide nanoparticles in aqueous solutions. Water science and technology, 61(1), 127-133.

Tu, Y. J., You, C. F., & Kuo, T. Y. (2020). Source identification of Zn in Erren River, Taiwan: an application of Zn isotopes. Chemosphere, 248, 126044.

Umar, W., Ayub, M. A., Ahmad, H. R., Farooqi, Z. U. R., Shahzad, A., Rehman, U., ... & Nadeem, M. (2020). Nitrogen and phosphorus use efficiency in agroecosystems. In Resources Use Efficiency in Agriculture (pp. 213-257). Springer, Singapore.

Umar, W., Czinkota, I., Gulyás, M., Aziz, T., & Hameed, M. K. (2022). Development and characterization of slow release N and Zn fertilizer by coating urea with Zn fortified nano-bentonite and ZnO NPs using various binders. Environmental Technology & Innovation, 102250.

Umar, W., Hameed, M. K., Aziz, T., Maqsood, M. A., Bilal, H. M., & Rasheed, N. (2021). Synthesis, characterization and application of ZnO nanoparticles for improved growth and Zn biofortification in maize. Archives of Agronomy and Soil Science, 67(9), 1164-1176.

Ussiri, D., & Lal, R. (2013). The role of nitrous oxide on climate change. In Soil Emission of Nitrous Oxide and its Mitigation (pp. 1-28). Springer, Dordrecht.

Van Groenigen, J. W., Velthof, G. L., Oenema, O., Van Groenigen, K. J., & Van Kessel, C. (2010). Towards an agronomic assessment of N2O emissions: a case study for arable crops. European journal of soil science, 61(6), 903-913.

Versino, F., Urriza, M., & García, M. A. (2019). Eco-compatible cassava starch films for fertilizer controlled-release. International journal of biological macromolecules, 134, 302-307.

Vinutha, H. P., Poornima, B., & Sagar, B. M. (2018). Detection of outliers using interquartile range technique from intrusion dataset. In Information and decision sciences (pp. 511-518). Springer, Singapore.

Wadgave, U. (2019). Parametric test for non-normally distributed continuous data: For and against: Array. Electronic Physician, 11(2), 7468-7470.

Walling, E., & Vaneeckhaute, C. (2020). Greenhouse gas emissions from inorganic and organic fertilizer production and use: A review of emission factors and their variability. Journal of Environmental Management, 276, 111211.

Wang, B., Smith, S. M., & Li, J. (2018a). Genetic regulation of shoot architecture. Annual review of plant biology, 69, 437-468.

Wang, F., Adams, C. A., Shi, Z., & Sun, Y. (2018b). Combined effects of ZnO NPs and Cd on sweet sorghum as influenced by an arbuscular mycorrhizal fungus. Chemosphere, 209, 421-429.

Wang, H., Ma, S., Shao, G., & Dittert, K. (2021a). Use of urease and nitrification inhibitors to decrease yield-scaled N2O emissions from winter wheat and oilseed rape fields: A two-year field experiment. Agriculture, Ecosystems & Environment, 319, 107552.

Wang, J., Hang, D. W., Ren, G., Guo, J. Q., Zhang, Y. S., Wei, C. Z., & Song, Y. M. (2006). A study on relation between SPAD value, chlorophyll and nitrogen content in cotton. Xinjiang Agricultural Sciences, 43(3), 167-170.

Wang, S., Chen, A., Xie, K., Yang, X., Luo, Z., Chen, J., ... & Xu, G. (2020). Functional analysis of the OsNPF4. 5 nitrate transporter reveals a conserved mycorrhizal pathway of nitrogen acquisition in plants. Proceedings of the National Academy of Sciences, 117(28), 16649-16659.

Wang, S., Li, M., Liu, K., Tian, X., Li, S., Chen, Y., & Jia, Z. (2017a). Effects of Zn, macronutrients, and their interactions through foliar applications on winter wheat grain nutritional quality. PLoS One, 12(7), e0181276.

Wang, S., Wang, Z., Gao, Y., Liu, L., Yu, R., Jin, J., ... & Li, M. (2017b). EDTA alone enhanced soil zinc availability and winter wheat grain Zn concentration on calcareous soil. Environmental and Experimental Botany, 141, 19-27.

Wang, W., Yang, Z., Zhang, A., & Yang, S. (2021b). Water retention and fertilizer slow release integrated superabsorbent synthesized from millet straw and applied in agriculture. Industrial Crops and Products, 160, 113126.

Wang, X., Bai, J., Xie, T., Wang, W., Zhang, G., Yin, S., & Wang, D. (2021c). Effects of biological nitrification inhibitors on nitrogen use efficiency and greenhouse gas emissions in agricultural soils: A review. Ecotoxicology and Environmental Safety, 220, 112338.

Wang, X., Zou, C., Gao, X., Guan, X., Zhang, W., Zhang, Y., ... & Chen, X. (2018c). Nitrous oxide emissions in Chinese vegetable systems: a meta-analysis. Environmental Pollution, 239, 375-383.

Wang, Y., Zhang, X., & Huang, C. (2009). Spatial variability of soil total nitrogen and soil total phosphorus under different land uses in a small watershed on the Loess Plateau, China. Geoderma, 150(1-2), 141-149.

Wei, X. R., Hao, M. D., Xue, X. H., Shi, P., Horton, R., Wang, A., & Zang, Y. F. (2010). Nitrous oxide emission from highland winter wheat field after long-term fertilization. Biogeosciences, 7(10), 3301-3310.

World Meteorological Organization (2019) (WMO Greenhouse Gas Bulletin No. 15) https://library.wmo.int/index.php?lvl=notice_display&id=21620#.Xtf9PZ5KhN0 (2019)

WRB, I. W. G. (2014). World Reference Base for soil resources 2014: international soil classification system for naming soils and creating legends for soil maps. World Soil Resources Report, 106, 12-21.

Wu, K., Wang, S., Song, W., Zhang, J., Wang, Y., Liu, Q., ... & Fu, X. (2020). Enhanced sustainable green revolution yield via nitrogen-responsive chromatin modulation in rice. Science, 367(6478), eaaz2046.

Wu, L., & Liu, M. (2008). Preparation and properties of chitosan-coated NPK compound fertilizer with controlled-release and water-retention. Carbohydrate Polymers, 72(2), 240-247.

Wu, L., Zhang, W., Ding, Y., Zhang, J., Cambula, E. D., Weng, F., ... & Li, G. (2017). Shading contributes to the reduction of stem mechanical strength by decreasing cell wall synthesis in japonica rice (Oryza sativa L.). Frontiers in plant science, 8, 881.

Wu, Z., Wang, X., Song, B., Zhao, X., Du, J., & Huang, W. (2021). Responses of photosynthetic performance of sugar beet varieties to foliar boron spraying. Sugar Tech, 23(6), 1332-1339.

Xiaoyu, N., Yuejin, W., Zhengyan, W., Lin, W., Guannan, Q., & Lixiang, Y. (2013). A novel slow-release urea fertiliser: Physical and chemical analysis of its structure and study of its release mechanism. Biosystems engineering, 115(3), 274-282.

Xie, J., Shi, X., Zhang, Y., Wan, Y., Hu, Q., Zhang, Y., ... & Evgenia, B. (2022). Improved nitrogen use efficiency, carbon sequestration and reduced environmental contamination under a gradient of manure application. Soil and Tillage Research, 220, 105386.

Xie, K., Ren, Y., Chen, A., Yang, C., Zheng, Q., Chen, J., ... & Xu, G. (2021). Plant nitrogen nutrition: The roles of arbuscular mycorrhizal fungi. Journal of Plant Physiology, 153591.

Xie, Y., Tang, L., Han, Y., Yang, L., Xie, G., Peng, J., ... & Zhang, Y. (2019). Reduction in nitrogen fertilizer applications by the use of polymer-coated urea: effect on maize yields and environmental impacts of nitrogen losses. Journal of the Science of Food and Agriculture, 99(5), 2259-2266.

Xu, G., Fan, X., & Miller, A. J. (2012). Plant nitrogen assimilation and use efficiency. Annual review of plant biology, 63, 153-182.

Xu, P., Li, Z., Wang, J., & Zou, J. (2022). Fertilizer-induced nitrous oxide emissions from global orchards and its estimate of China. Agriculture, Ecosystems & Environment, 328, 107854.

Yan, Z., Eziz, A., Tian, D., Li, X., Hou, X., Peng, H., ... & Fang, J. (2019). Biomass allocation in response to nitrogen and phosphorus availability: insight from experimental manipulations of Arabidopsis thaliana. Frontiers in plant science, 10, 598.

Yang, G., Yuan, H., Ji, H., Liu, H., Zhang, Y., Wang, G., ... & Guo, Z. (2021). Effect of ZnO nanoparticles on the productivity, Zn biofortification, and nutritional quality of rice in a life cycle study. Plant Physiology and Biochemistry, 163, 87-94.

Yang, J. T., Schneider, H. M., Brown, K. M., & Lynch, J. P. (2019). Genotypic variation and nitrogen stress effects on root anatomy in maize are node specific. Journal of Experimental Botany, 70(19), 5311-5325.

Yang, X., Jiang, R., Lin, Y., Li, Y., Li, J., & Zhao, B. (2018). Nitrogen release characteristics of polyethylene-coated controlled-release fertilizers and their dependence on membrane pore structure. Particuology, 36, 158-164.

Yang, X., Lu, Y., Ding, Y., Yin, X., & Raza, S. (2017). Optimising nitrogen fertilisation: a key to improving nitrogen-use efficiency and minimising nitrate leaching losses in an intensive wheat/maize rotation (2008–2014). Field Crops Research, 206, 1-10.

Yaseen, M., Ahmad, A., Naveed, M., Ali, M. A., Shah, S. S. H., Hasnain, M., ... & Mustafa, A. (2021). Subsurface-applied coated nitrogen fertilizer enhanced wheat production by improving nutrient-use efficiency with less ammonia volatilization. Agronomy, 11(12), 2396.

Ye, H. M., Li, H. F., Wang, C. S., Yang, J., Huang, G., Meng, X., & Zhou, Q. (2020). Degradable polyester/urea inclusion complex applied as a facile and environment-friendly strategy for slow-release fertilizer: Performance and mechanism. Chemical Engineering Journal, 381, 122704.

Yi, J., Gao, J., Zhang, W., Zhao, C., Wang, Y., & Zhen, X. (2019). Differential uptake and utilization of two forms of nitrogen in japonica rice cultivars from north-eastern China. Frontiers in plant science, 1061.

Yi, Q., Tang, S., Fan, X., Zhang, M., Pang, Y., Huang, X., & Huang, Q. (2017). Effects of nitrogen application rate, nitrogen synergist and biochar on nitrous oxide emissions from vegetable field in south China. Plos one, 12(4), e0175325.

Yusefi-Tanha, E., Fallah, S., Rostamnejadi, A., & Pokhrel, L. R. (2020). Zinc oxide nanoparticles (ZnONPs) as a novel nanofertilizer: Influence on seed yield and antioxidant defense system in soil grown soybean (Glycine max cv. Kowsar). Science of the Total Environment, 738, 140240.

Yuvaraj, M., & Subramanian, K. S. (2018). Development of slow release Zn fertilizer using nano-zeolite as carrier. Journal of plant nutrition, 41(3), 311-320.

Zhang, H., Wang, R., Chen, Z., Cui, P., Lu, H., Yang, Y., & Zhang, H. (2021a). The Effect of Zinc Oxide Nanoparticles for Enhancing Rice (Oryza sativa L.) Yield and Quality. Agriculture, 11(12), 1247.

Zhang, L., Yan, M., Li, H., Ren, Y., Siddique, K. H., Chen, Y., & Zhang, S. (2020). Effects of zinc fertilizer on maize yield and water-use efficiency under different soil water conditions. Field Crops Research, 248, 107718.

Zhang, S., Shen, T., Yang, Y., Ma, X., Gao, B., Li, Y. C., & Wang, P. (2021b). Novel environment-friendly superhydrophobic bio-based polymer derived from liquefied corncob for controlled-released fertilizer. Progress in Organic Coatings, 151, 106018.

Zhang, T., Sun, H., Lv, Z., Cui, L., Mao, H., & Kopittke, P. M. (2017a). Using synchrotron-based approaches to examine the foliar application of ZnSO4 and ZnO nanoparticles for field-grown winter wheat. Journal of agricultural and food chemistry, 66(11), 2572-2579.

Zhang, W., Wu, L., Ding, Y., Yao, X., Wu, X., Weng, F., ... & Wang, S. (2017b). Nitrogen fertilizer application affects lodging resistance by altering secondary cell wall synthesis in japonica rice (Oryza sativa). Journal of plant research, 130(5), 859-871.

Zhang, Z., Wang, H., Niu, M., Peng, K., & Guo, P. (2022). Adsorption properties of millimeter porous spheres constructed by montmorillonite nanosheets. Applied Clay Science, 216, 106324.

Zhao, Z., Yan, S., Hu, S., & Qu, K. (2022). Nitrogen distribution in apple orchard soil profile under fertilization with different water and fertilizer coupling techniques. International Journal of Agricultural and Biological Engineering, 15(5), 146-154.

Zhong, L., Bowatte, S., Newton, P. C., Hoogendoorn, C. J., & Luo, D. (2018). An increased ratio of fungi to bacteria indicates greater potential for N2O production in a grazed grassland exposed to elevated CO2. Agriculture, Ecosystems & Environment, 254, 111-116.

Zhou, J., Qu, T., Li, Y., Van Zwieten, L., Wang, H., Chen, J., ... & Zhong, Z. (2021). Biochar-based fertilizer decreased while chemical fertilizer increased soil N2O emissions in a subtropical Moso bamboo plantation. Catena, 202, 105257.

Zia, M. H., Ahmed, I., Bailey, E. H., Lark, R. M., Young, S. D., Lowe, N. M., ... & Broadley, M. R. (2020). Site-specific factors influence the field performance of a Zn-biofortified wheat variety. Frontiers in Sustainable Food Systems, 135.

Zulfiqar, F., Navarro, M., Ashraf, M., Akram, N. A., & Munné-Bosch, S. (2019). Nanofertilizer use for sustainable agriculture: Advantages and limitations. Plant Science, 289, 110270.

Zunfu, L., Ruoyi, J., Lijuan, D., Weichen, H., Ximing, X., Yongxin, L., ... & Guoquan, L. (2022). A model of plant and ear nitrogen for the diagnosis of nitrogen nutrition of malting barley to coordinate the relationship between grain yield and quality. European Journal of Agronomy, 136, 126488.